CONTROL OF STRESS RESPONSES BY VIRAL AND CELLULAR BASIC

LEUCINE ZIPPER TRANSCRIPTION FACTORS

by

Madeleine L. Stolz

Submitted in partial fulfillment of the requirements

for the degree of Master of Science

at

Dalhousie University

Halifax, Nova Scotia

August 2022

Table of Contents

LIST OF TABLES

LIST OF FIGURES

ABSTRACT

Glycoproteins are processed through the secretory pathway and require folding in the endoplasmic reticulum (ER). When unfolded proteins accumulate in the ER, the sensor protein ATF6 is activated, translocated to the Golgi, and proteolytically processed into ATF6-N, a member of the heterodimerizing family of basic leucine zipper (bZIP) transcription factors. ATF6-N restores proteostasis by upregulating chaperones and ER-associated degradation genes. Kaposi's sarcoma-associated herpesvirus (KSHV) activates ATF6 cleavage but suppresses the downstream production of antiviral effectors. I hypothesized that ATF6-N is antiviral and KSHV must subvert its antiviral activity. Indeed, I showed that ectopically expressed ATF6-N reduces viral titers. I investigated if K-bZIP, a viral bZIP and multifunctional transcriptional repressor essential for viral replication, is an inhibitor of ATF6, but found that K-bZIP does not perturb ATF6-N signaling. Conversely, ATF6-N impairs nuclear import of K-bZIP. I concluded that ATF6-N is antiviral to KSHV, but the mechanism of action remains unknown.

LIST OF ABBREVIATIONS AND SYMBOLS USED

%	Percent
°C	Degrees Celsius
2'-5' OAS	2'-5' oligoadenylate synthetase
ΔΔCt	Delta-delta threshold cycles
μg	Microgram
μg/mL	Micrograms per milliliter
μL	Microliter
μM	Micromolar
μM	Micromolar
A	Adenine
A	Alanine
aa	Amino acid
AARE	Amino acid response element
AIDS	Acquired immunodeficiency syndrome
AMP	Adenosine monophosphate
ANOVA	Analysis of variance
AP-1	Activator protein 1
AP-2	Adaptor protein complex 2
ART	Antiretroviral therapy
ASNS	Asparagine synthetase
ATF	Activating transcription factor

ATF6-N	ATF6 N-terminal fragment
ATG5	Autophagy-related gene 5
ATP	Adenosine triphosphate
BC-3	Body-cavity based lymphoma cells
BCBL-1	Body-cavity-based lymphoma cells
Bcl-2	B-cell lymphoma 2
BiP	Binding immunoglobulin protein
bp	Base pair
bZIP	Basic leucine zipper
C	Cytidine
C/EBP	CCAAT/enhancer-binding protein
C33A	Cervical cancer cells
Ca^{2+}	Calcium ion
CALR	Calreticulin
CBP	CREB-binding protein
cccDNA	Covalently closed circular DNA
CCL5	C-C Motif Chemokine Ligand 5
CD20	Cluster of differentiate 20
cDNA	Circular DNA
cGAS	cytosolic dsDNA sensor cyclic GMP-AMP synthase
CHiP-seq	Chromatin immunoprecipitation sequencing
CHO	Chinese hamster ovary cells
CHOP	C/EBP homologous protein

cm	Centimeter
CO_2	Carbon dioxide
Co-IP	Co-immunoprecipitation
COPII	Coat protein II
COX-2	Cyclooxygenase-2
CpG	5'-C-phosphate-G-3'
CRE	cAMP response element
CREB	CRE-binding protein
C-terminus	Carboxyl-terminus
DAPK1	Death-associated protein kinase 1
DC-SIGN	Dendritic cell-specific ICAM-3-grabbing nonintegrin
DDIT3	DNA damage-inducible transcript 3
DNA	Deoxyribonucleic acid
DNAJB9	DNA J-domain heat shock protein family member B9
dpi	Days post-infection
DR	Direct repeat
dsDNA	double-stranded DNA
E	Early gene
EBV	Epstein-Barr virus
EDEM	ER degradation enhancing alpha-mannosidase like protein
EF-1-α	Elongation factor 1-α
(E)GFP	(enhanced) Green fluorescent protein
eIF	Eukaryotic translation initiation factor

EphA2	Ephrin type-A receptor 2
ER	Endoplasmic reticulum
ERAD	ER-associated degradation
ERdj4	Endoplasmic reticulum-localized DNA J domain-containing protein 4
ERK	Extracellular signal-regulated kinase
ERManI	ER mannosidase I
ERp18	ER protein 18
ERSE	ER stress-response element
EZH2	Enhancer of zeste homolog 2
FCID	FIC-domain-containing ER-localized enzyme
Fig.	Figure
G	Guanine
GADD34	Growth arrest and DNA damage-inducible protein 34
gB/H/L	Glycoprotein B/H/L
GCN2	General control non-derepressible-2
GDP	Guanosine diphosphate
GFAP	Glial fibrillary acidic protein
GLS	Golgi localization signal
GMP	Guanosine monophosphate
GRP	Glucose-related protein
GTP	Guanosine triphosphate
H	Histone
h	Hour

H_2O_2	Hydrogen peroxide
HBZ	HTLV-1 bZIP factor
HCMV	Human cytomegalovirus
HCV	Hepatitis C Virus
HDAC	Histone deacetylase
HEK	Human embryonic kidney cells
HERPUD1	Homocysteine-inducible ER protein with ubiquitin-like domain 1
HHV-8	Human gammaherpesvirus 8
HIF-1α	Hypoxia-inducible factor-1α
HIV	Human immunodeficiency virus
hpi	Hours post-infection
HRI	Heme-regulated inhibitor HRI
hSet1	Human SET domain-containing 1
(h)SNF5	(Human) subunit sucrose non-fermentable 5
HSPA5	Heat shock family A member 5
HSV-1	Herpes simplex virus type 1
HTLV-1	Human T-lymphotropic virus 1
HVS	Herpesvirus saimiri
IAV	Influenza A virus
ICAM-3	Intercellular adhesion molecule-3
ICP27	Infected cell culture polypeptide 27
IE	Immediate early gene
IFN	Interferon

IL	Interleukin
IRE1	Inositol-requiring enzyme 1
IRF	Interferon response factor
ISG	Interferon-stimulated gene
ISGF	Interferon-stimulated gene factor
ISRE	Interferon-sensitive response element
IU/mL	Infectious units per milliliter
JMJD3	Jumonji domain containing 3
JNK	c-Jun N-terminal kinase
K	Lysine
kDA	Kilodalton
KICS	KSHV inflammatory cytokine syndrome
KIF3A	Kinesin family member 3A
KS	Kaposi's sarcoma
KSHV	Kaposi's sarcoma-associated herpesvirus
L	Late gene
LANA	Latency-associated nuclear antigen
LAP	C/EBPβ liver-enriched activating protein
LC3B	Microtubule-associated proteins 1A/1B light chain 3B
LIP	C/EBPβ liver-enriched inhibitory protein
Maf	Musculoaponeurotic fibrosarcoma
MAPK	Mitogen-activated protein kinase
MARE	Maf response element

MCD	Multicentric Castleman disease
MCM	Minichromosome maintenance
MCMV	Murine cytomegalovirus
MCP	Major capsid protein
MDV	Marek's disease virus
me	Methyl
MEF	Mouse embryonic fibroblast
MEQ	MDV Eco Q
Met-tRNA$_i$	Initiator methionyl-tRNA
MHC	Major histocompatibility complex
MIEP	Major immediate-early promoter
min	Minutes
miRNA	Micro RNA
MK2	MAPK-activated protein kinase 2
MLL2	Mixed-lineage leukemia protein 2
MOI	Multiplicity of infection
mRNA	Messenger RNA
NaB	Sodium butyrate
NFAT	Nuclear factor of activated T cells
NF-Y	Nuclear factor Y
NF-κ-B	Nuclear factor kappa B
ng	Nanogram
NLS	Nuclear localization signal

NPC	Nuclear pore complex
NRIF	Neurotrophin receptor interacting factor
NS4B	Non-structural protein 4B
nt	Nucleotide
N-terminus	Amino-terminus
OASIS	Old astrocyte specifically induced substance
ORC	Origin recognition complexes
ORF	Open reading frame
oriLyt	Lytic origin of replication
PAF	Primase-associated factor
PAN RNA	Polyadenylated nuclear RNA
PDIA	Protein disulfide isomerase
PEL	Primary effusion lymphoma
PERK	Protein kinase R-like endoplasmic reticulum kinase
PFAS	Phosphoribosylformyl-glycinamidine synthetase
PIC	Pre-initiation complex
PKR	Protein kinase double-stranded RNA-dependent
PML bodies	Promyelocytic leukemia nuclear bodies
Pol	Polymerase
Poly(I:C)	Polyinosinic:polycytidylic acid
PRC2	Polycomb repressive complex 2
PRMT5	Protein arginine methyltransferase 5
PRR	Pattern recognition receptor

PTM	Post-translational modification
R	Arginine
Ran	Ras-related nuclear protein
RE	Response element
RFU	Relative fluorescent units
RIDD	Regulated IRE1-dependent decay
RLU	Relative light units
RNA	Ribonucleic acid
ROS	Reactive oxygen species
RRE	RTA response element
RTA	Replication and transcription activator
RT-qPCR	Real-time quantitative polymerase chain reaction
SCAF	Scaffolding protein
SCP	Small capsid protein
SDS-PAGE	Sodium dodecyl sulfate-polyacrylamide gel electrophoresis
Sec gene	Secretory gene
SEM	Standard error of the mean
SERCA	Sarco/endoplasmic reticulum Ca^{2+} ATPase
SIM	SUMO interaction motif
SLK	KS renal carcinoma cells
SNAT2	Sodium-dependent neutral amino acid transporter-2
SOX	Shutoff and exonuclease
Sp	Specificity protein

SP-1/-2	Serine protease-1/-2
SRT1	Sirtuin 1
SSB	Single-stranded DNA binding protein
STING	Stimulator of interferon genes
STUbL	SUMO-targeting ubiquitin ligase
SUMO	Small ubiquitin-like modifier
T	Threonine
T	Thymine
Tat	Transactivator of transcription
TBK1	TANK-binding kinase 1
TBP	TATA-binding protein
TF	Transcription factor
Tg	Thapsigargin
TGF	Tumor growth factor
TLR	Toll-like receptor
TPA	12-O-tetradecanoyl-phorbol-13-acetate
TR	Terminal repeat
TRE	TPA response element
tRNA	Transfer RNA
U	Uracil
U/mL	Units per milliliter
UL	Unique long
uORF	Upstream ORF

UPR	Unfolded protein response
UPRE	Unfolded protein response element
UTR	Untranslated region
UTX	Ubiquitously transcribed tetratricopeptide repeat protein X-linked
v	Viral
v-Cyclin	Viral cyclin D homologue
vFLIP	Fas-associated death domain-like IL-1β-converting enzyme-inhibitory protein
VGEF	Vascular endothelial growth factor
vGPCR	Viral G protein-coupled receptor
VP16	Viral protein 16
vPIC	Viral pre-initiation complex
vPK	Viral protein kinase
VSV	Vesicular stomatitis virus
VZV	Varicella-Zoster virus
X	-times
XBP1s	X-box binding protein 1 spliced
XBP1u	X-box binding protein 1 unspliced
xCT	Cysteine/glutamate exchange transporter
ZIKV	Zika virus
ZIP	Zipper
Zta	BamHI Z EBV replication activator

ACKNOWLEDGEMENTS

First and foremost, I would like to thank my supervisor Dr. Craig McCormick for allowing me to work in his wonderful lab and for supporting me throughout my studies and beyond. His suggestions, ideas, and feedback have made me a better critical thinker and scientist. His continuing concern for my studies and my mental health and wellbeing have allowed me to complete this project. I deeply appreciate all he has done to help me reach this point in my studies and all he continues to do to secure a successful future for me.

I would like to thank all past and present members of the McCormick lab for their support and help with experimental setups, presentations, scholarship applications, and for accepting me for who I am. I would especially like to thank Dr. Brett Duguay for his seemingly endless patience and for always having a solution to every problem, and Dr. Eric Pringle, who I value most for his expertise with various cellular techniques and for being so beautifully direct and straightforward.

I would like to thank Derek Rowter and the members of the Dalhousie flow cytometry facility for their excellent help with my flow cytometry experiments.

Lastly, I would like to thank my family, who have not only made me the person I am, but who support me and my personal development limitlessly and who have always loved me for my flaws without wanting to correct them. Time and time again they have put my best interest ahead of their own. I am thankful for having such a loving, caring, and supportive family without whom I surely would not be where I am today.

CHAPTER 1: INTRODUCTION

1.1 KSHV Epidemiology and Pathogenesis

Kaposi's sarcoma associated herpesvirus (KSHV) or human gammaherpesvirus 8 (HHV-8) is a human oncogenic, double-stranded DNA gammaherpesvirus and close relative of Epstein-Barr virus (EBV) and various gammaherpesviruses of other mammals, including non-human primates [1]. The DNA genome of KSHV is ~165,000 base pairs in length and encodes more than 80 proteins, many of which are homologous to proteins expressed by other herpesviruses [371]. Some KSHV genes, *ORFs K1-K15*, encode proteins that are unique to KSHV and have no known homologues [372]. KSHV displays differential global distribution and is most common in sub-Saharan Africa and parts of the Mediterranean, with seroprevalence rates of greater than 50% and up to 30%, respectively. KSHV is uncommon in the Americas, Europe, and Asia with seroprevalence rates of less than 10%. Seroprevalence is also higher in certain ethnic groups, as well as in men who have sex with men [2,3].

KSHV is the etiologic agent of two distinct cancers and two inflammatory disorders: the AIDS-defining Kaposi's sarcoma (KS), primary effusion lymphoma (PEL), HHV-8 associated multicentric Castleman disease (MCD), and KSHV inflammatory cytokine syndrome (KICS) [2,3]. The biggest determinant of KSHV-associated pathogenesis is immune status; individuals with compromised immune systems, such as HIV-positive individuals, organ transplant recipients [3], and diabetics [4], are most at risk of developing KSHV malignancies. KS is an endothelial-derived tumor that affects the skin and organs [5]. KS is one of the most common cancers in HIV/AIDS patients but may also occur in individuals without HIV co-infection [2,6]. PEL is a B-cell lymphoma that manifests as pleural effusions collecting in body cavities but can also manifest as solid tumors in the skin, lymph nodes, gastrointestinal tract, central nervous system, and lungs [3]. PEL most commonly affects HIV/AIDS patients and may occur concurrently with KS and MCD [7]. The B-cell lymphoproliferative disorder and inflammatory disease HHV-8-associated MCD, like KS and PEL, is most common in HIV/AIDS patients [3], and involves inflammatory symptoms, such as fever, thrombocytopenia, anemia, and hepatosplenomegaly caused by high levels of pro-inflammatory cytokines. Untreated

HHV-8 associated MCD is almost always fatal [2]. KICS, the most recently identified KSHV-associated disease, shares many of its symptoms with HHV-8-associated MCD and is characterized by high serum levels of IL-6 and IL-10 but does not involve lymphoproliferation and other MCD-associated pathologies [2,3].

A hallmark feature of herpesviruses is their ability to undergo latency and establish life-long persistence in their hosts. During latency, KSHV expresses only a few genes needed to maintain the viral plasmid-like genome, the episome, and spreads passively to daughter cells during cell division. Infectious progeny is only made once the virus switches to the lytic cycle and expresses the proteins required to regulate viral gene expression, facilitate immune evasion, and assemble new virions [8]. Latent and lytic replication both contribute to viral tumorigenesis [9,10].

KSHV infection is life-long and cannot be cured, but KSHV-associated malignancies can be treated. Chemotherapy with one or multiple therapeutic agents, such as doxorubicin, an inhibitor of DNA synthesis, is commonly used to treat KS tumors [11] and PEL [12]. For HIV positive patients, antiretroviral therapy (ART) is also effective at controlling KSHV malignancies like PEL [12], but has limited efficiency at treating AIDS-associated KS [11] and HHV-8 associated MCD [13]. HHV8-associated MCD is more difficult to treat and does not respond well to ART or chemotherapy and is instead treated with the monoclonal anti-CD20 antibody rituximab alone or in combination with ART to prolong survival of patients [13].

1.2 KSHV Tropism and Replication Cycles

KSHV is primarily transmitted between individuals by saliva, but is also present in other bodily fluids, which include the blood, semen, and vaginal excretions. As such, KSHV can be transmitted sexually and non-sexually [14]. KSHV may also be transmitted vertically from mother to child [15,16]. Once inside the host, KSHV infects a range of cell types, including epithelial cells, endothelial cells [17], B cells [18], macrophages, and dendritic cells [19]. Cell entry is initiated by interaction of the viral surface glycoproteins glycoprotein B (gB) [19,20], K8.1A [21,22], and gH/gL [23] with cellular heparan sulfate sugars that act as binding receptors [20] and integrins [24,25], ephrin type-A receptor 2 (EphA2) [26], and dendritic cell-specific intercellular adhesion molecule-3- (ICAM-3)

grabbing nonintegrin (DC-SIGN) that act as entry receptors [19]. Following successful attachment, KSHV enters target cells by clathrin-mediated endocytosis [27,28], or micropinocytosis [29], and releases its capsid into the cytosol by fusion of the viral envelope with the endosomal membrane (Fig. 1). The precise mechanism of membrane fusion is not fully understood but requires the viral glycoproteins gB and gH/gL [30] as well as the cellular cysteine/glutamate exchange transporter xCT [31]. KSHV induces the hyperacetylation of microtubules and initiates transport of the viral capsid to the nucleus via the motor protein dynein [32]. The capsid then docks at the nuclear pore and the viral dsDNA is injected into the nucleus [33] and circularized into covalently closed circular DNA (cccDNA), known as the episome (Fig. 1). cccDNA is the most abundant form of viral DNA present during latency, whereas linear DNA is the primary form that accumulates during lytic replication [34].

1.3 Latency

To establish and maintain latency, the viral transcription program needs to shift to the activation of latent genes and the repression of lytic genes. Importantly, expression of the potent lytic viral replication and transcription activator (RTA) must be tightly controlled during latency, because overexpression of RTA alone is sufficient to reactivate latent KSHV in PEL body-cavity-based lymphoma (BCBL-1) and KS renal carcinoma (SLK) cell lines [35,36]. Modification of the viral gene expression landscape takes place by histone modification and methylation of cytidine (C) residues in CpG islands on the KSHV genome. These reversible, epigenetic changes convert regions of the genome, specifically those encoding immediate early (IE) or early (E) lytic genes, to transcriptionally silent heterochromatin [36,37]. During the initial stages of infection, starting as early as 4 hours post-infection (hpi), histones localized on promoter regions of the viral genome acquire modifications, such as acetylation of lysine 27 on histone 3 (H3K27-ac), tri-methylation of lysine 4 on H3 (H3K4-me3) [36], and acetylation of lysine 9 and/or 14 on H3 (H3K9/14-ac) [37], that positively regulate transcription. By contrast, the activating histone modifications are replaced 24-72 hpi by repressive modifications, such as tri-methylation of lysine 4 or 27 on H3 (H3K4-me3/H3K27-me3) [36,37]. Enhancer of zeste homolog 2 (EZH2) is a cellular methyltransferase and part of the

3

Figure 1. **Phases of KSHV infection.**

Following reversible attachment to cellular attachment and entry receptors, KSHV enters target cells by endocytosis or micropinocytosis depending on cell type. KSHV escapes the endosome by membrane fusion and is transported to the nucleus, where LANA tethers the viral episome to the cellular DNA to establish latency. Latency is disrupted by expression of RTA from *ORF50* and initiates lytic replication, which culminates in viral gene expression, capsid assembly, and genome packaging. Viral capsids escape the nucleus and acquire a lipid envelope decorated with viral glycoproteins by budding into vesicles of the ER-Golgi intermediate compartment (ERGIC) or the Golgi. Virions leave the cell by exocytosis.

Figure 1. **Phases of KSHV infection.**
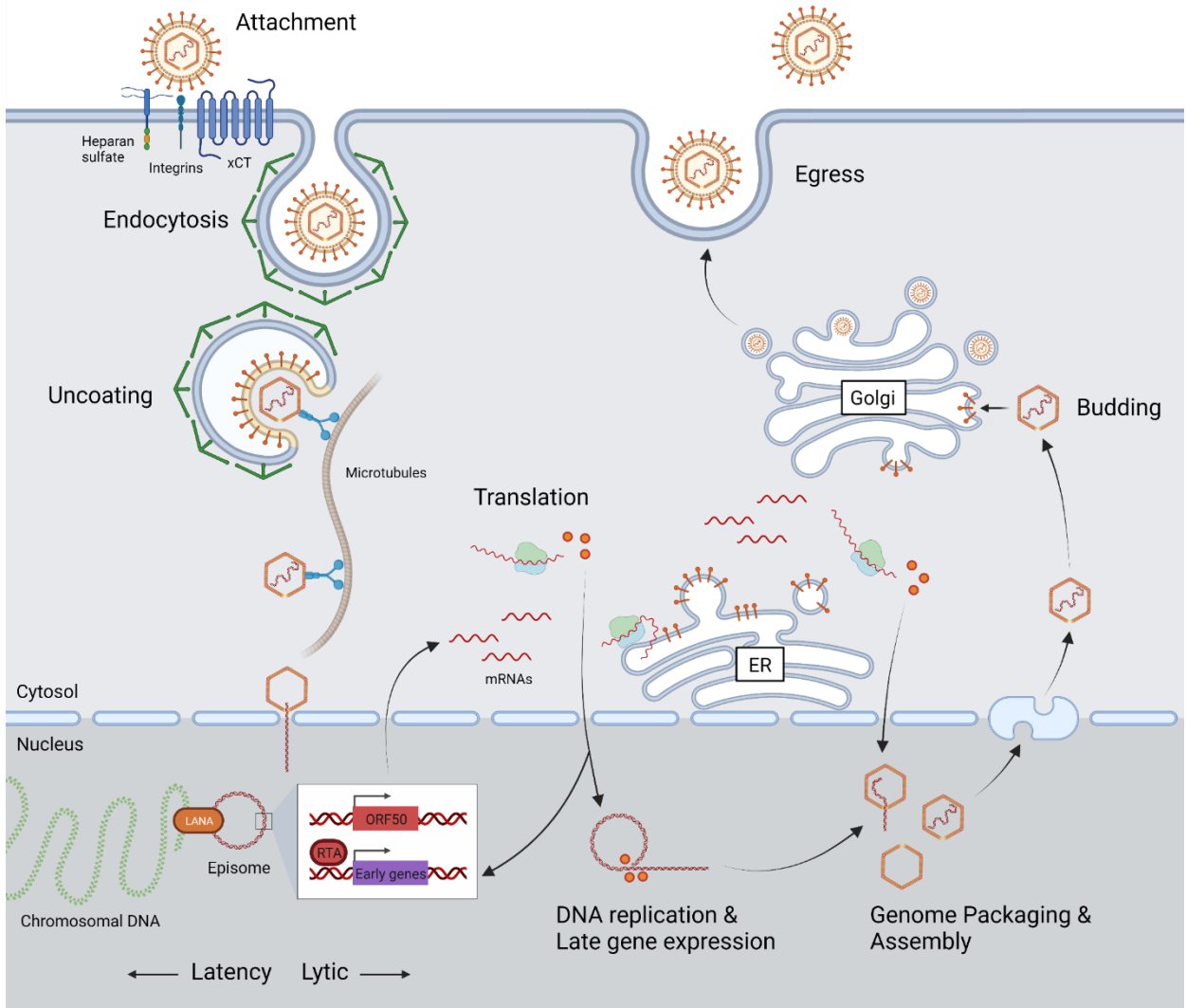
Polycomb repressive complex 2 (PRC2) that mediates tri-methylation of H3K27. The viral latency-associated nuclear antigen (LANA) co-localizes and forms complexes with PRC2 24 hpi to facilitate widespread transcriptional repression of the viral genome and help establish latency [38]. Histone modification across the KSHV genome is variable and some promoters, such as the *ORF50* promoter from which the viral RTA is encoded, carry both activating and repressive histone modifications during latency, whereas the LANA promoter almost exclusively carries activating histone modifications [36]. The cellular histone deacetylase (HDAC) sirtuin 1 (SRT1) also assists in the transcriptional silencing of early lytic KSHV genes by binding the *ORF50* promoter. SIRT1 inhibition or knockdown leads to an increase in H3K4-me3 and a decrease in H3K27-me3 on the *ORF50* promoter, which reactivates KSHV from latency in BCBL-1 cells [39].

Methylation of CpG motifs provides an additional mechanism for gene silencing and maintaining latency. The KSHV genome is subject to CpG methylation and becomes abundantly methylated at 5 days post-infection (dpi) in BCBL-1 and SLK cells [37]. Like histone modification, methylation of the KSHV genome is variable. As such, the *ORF50* gene encoding RTA is hypermethylated during latency in some KSHV-infected cell lines but not in others, and the *ORF73* gene encoding LANA is not subject to DNA methylation [37,40]. Therefore, establishment and maintenance of viral latency is a multifactorial process that requires multiple layers of transcriptional regulation.

1.3.1 Latency-Associated Nuclear Antigen (LANA)

LANA is a multifunctional, DNA-binding protein that is encoded from *ORF73* and is abundantly expressed in latently infected cells [41–43]. The protein localizes to the nucleus and forms nuclear aggregates by oligomerization of its C-terminal DNA-binding domain. Oligomerization is critical to LANA function and required for DNA binding and episome maintenance. Oligomerization-deficient LANA mutants fail to associate with the viral terminal repeat (TR) sequence and display a diffuse pattern of localization inside the nucleus instead of forming nuclear aggregates [44]. LANA allows the episome to persist in infected cells by binding the viral TR sequence and cellular chromosomes and therefore tethering the episome to the cellular DNA (Fig. 1). LANA also recruits cellular origin recognition complexes (ORCs) and minichromosome maintenance (MCM) proteins to

the viral TR that initiate episome unwinding and DNA replication. As such, LANA is not only essential for episome maintenance but also allows the episome to be passed on to daughter cells [45–47]. LANA also regulates the latent gene expression landscape by binding viral latent promoters and recruiting the human SET domain-containing 1 (hSet1) methyltransferase that tri-methylates H3K4 and permits transcriptional initiation. Cellular promoters may also be subject to LANA-mediated epigenetic control because LANA associates with H3K4-me3 at various cellular promoters, including those that regulate chromosome organization and apoptosis [43,48]. Other functions of LANA include promoting cell survival and oncogenesis, which the protein facilitates by inhibiting the tumor suppressor protein p53 [49] and by dysregulating tumor growth factor β (TGF-β) signaling through silencing of the TGF-β receptor II [50].

1.3.2 Other Latent Transcripts

Most latent viral transcripts found in all KSHV-associated malignancies are expressed from the latency locus, a region on the KSHV genome that encodes multiple polycistronic transcripts. One of these transcripts is transcribed from three distinct ORFs and encodes LANA (from *ORF73*), a viral cyclin D homologue (v-Cyclin, encoded from *ORF72*), and Fas-associated death domain (FADD)-like IL-1β-converting enzyme (FLICE)-inhibitory protein (vFLIP, encoded from *ORF71*) from a single promoter [51–53]. Adjacent to *ORFs 73-71* are *ORF K12* and two GC-rich direct repeat (DR) sequences, which comprise the Kaposin locus that encodes Kaposin A-C from a single promoter by use of alternative, non-AUG, start codons [54,55]. The region that separates *ORFs 71-73* from *ORF K12* also contains promoters and expresses 13 micro RNAs (miRNAs) from the sense and antisense strand that are then processed into a total of 25 mature miRNA derivatives [56–58]. miRNAs are short, non-coding RNAs ~22 nucleotides (nt) in length that are initially made as pre-miRNAs and are then processed into mature miRNAs. They can base-pair with complementary 5' and 3' untranslated regions (UTRs) of mRNAs and promoter regions of genomic DNA to regulate gene expression by silencing at the transcriptional and post-transcriptional level [59]. The KSHV-encoded miRNAs are multifunctional and target cellular transcripts, such as those encoding p21 [60], inhibitor of nuclear factor kappa B (IκBα) [61,62], and CCAAT/enhancer-binding protein α (C/EBPα),

to inhibit expression of all classes of lytic genes [63], and regulate the NF-κB pathway to prevent growth arrest, protect from apoptosis of infected cells [64], and promote oncogenesis [62]. Likewise, v-Cyclin and vFLIP prevent G_0/G_1 cell cycle arrest [65,66] and inhibit lytic gene expression [67], respectively. v-Cyclin and vFLIP are also oncogenes and induce tumorigenesis in mouse models and therefore most likely contribute to the tumorigenesis of KSHV in human patients as well [68–70].

Another latently expressed contributor to KSHV pathogenesis is Kaposin B, the most abundant protein product of the Kaposin locus expressed in the BCBL-1 PEL cell line [54]. Transcription from *ORF K12* yields a transcript that spans *ORF K12* as well as the DRs immediately downstream of *K12*. The transcript is spliced and translation initiation from different sites within the transcript yields the three Kaposin proteins A-C. Translation of the DR sequences is initiated from a CUG codon located in the 5' region of the DR sequences and produces Kaposin B [54,55]. The presence and length of additional repeat elements 5' to the DR sequences varies between PEL and KS isolates and affects translation, such that some KS and PEL tumors lack Kaposin B, but still express Kaposin A and C [55]. During latency, Kaposin B activates the cellular mitogen-activated protein kinase (MAPK) p38, and MAPK-activated protein kinase 2 (MK2) - a target of p38-mediated phosphorylation - which are implicated in inflammatory responses and cell proliferation. The Kaposin B-mediated dysregulation of the p38/MK2 pathway results in the upregulation of cytokine-expressing genes, such as *IL-6*, which in turn provide a favourable environment for the survival and proliferation of KS spindle cells [71].

1.4 Lytic Replication

A small percentage of latently infected cell populations can undergo spontaneous reactivation and lytic replication. Spontaneous expression of lytic markers, such as RTA and the capsid protein ORF65, has been observed in KSHV-positive PEL cell lines, KS skin biopsies, and other latently infected cells [72–77]. Lytic replication culminates in a temporally regulated cascade of gene expression, DNA replication, and virion production and allows the virus to spread to new tissues in the host (Fig. 1). KSHV episomes are not stably maintained in all cell types and may be lost after repeated rounds of cell division.

Therefore, lytic replication may provide a mechanism to sustain viral infection and pathogenesis in the host [78]. Reactivation from latency is accompanied by epigenetic changes and chromatin remodeling that permit the efficient transcription of lytic genes. During latency, the *ORF50* promoter is bivalent and occupied by histones carrying both repressive (H3K27-me3) and activating (H3K4-me3) histone modifications. This bivalent chromatin profile contributes to RTA suppression during latency but allows for more rapid RTA expression following reactivation. Some early genes, including *K4.2*, *K8*, *ORF45*, and *ORF48*, are likewise tri-methylated during latency and display the same bivalent histone modification profile as the *ORF50* promoter. During early lytic replication, the repressive H3K27-me3 modifications of the bivalent promoters decrease and the activating H3K4-me3 modifications increase, which permits the expression of RTA and early lytic genes. Most E gene promoters are occupied by histones carrying activating modifications during latency and lytic reactivation but depend on RTA for their expression. Conversely, promoters of most late (L) genes retain their repressive histone modifications during E gene expression to provide additional temporal control to the lytic gene expression program [37,79]. The viral early gene product, ORF59, a DNA polymerase processivity factor, and the viral non-coding polyadenylated nuclear RNA (PAN RNA) transcript co-operate to restructure the epigenetic landscape of the *ORF50* promoter during lytic reactivation. PAN RNA binds the *ORF50* promoter and forms a scaffold that allows ORF59 to interact with the cellular demethylases ubiquitously transcribed tetratricopeptide repeat protein X-linked (UTX) and Jumonji domain containing 3 (JMJD3). The interaction between PAN RNA and ORF59 mediates the recruitment of UTX and JMJD3 to the *ORF50* promoter where the demethylases remove the repressive H3K27-me3 histone modification and relieve *ORF50* silencing [80,81]. More recently, ORF59 has also been found to inhibit the cellular protein arginine methyltransferase 5 (PRMT5) during early lytic replication. PRMT5 di-methylates arginine 3 of H4 (H4R3me2s) and promotes placement of the repressive H3K27-me3 modification, therefore converting the viral episome to heterochromatin and maintaining latency. The association of ORF59 with the methyltransferase site of PRMT5 prevents its association with the viral chromatin and reduces H4R3me2s enrichment while simultaneously increasing H3K4-me3 modifications on viral promoters [82]. Lastly, PAN

RNA has been shown to interact with the methyltransferase myeloid/lymphoid or mixed-lineage leukemia protein 2 (MLL2), which tri-methylates H3 at lysine 4 (H3K4-me3) and might promote viral reactivation [80]. As such, ORF59 and PAN RNA may assist in converting the viral heterochromatin to transcriptionally active euchromatin during lytic reactivation.

1.4.1 Immediate Early and Early Gene Products

RTA is the only viral IE gene product, and its expression is crucial to lytic viral replication. The potent viral transcription factor drives expression of all classes of lytic genes during infection [83] and is required for origin-dependent DNA replication of the viral genome [84,85]. The early gene product and transcription factor (TF) KSHV basic leucine zipper (K-bZIP), expressed from the *K8* gene, fine-tunes the lytic transcription program by interaction with RTA. K-bZIP functions as a co-factor and repressor of RTA [86,87] and modulates the transactivation activity of RTA to enhance expression of E and L genes while repressing expression of RTA. Thus, K-bZIP provides temporal control to lytic gene expression [83]. The abundantly expressed PAN RNA also plays a regulatory role during lytic reactivation and permits efficient viral gene expression. PAN RNA deficient viruses are not able to produce progeny virions and viral gene expression is reduced in the absence of PAN RNA [80]. The non-coding RNA binds the promoter regions of the viral episome and the cellular genome and might influence gene expression by recruiting transcription factors and histone methyltransferases or preventing promoter access [80,88].

Viral transcripts are synthesized in the host cell nucleus and are exported to the cytoplasm with the aid of the early gene product and RNA-binding protein ORF57. ORF57 interacts with viral transcripts and facilitates the nuclear export of intronless RNAs [89–91], protects protein-coding and non-coding RNAs from RNA decay [92,93], and enhances the translation of viral transcripts by mediating their splicing [94]. ORF57 enhances lytic gene expression at the post-transcriptional level and is required for efficient viral replication and virion production [95].

1.4.2 Immune modulation

Multiple early gene products serve to create an environment conducive for efficient viral replication. Type 1 interferons (IFNs) are cytokines produced in response to viral infection and constitute signaling pathways that induce a range of cellular processes involved in antigen presentation, induction of apoptosis, and inhibition of viral replication and gene expression. Cellular pattern recognition receptors (PRRs) sense viral DNA, RNA, and peptides, and activate interferon regulatory transcription factors (IRFs), such as IRF3 and IRF7, that transactivate the expression of type 1 IFNs. These type 1 IFNs then act in a paracrine and autocrine fashion and signal through various adaptors, such as the interferon-stimulated gene factor 3 (ISGF3), comprised of signal transducer and activator of transcription 1 (STAT), STAT2, and IRF9, to activate the expression of interferon-stimulated genes (ISGs) that encode antiviral effectors [96]. KSHV encodes four individual proteins with homology to cellular IRFs. These viral IRFs, vIRF1-4, interfere with type 1 IFN production and signaling by various mechanisms [97]. vIRF4, expressed from *ORF K10*, prevents the dimerization of the cellular IRF7 and subsequent transactivation of the IFN-α promoter, therefore reducing intracellular IFN levels [98]. Similarly, vIRF3, expressed from *ORF K10.5*, also targets IRF7 and interferes with its ability to bind and transactivate the IFN-α promoter [99]. Downstream of type 1 IFN production, vIRF2, expressed from *ORF K11*, inhibits the ISGF3 complex from transactivating interferon-stimulated response elements (ISREs) in the promoters of ISGs [100].

Other viral proteins that interfere with type 1 IFN signaling include the E gene product of *ORF45*, which inhibits the phosphorylation and nuclear localization of IRF7 and therefore inhibits type 1 IFN production [101]. The late gene product and tegument protein ORF52 binds and inhibits the sensor of viral cytosolic dsDNA cyclic GMP-AMP synthase (cGAS) and prevents the downstream activation of IRF3 and type 1 IFN production [102]. The early gene products and ubiquitin ligases K3 and K5 downregulate the expression of surface major histocompatibility complex (MHC) class I to prevent activation of innate immune effector cells [103,104]. Lastly, broad inhibition of host gene expression by a process termed host shutoff may also facilitate immune evasion and

allow for more efficient co-opting of the cellular replication machinery in favour of enhanced viral replication [105]. The viral shutoff and exonuclease (SOX), encoded from *ORF37* early during lytic viral replication, possesses endoribonuclease (RNase) and deoxyribonuclease (DNase) activity and facilitates the degradation of most host mRNAs in the cytoplasm [105,106]. Only 20% of cellular transcripts, such as the one encoding IL-6, are refractory to SOX-mediated host shutoff and accumulate normally during lytic replication [107,108]. SOX is site-specific and targets and cleaves mRNAs that contain adenine dimers or trimers [109] as well as stem loops or bulge structures [105]. The cleaved mRNAs then become substrates for the cellular exoribonuclease 1 (Xrn1), which mediates the decay of the cleaved transcripts and results in a global downregulation of cellular gene expression [105,110]. Virus mediated host shutoff may therefore provide KSHV with an additional mechanism for controlling the expression of type 1 IFNs and class I MHC.

1.4.3 Oncogenesis and Angiogenesis

Multiple lytic viral gene products contribute to oncogenesis and survival of infected cells [10]. vIRF1, expressed from *ORF K9*, downregulates the expression of the tumor suppressor protein p53 and the cyclin-dependent kinase inhibitor p21 to prevent cell cycle arrest and apoptosis in KSHV-infected cells [111–113]. vIRF3, the only vIRF also expressed in latently infected cells, is required for the proliferation and survival of KSHV-infected PEL cells. In vIRF3 knock-down body-cavity based lymphoma (BC-3) cells, caspases 3 and 7 are cleaved and infected cells undergo apoptosis [114]. KSHV also expresses a constitutively active G protein-coupled receptor (vGPCR, from *ORF74*) with homology to human IL-8 early during lytic replication [115,116]. vGPCR induces tumorigenesis and angiogenesis *in vitro* and *in vivo* [115] by signaling through the phosphoinositide-3 kinase (PI3K) and protein kinase B (Akt) pathway [116], and MAPK and p38 pathways [117] to activate NF-κB, activator protein 1 (AP-1) [118], vascular endothelial growth factor (VEGF) [117], and cyclooxygenase-2 (COX-2) [119] to promote the production of proinflammatory and angiogenic cytokines and chemokines [118]. K-bZIP and ORF45 directly and independently associate with and inhibit the transactivation

activity of the tumor suppressor p53 and potentially facilitate tumor persistence by preventing apoptosis of infected cells [120,121].

1.4.4 DNA Replication

Six E genes encode proteins that are directly involved in lytic DNA replication and include the viral DNA polymerase. During latency, genome replication is initiated from the viral TR and requires the host machinery, including the cellular DNA polymerase, to replicate the viral episome. By contrast, lytic DNA replication is initiated at two homologous lytic origins of replication (oriLyt), termed oriLyt-L and oriLyt-R, and the DNA is subsequently amplified by rolling circle replication using the viral DNA polymerase, ORF9. OriLyt-L is located between *ORFs K4.2* and *5* and is an inverted homolog of oriLyt-R, which is located about 50,000 bp away from oriLyt-L, between *ORFs 69* and *71* [84,122]. Efficient DNA replication relies upon cis- and trans-acting elements: both oriLyt sequences contain eight C/EBPα binding sites organized into four palindromes, two AT-rich palindromic sequences, an RTA response element (RRE), a TATA box, and three cyclic AMP response elements (CREs), all of which are required for efficient DNA replication [84,123]. The trans-acting factors required for DNA replication are RTA, K-bZIP, and the viral pre-initiation complex (vPIC) consisting of the viral DNA polymerase (ORF9), processivity factor (ORF59), helicase (ORF44), primase (ORF56), primase-associated factor (PAF, ORF40/41), and single-stranded DNA binding protein (SSB, ORF6). RTA and K-bZIP do not actively partake in genome replication but act as origin-binding proteins and allow DNA replication to initiate. K-bZIP is likely recruited to the C/EBPα binding sites through its interaction with C/EBPα, whereas RTA associates with the RRE directly. oriLyt-L/R contain a promoter that is RTA-inducible; transactivation of this promoter may license DNA replication and allow the vPIC to assemble on the DNA and commence genome replication [84,123].

1.4.5 Late Gene Expression

Continuous viral genome replication is necessary for L gene expression. The exact mechanism by which ongoing genome replication licenses L gene expression is unknown but may involve the maintenance of nuclear replication compartments that permit transcription from newly synthesized genomes. In addition to viral DNAs, these

replication compartments may also contain viral and cellular transcription factors needed for L gene expression or may exclude histones and other DNA-binding proteins that would otherwise render the DNA inaccessible to transcription factors. Blocking viral DNA replication leads to the dissolution of nuclear replication compartments and abolishes L gene expression [124]. L gene expression is regulated differently from early gene expression and requires a set of viral transcription factors that are conserved across all γ-herpesviruses. In KSHV, these transcription factors are encoded by *ORFs 66*, *31*, *18*, *30*, *34*, and *24* [125,126]. *ORF24* encodes a functional analog of the cellular TATA-binding protein (TBP) that binds the C-terminal domain repeats of the cellular RNA polymerase II (Pol II) [127] to recruit Pol II to viral L promoters and initiate gene expression [128]. ORF24 mutants that cannot bind Pol II are unable to induce L gene expression [128]. ORF34 is likewise required for L gene expression and acts as a scaffold to connect the viral TFs ORF66, 31, 18, 23, and 30 to ORF24 and Pol II and therefore promotes the assembly of a transcription-competent pre-initiation complex on viral L promoters [125,126].

1.4.6 Genome Packaging, Capsid Assembly, and Egress

Multiple L genes encode capsid, envelope, and tegument proteins that collectively make up progeny virus particles. The icosahedral capsid is composed of around 3,000 proteins and includes the major capsid protein (MCP, encoded from *ORF25*), which organizes into hexamers (hexons) or pentamers (pentons) to form the capsid structure. The protein products of *ORFs 62*, *26*, and *65* provide further structural support by cross-linking neighboring hexons and pentons. The small capsid protein (SCP, encoded from *ORF65*) joins adjacent MCP at their tips (called the floor), whereas the triplex, comprised of one Tri1 protein (encoded from *ORF62*) and two Tri2 proteins (encoded from ORF26), joins adjacent MCP at their base (called the tower) [129,130]. Capsid assembly is similar for all herpesviruses and takes place in the nucleus (Fig. 1). The KSHV scaffolding protein (SCAF, encoded from *ORF17.5*) assists in the assembly of a pro-capsid by forming a lattice upon which the MCP units are layered. As the initially spherical pro-capsid matures, it becomes angular and the SCAF protein is digested by the viral protease ORF17 and extruded from the capsid [131–133]. Three distinct types of mature capsids can

be recovered from herpesviruses: A, B, and C capsids. All mature capsids contain the capsid shell comprised of MCP, SCP, and triplexes. A-capsids only contain the capsid shell and lack the scaffolding protein and viral DNA. B-capsids contain the capsid shell, internal scaffold and the ORF17 protease, but lack DNA. C-capsids are the only capsids that give rise to infectious virions and contain the capsid shell and DNA, but no scaffolding protein [132]. Viral dsDNA head-to-tail concatemers are fed into pro-capsids through a portal ring that consists of 12 copies of the ORF43 portal protein [134,135] by action of an ATP-powered terminase complex thought to consist of ORF7, ORF29, and ORF67.5 [136,137]. The E protein ORF68 also assists genome packaging and forms a pentameric ring that might couple the terminase to the portal complex and cleave concatemeric DNA [138,139]. Herpesviruses, including KSHV, acquire their membrane glycoproteins and lipid envelope by budding into intracellular membranes. The egress mechanism is not fully understood and might involve an intermediary budding step through the nuclear membrane as well as transient acquisition of an envelope [140,141]. Inside the cytoplasm, the viral particles acquire a tegument layer that later forms the interface between the capsid and the envelope. Tegument proteins include ORFs 63, 64, and 45, and are involved in the intracellular transport of virus capsids during entry and egress, and mediate virion assembly by positioning the capsid at the Golgi network from which the lipid envelope will be acquired [142–144]. Of those, the outer tegument protein ORF45 is crucial to viral egress and mediates the transport of the mature capsids along microtubules by interaction with the cellular kinesin family member 3A (KIF3A) subunit of the kinesin-2 motor protein [145]. ORF45 also promotes budding by associating with membrane microdomains, called lipid rafts, of the Golgi network [141]. Finally, virus particles acquire their lipid envelope by budding into Golgi-derived vesicles and exit the cell by exocytosis [140,141] (Fig. 1). Release of infectious virions permits transmission to neighboring cells and facilitates spread.

1.5 Reactivation from Latency

RTA expression alone is sufficient to reactivate KSHV from latency and induce the expression of early lytic genes [35,146]. Viral and cellular factors co-operate with RTA to augment expression from the *ORF50* gene for sustained lytic replication [147,148].

Reactivation from latency is controlled by suppression of the *ORF50* promoter. Relief of this suppression or induction of *ORF50* expression facilitates the lytic switch. For instance, the DNA methyltransferase inhibitor 5-azacytidine removes suppressive CpG methylation from the *ORF50* promoter and permits RTA production [40]. The histone deacetylase inhibitor sodium butyrate (NaB) increases acetylation of histones H3 and H4 at the *ORF50* promoter and restructures the nucleosomes to free a binding site for the cellular transcription factors specificity protein 1 and 3 (Sp1/Sp3) that then transactivate *ORF50* [149,150]. The proto-oncogenic serine/threonine kinases proviral insertion in murine 1 (Pim1) and Pim3 phosphorylate LANA and prevent the LANA-mediated inhibition of transcription from *ORF50* to also relieve suppression of the *ORF50* promoter [151]. The *ORF50* promoter also contains binding sites for hypoxia-inducible factor-1α (HIF-1α), X-box binding protein 1 spliced (XBP1s), and AP-1, which are cellular transcription factors that can transactivate *ORF50* and facilitate KSHV reactivation [152–154]. HIF-1α is expressed in response to hypoxia and transactivates the *ORF50* promoter in co-operation with LANA [152]. XBP1s is produced during ER stress as part of the unfolded protein response (UPR) [155]. AP-1 expression is activated by multiple MAPKs, including extracellular signal-regulated kinases (ERKs), c-Jun N-terminal kinase (JNK), and p38, in response to the chemical 12-O-tetradecanoyl-phorbol-13-acetate (TPA) [154]. Aside from TPA, MAPK signaling pathways can also be induced by members of the Ras family of GTPases [156], co-infection with herpes simplex virus type 1 (HSV-1) [157], the reactive oxygen species (ROS) hydrogen peroxide (H_2O_2) [77], and the signaling molecule histamine [158], all of which reactivate KSHV from latency in BC-3, BCBL-1, or renal carcinoma iSLK.219 cell lines. Co-infection with other viruses, including HIV [159] and vesicular stomatitis virus (VSV), can also trigger the lytic switch by activating cellular signaling pathways, such as toll-like receptor (TLR) 7 and 8 signaling [160].

1.6 The Unfolded Protein Response

The following section 1.6 was adapted from the review titled "The bZIP Proteins of Oncogenic Viruses" [161].

The unfolded protein response (UPR) is a cellular stress response that responds to accumulation of unfolded proteins in the endoplasmic reticulum (ER), the site of

synthesis and folding of secreted and transmembrane proteins [162]. Nutrient deprivation, Ca^{2+} depletion, hypoxia, heart disease, diabetes and viral infection are all factors that can cause accumulation of unfolded proteins in the ER lumen and trigger stress responses [163]. Cells sense ER stress through the ER-resident transmembrane receptors inositol-requiring enzyme 1 (IRE1), protein kinase R-like endoplasmic reticulum kinase (PERK) and activating transcription factor 6 (ATF6) (Fig. 2). In the absence of ER stress, the luminal domains of IRE1, PERK, and ATF6 are bound by the cellular chaperone binding immunoglobulin protein (BiP), which represses activation of each of these sensors [164]. The dual function of BiP as a chaperone and repressor of the UPR sensors is controlled by a post-translational modification (PTM) that involves addition of adenosine monophosphate (AMP) to threonine 158 of BiP. This modification is carried out by the cellular protein adenylyltransferase FIC-domain-containing ER-localized enzyme (FICD) and is called AMPylation. BiP AMPylation reduces substrate binding affinity and switches BiP to a repressor of the UPR sensors. When unfolded proteins accumulate in the ER, FICD de-AMPylates BiP to increase substrate affinity and switch BiP to a chaperone [165]. As BiP becomes active as a chaperone, it dissociates from the stress sensors, therefore activating the UPR [166]. The UPR sensors may also respond to unfolded proteins directly, as IRE1 can become activated upon association with unfolded proteins [167]. The IRE1, PERK, and ATF6 arms of the UPR collectively function to increase the ER folding capacity and restore homeostasis. This includes mediating the degradation of unfolded proteins, upregulating chaperone synthesis, and enhancing lipid biogenesis. If ER stress cannot be resolved, the cell switches from an adaptive response to an apoptotic response [162].

1.6.1 The ATF6 Arm of the UPR

ATF6 is a constitutively expressed type II transmembrane protein that resides in the ER but undergoes ER-to-Golgi localization and proteolytic processing upon ER stress sensing and activation [168,169]. In the ER, ATF6 exists as dimers stabilized by interchain disulfide bonds formed between cysteines at amino acid (aa) positions 467 or 618 in the luminal domain of ATF6 [170,171]. Under normal physiological conditions, BiP associates with the luminal domain of ATF6 and sequesters ATF6 in the ER by masking its Golgi

Figure 2. **The unfolded protein response responds to ER stress to restore homeostasis.** The UPR transmembrane sensors PERK, IRE1, and ATF6 are suppressed by the ER chaperone BiP in the absence of ER stress. When unfolded proteins accumulate in the ER lumen, BiP dissociates from the sensors to assist in protein folding, thereby activating the UPR. The kinase PERK oligomerizes, autophosphorylates, and phosphorylates translation initiation factor eIF2α, which attenuates global translation. Transcripts containing 5' uORFs, such as the *ATF4* transcript, are preferentially translated when eIF2α is phosphorylated. Translation of the *ATF4* transcript yields the bZIP transcription factor ATF4, which induces genes involved in restoring homeostasis and regulating apoptosis. The ribonuclease IRE1 oligomerizes, is phosphorylated, and excises an intron from the *xbp1* transcript. Excision of the intron results in a frameshift that allows expression of the bZIP XBP1s, which induce the expression of BiP and genes involved in ERAD. ATF6 is shipped to the Golgi and proteolytically processed by proteases S1P and S2P to liberate its N-terminus, ATF6-N, which is a bZIP transcription factor that induces genes encoding *xbp1* and chaperones, including BiP.

Figure 2. **The unfolded protein response responds to ER stress to restore homeostasis.**
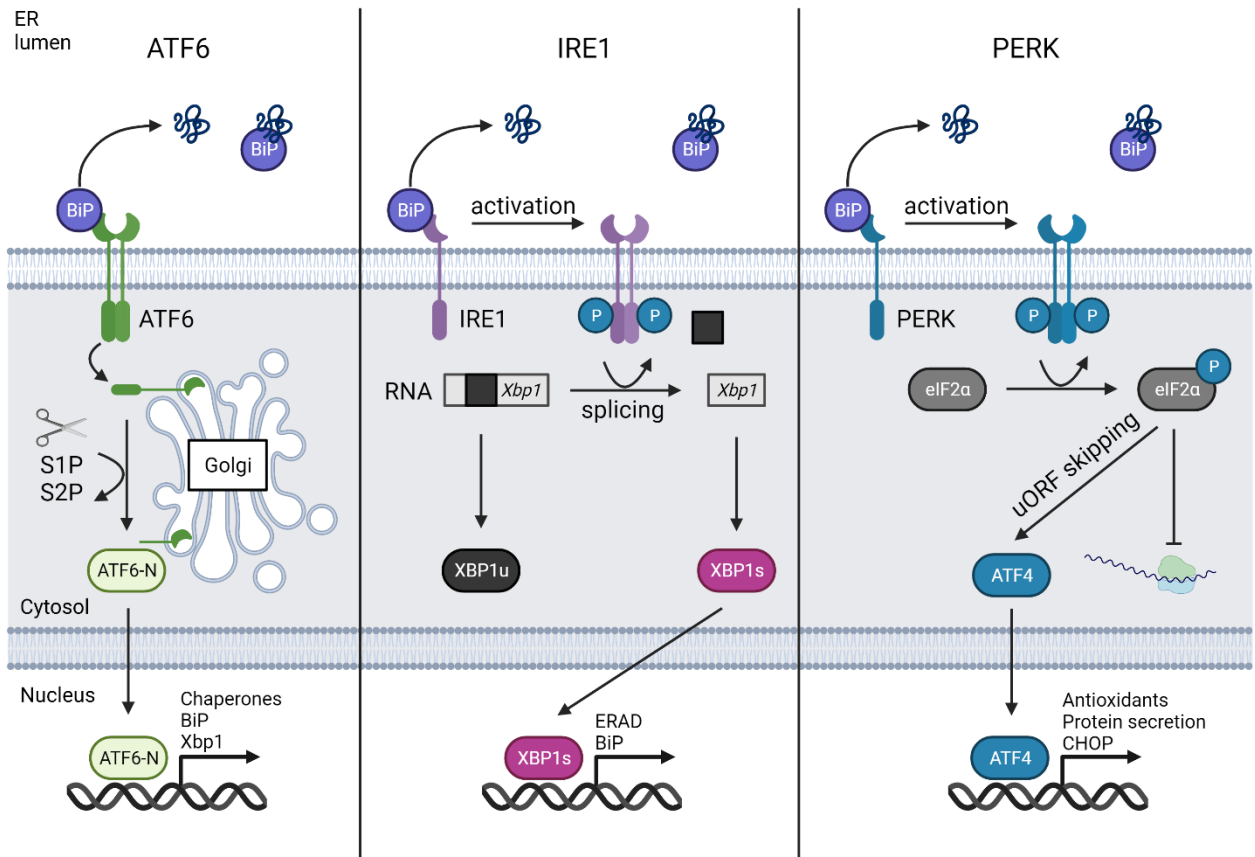
localization signals (GLS) [172]. Upon induction of ER stress and BiP dissociation, these GLS become unmasked, but the ER-resident oxidoreductase ER protein 18 (ERp18) retains ATF6 in the ER until ATF6 dimers are successfully reduced to monomers [170]. Monomers are then transported to the Golgi in coat protein II (COPII)-coated vesicles [173]. The Golgi-resident serine proteases 1 and 2 (SP-1 and SP-2) cleave the luminal domain of ATF6 near aa 418 and in the adjacent transmembrane domain in a two-step process to remove the C-terminal portion of the protein and release the 373 aa N-terminal portion that represents the transcriptionally active ATF6-N [169]. ATF6-N localizes to the nucleus and induces or upregulates the expression of genes encoding the chaperones BiP, glucose-related protein 94 (GRP94), calreticulin, and protein disulfide isomerases (PDIA) 4 and 6 [174] (Table 1). Some of the protein products of ATF6-N target genes, including the TF XBP1s, the DNA J domain-containing (DnaJ) family of co-chaperones and the ER degradation enhancing alpha-mannosidase like protein (EDEM) family, are involved in mediating ER-associated degradation (ERAD) of unfolded or misfolded proteins [174]. As such, ATF6 is pivotal to the proper folding or degradation of excess proteins during ER stress. ATF6-N also increases ER folding capacity by transactivating genes whose protein products participate in the synthesis of lipids and fatty acids that increase ER surface area. Indeed, lipotoxic stress can activate ATF6 in a BiP-independent manner and represents a pathway for ATF6 activation in the absence of ER stress [175]. ATF6 mounts a rapid response to ER stress and localizes to the Golgi as soon as 30-45 minutes following activation [170]. The ATF6-N-mediated response to ER stress is controlled - and perhaps limited - by a half-life of only about 40 minutes [176]. The N-terminus of ATF6 contains a short 8 aa sequence with 75% aa homology to the VN8 region of the HSV viral protein 16 (VP16). The VN8 sequence renders VP16 and ATF6 susceptible to rapid, proteasomal degradation [177]. ATF6 is also a substrate of ERAD and can be degraded in a SEL1-dependent manner that requires the C-terminal, luminal domain of ATF6 [176].

1.6.2 The IRE1 Arm of the UPR

The IRE1 arm is the sole arm that governs the UPR in budding yeast [178]. IRE1 is a type I transmembrane serine/threonine kinase and RNase that resides in the ER. In mammals, two genes encode the homologues IRE1α and IRE1β. Both proteins contain

Table 1. **Promoters of ATF6-N and XBP1s target genes contain conserved transcription factor binding sites.** ATF6-N and XBP1s can recognize and bind ERSE-I, ERSE-II, UPRE, and UPRE-II sequences with different affinities. ERSE-I, ERSE-II, and UPRE-II contain 5'-CCAAT-3' sites that facilitate binding of NF-Y, which is required for ATF6-N and XBP1s binding to the downstream 5'-CCACGT-3' or 5'-CCGCGT-3' [186,187]. NF-Y binding is not required for XBP1s binding to ERSE-II and UPRE-II [187]. The promoters of some UPR-sensitive genes, such as *HSPA5*, *HERPUD1*, and *CHOP*, can be induced by ATF6-N, XBP1s, and ATF4 [174,188–192].

Table 1. **Promoters of ATF6-N and XBP1s target genes contain conserved transcription factor binding sites.**

DNA-binding Motif	Consensus Sequence (5'-3')	Contained in Gene	Transcription Factor Binding	NF-Y Dependency	
				XBP1s	ATF6-N
ERSE-I	CCAAT-N$_9$-CCACG	*HSPA5* (x3) (BiP), *CALR* (x2), *XBP1*, *PDIA4* (x2), *SYVN1* (x2) (HRD1), *DDIT3* (CHOP), *HSP90B1* (x3), *HYOU1*, *HERPUD1* (x2)	ATF6-N > XBP1s	Yes	Yes
ERSE-II	ATTGG-N$_1$-CCACGT	*SYVN1* (HRD1), *HYOU1* (reverse), *HERPUD1*	XBP1s > ATF6-N	No	Yes
UPRE-II (ERSE-II-like)	ATTGG-N$_1$-CCGCGT	*SYVN1* (HRD1)	XBP1s > ATF6-N	No	Yes
UPRE (CRE-like)	TGACGTG(G/A)	*PDIA4* (x2) (reverse), *HYOU1*, *EDEM1*	XBP1s/ATF6-N, XBP1s, ATF4?	N/A	N/A
CRE	TGACGTCA	*SYVN1* (HRD1), *HSPA5* (BiP)	ATF4, XBP1s? ATF6-N?	N/A	N/A
XBP1s binding Motif	GCCACGT	*PDIA4*, *SYVN1* (HRD1), *HYOU1* (reverse), *HERPUD1*	XBP1s	N/A	N/A
AARE	(R/T)TT(G/T)CRTCA TGATG(C/A)AA	*DDIT3* (CHOP), *HERPUD1*	ATF4	N/A	N/A

conserved domains and carry out conserved functions to regulate the UPR, but IRE1α is expressed in all cell types whereas IRE1β is only expressed in intestinal epithelial cells [179–183]. IRE1α (from here on called IRE1 for simplicity) dimerization and phosphorylation is required for its activation in response to ER stress [167,179,181,182,184]. Unfolded or misfolded proteins might also contribute to IRE1 activation by binding an MHC-like peptide binding groove in the luminal domain of IRE1 [167,185]. In the absence

of ER stress, BiP is recruited onto the luminal domain of IRE1 by the co-chaperone endoplasmic reticulum-localized DnaJ protein 4 (ERdj4) and represses IRE1 activation and RNase activity by promoting IRE1 monomerization [193,194]. BiP dissociation permits the formation of back-to-back dimers of IRE1 where the kinase active sites of the individual monomers face and phosphorylate each other to generate RNase-competent IRE1 complexes [184,195]. Phosphorylation of the activation loop located in the kinase domain is critical to conferring RNase function [183]. Activated IRE1 oligomers utilize their C-terminal, cytoplasmic RNase domains to excise an intron from the yeast *Hac1* transcript and its mammalian homologue *Xbp1* in a spliceosome-independent manner [155,178]. Conventional RNA splicing is a multi-step process that relies on several small nuclear RNAs (snRNAs) and proteins working in concert. Canonical introns contain conserved 5' and 3' flanking sequences, as well as an intronic branch point containing a critical A nucleotide. During conventional splicing, the ribonucleoprotein complexes assemble on the intron and cleave and attach the 5' splice site (SS) to the branch point A to generate a branched intermediate known as the lariat. The 5' SS and 3' SS are then joined, the lariat is removed, and the splice sites are re-ligated to generate a spliced transcript [196]. By contrast, the IRE1-mediated splicing of *Hac1/Xbp1* only requires two enzymes: IRE1 and a cellular tRNA ligase. IRE1 recognizes two stem-loops in the *Hac1/Xbp1* transcript and cleaves each loop once to excise a 252/26-nt intron. The tRNA ligase then re-joins the resulting fragments [155,178,197,198]. *Hac1/Xbp1* is not the only target of IRE1-mediated splicing; IRE1 dimers can also cleave other RNAs by regulated IRE1-dependent decay (RIDD) to reduce the number of transcripts that need to be translated and polypeptides that need to be folded in the ER [199,200].

Xbp1 splicing results in a frameshift that produces the TF XBP1s upon translation [155]. XBP1s induces or upregulates the expression of ERAD genes and chaperones in co-operation with ATF6-N to maximize protein folding and reduce the burden on the ER folding machinery [174,189]. Additionally, XBP1s co-ordinates the expression of secretory (*Sec*) genes whose protein products constitute the COPII ER to Golgi trafficking pathway and mediate lipoprotein secretion in the liver. XBP1s not only responds to ER stress but also nutrient availability, because it promotes COPII-mediated lipoprotein secretion when nutrients are abundant and suppresses the COPII pathway when nutrients are limited [201]. Unspliced *Xbp1* produces the truncated XBP1u that shares its N-terminus with XBP1s, but not its C-terminus. XBP1u is not a transcriptional activator but plays an important role in restoring homeostasis by binding and destabilizing XBP1s and ATF6-N and targeting them for degradation by the proteasome during the resolution phase of ER stress [202,203].

1.6.3 The PERK Arm of the UPR

PERK, like IRE1, is a type I transmembrane serine/threonine kinase that becomes activated upon oligomerization and autophosphorylation [204,205]. BiP and the cellular chaperone GRP94 bind the N-terminal luminal domain of PERK and prevent its activation, possibly by keeping PERK in a monomeric or dimeric state and preventing oligomerization [204]. Upon BiP and GRP94 dissociation, PERK forms kinase-competent oligomers that phosphorylate the eukaryotic translation initiation factor 2 subunit alpha (eIF2α) to attenuate global translation and stall cell cycle progression [204,206]. Misfolded proteins may also promote PERK oligomerization and activation by engaging with a peptide binding groove located in the luminal domain of PERK and tethering adjacent PERK dimers together [167,207]. PERK, like IRE1, forms back-to-back dimers, but unlike IRE1, the C-terminal kinase activation loops of the PERK monomers face away from each other. PERK phosphorylation might therefore be achieved by adjacent dimers phosphorylating each other once they have assembled into oligomers. Upon phosphorylation, the unstructured kinase activation loop of PERK becomes ordered and binds eIF2α [205]. eIF2α is a subunit of the GTP-bound eIF2 protein complex that together with the initiator methionyl-tRNA (Met-tRNA$_i$) and the 40S small ribosomal subunit

forms the 43S pre-initiation complex (PIC). The PIC initiates translation by scanning mRNAs for the AUG start codon and recruiting the 60S large ribosomal subunit. Once the AUG has been identified, the PIC locks onto the mRNA, the GTP bound to eIF2 is hydrolyzed to GDP, and eIF2 is released. To begin another round of translation initiation, eIF2-GDP needs to be re-cycled to eIF2-GTP by the guanine nucleotide exchange factor eIF2B [208]. eIF2α makes direct contact with the α, β, and δ subunits of eIF2B during the exchange. Phosphorylation of eIF2α at serine 51 stabilizes the interaction between eIF2 and eIF2B and prevents the re-cycling of eIF2-GDP to eIF2-GTP, thereby preventing the assembly of another PIC [209]. By phosphorylating eIF2α, PERK inhibits global translation and relieves the burden on the ER folding machinery during ER stress. The kinases protein kinase double-stranded RNA-dependent (PKR), general control non-derepressible-2 (GCN2), and heme-regulated inhibitor (HRI) are activated by diverse stresses and likewise phosphorylate eIF2α and represent a complex and versatile machinery to control translation [210].

Not all mRNA translation is attenuated while eIF2α is phosphorylated. Translation of the *Atf4* transcript is upregulated when eIF2-GTP is limited and produces the TF ATF4 [211]. The 5' UTR of the *Atf4* transcript contains two short upstream ORFs (uORFs), uORF1 and uORF2, that regulate translation of the downstream ORF that encodes ATF4. uORF2 overlaps with the coding region of ATF4. As such, the ATF4 coding region cannot be translated when uORF2 is translated and vice versa. *Atf4* translation begins when the scanning PIC encounters the uORF1 start codon and the 80S ribosome assembles for translation. Once uORF1 has been translated, the 80S ribosome disassembles and the 40S subunit resumes scanning until it finds the next start codon. When eIF2-GTP levels are high, the 40S ribosome may acquire eIF2-GTP before it reaches the uORF2 start codon, the PIC assembles, and uORF2 is translated. When eIF2-GTP is low, the 40S ribosome may not acquire eIF2-GTP before it reaches the uORF2 start codon and resumes scanning without translating uORF2. If the ribosome then acquires eIF2-GTP before it reaches the start codon of the ATF4 coding region, the *Atf4* transcript is successfully translated and ATF4 is made [212]. ATF4 is at the center of responses to ER stress, hypoxia, infection, and amino acid starvation [210] and responds by inducing the expression of gene products involved in protein folding, amino acid

metabolism [191,211,213,214] autophagy [215,216], and tumor progression and survival [217]. The ATF4 target and TF C/EBP homologous protein (CHOP) governs cell fate by balancing between autophagy, apoptosis, and ER stress resolution. CHOP and ATF4 cooperatively induce the expression of autophagy genes and promote cell survival by increasing the metabolite recycling capacity of the cell [215,218]. Prolonged ER stress and CHOP expression shift the balance from a pro-survival to an apoptotic response, which is coordinated by CHOP and its binding partner C/EBPβ [219] through multiple mechanisms [220]. On the other hand, the CHOP-inducible growth arrest and DNA damage-inducible protein 34 (GADD34) promotes recovery from ER stress and protects from apoptosis by recruiting the protein phosphatase 1 α (PP1α) that then de-phosphorylates eIF2α and allows protein translation to resume normally [221,222].

Together, the ATF6, IRE1, and PERK arms facilitate a coordinated response to ER stress and increase the ER folding capacity by attenuating global translation, promoting mRNA and protein turnover, maximizing protein folding, and increasing lipid biosynthesis to restore the cell to homeostasis. The UPR controls cell fate in response to a variety of stimuli and may initiate apoptotic programs if the stress cannot be resolved.

1.7 The Basic Leucine Zipper Family of Transcription Factors

The following section 1.7 was adapted from the review titled "The bZIP Proteins of Oncogenic Viruses" [161].

The UPR-governing TFs ATF6-N, XBP1s, ATF4, and CHOP are all members of the dimer-forming family of basic leucine zipper (bZIP) TFs. bZIPs are eukaryotic DNA-binding proteins that regulate gene expression programs that govern cell proliferation, apoptosis [223,224], response to ER stress, homeostasis [162], and long-term memory [225]. All bZIP TFs contain two common structural motifs: an α-helical leucine zipper (ZIP) dimerization domain, and a DNA-binding domain rich in basic amino acid (aa) residues (Fig. 3 & 4). The leucine zipper is 60–80 aa in length and organizes into repeats of seven aas (heptad repeats) that contain highly conserved leucines at every seventh position throughout the domain [226]. Each heptad repeat spans two α-helical turns, allowing ZIP domains to form homodimers or heterodimers with adjacent ZIP-helices through hydrophobic interactions between leucines in the 'd' positions and other, commonly

hydrophobic residues in the 'a' positions. Formation of salt bridges between charged aas in the 'e' and 'g' positions further stabilize dimer formation. The interaction between two monomers forms a coiled-coil structure [227]. The DNA-binding domain is located adjacent to the ZIP domain [228] and is connected to the first heptad repeat of the leucine zipper by a short hinge region. The DNA-binding domain, also called the basic domain, makes direct contact with specific DNA sequences known as response elements (REs) and provides transactivation specificity. This domain comprises highly conserved basic amino acid residues that stabilize DNA-protein interactions [226].

bZIPs organize into multiple families and subfamilies that evolved from common ancestors by diversification and gene duplications. Vertebrates contain the most diverse bZIPs and include the Jun, Fos, ATF, musculoaponeurotic fibrosarcoma (Maf), old astrocyte specifically induced substance (OASIS), CRE-binding protein (CREB), and C/EBP subfamilies of bZIPs [229]. A well-studied example of a heterodimeric bZIP TF is the AP-1 complex, which is commonly depicted as consisting of one c-Jun and one c-Fos monomer that together form a heterodimer. The AP-1 complex not only forms between members of the Jun and Fos families of bZIP proteins, but can also comprise members of the ATF, and Maf families of bZIPs [223]. bZIP assembly into homo- and heterodimers controls sequence-specific DNA binding [228,230]. For example, ATF homodimers bind the 5'-TGACGTCA-3' CREs and Maf family homodimers recognize 5'-TGCTGAC(G)TCAGCA-3' Maf response elements (MAREs), whereas ATF/Maf heterodimers recognize a hybrid 5'-TGCTGACGTCA(C/T)-3' motif that shares sequence similarities with both CREs and MAREs. Jun homodimers bind 5'-TGA(G/C)TCA-3' TPA response elements (TREs), and ATF4 homodimers recognize CREs, whereas Jun/ATF4 heterodimers bind both TREs and CREs [230]. Divergent bZIP proteins can bind common REs: for example, CREs are bound by ATFs, but also by CREB family members [225]. Heterodimer formation is ubiquitous between and within all families of bZIP proteins. The C/EBP family of bZIPs comprises six members (C/EBP-α, -β, -γ. -δ, -ε, and CHOP) that recognize 5'-(A/G)TTGCG(T/C)AA(T/C)-3' DNA consensus sites, called CAAT boxes [231]. C/EBPs do not participate in the formation of AP-1 complexes but can form homodimers or heterodimerize with other C/EBP family members, or with ATF, Jun, Fos, and Maf family members [232–234]. CREB family members also do not

Figure 3. **Structure of the c-Jun/c-Fos heterodimer.** The c-Jun/c-Fos complexes bind DNA as heterodimers. Each bZIP protein contains a leucine zipper (ZIP) and adjacent basic (b) DNA-binding domain that together constitute the bZIP domain. The ZIP domain organizes into heptad repeats with amino acid residues denoted as positions a–g. Hydrophobic interactions (black arrows) between a (blue) and d (red) residues and electrostatic interactions (dotted arrows) between g and e residues stabilize dimer formation) [161].

Figure 3. **Structure of the c-Jun/c-Fos heterodimer.**

Figure 4. **Sequence alignment of viral and human bZIPs.** Amino acid sequences were obtained from the National Center for Biotechnology Information (NCBI) gene database and from the UniProt Knowledgebase. Colored residues represent consensus (red and gray) or basic (blue) amino acids. The viral bZIPs Zta, K-bZIP, MEQ, HBZ, and NS4B are expressed by the viruses Epstein-Barr virus, Kaposi's Sarcoma associated herpesvirus, Marek's disease virus, human T-lymphotropic virus, and hepatitis C virus, respectively. NCBI Accession Numbers: c-Jun NP_002219.1; c-Fos NP_005243.1; C/EBPα AAC50235.1; CHOP NP_001181982.1; CREB1 NP_001358356.1; NFIL3 NP_001276928.1; XBP1s NP_001073007.1; ATF4 NP_001666.2; ATF6α NP_031374.2; ATF6β NP_004372.3; Zta YP_401673.1; K-bZIP AAD21530.1; MEQ AFU65791.1; HBZ BAX35088.1; NS4B PRO_0000037526 [161].

Figure 4. **Sequence alignment of viral and human bZIPs.**

```
bZIP              ------basic domain------ -----------ZIP domain------------

                                           abcdefgabcdefgabcdefgabcdefg

      c-Jun    251-ERIKAERKRMRNRIAASKCRKRKL ERIARLEEKVKTLKAQNSELASTANMLREQVAQLKQ-310
      c-Fos    136-EEEKRRIRRERNKMAAAKCRNRRR ELTDTLQAETDQLEDEKSALQTEIANLLKEKEKLEF-195
      C/EBPα   281-NSNEYRVRRERNNIAVRKSRDKAK QRNVETQQKVLELTSDNDRLRKRVEQLSRELDTLRGIFRQLPE-347
      CHOP     128-RKQSGHSPARAGKQRMKEKEQENE RKVAQLAEENERLKQEIERLTR-173
Cellular CREB1  268-AARKREVRLMKNREAARECRRKKK EYVKCLENRVAVLENQNKTLIEELKALKD-320
      NFIL3     72-KDAMYWEKRRKNNEAAKRSREKRR LNDLVLENKLIALGEENATLKAELLSLKL-124
      XBP1s     69-PEEKALRRKLKNRVAAQTARDRKK ARMSELEQQVVDLEEENQKLLLENQLLREKTHGLVVENQELRQ-135
      ATF4     277-KLDKKLKKMEQNKTAATRYRQKKR AEQEALTGECKELEKKNEALKERADSLAKEIQYLKD-336
      ATF6α    305-AVLRRQQRMIKNRESACQSRKKKK EYMLGLEARLKAALSENEQLKKENGTLKRQLDEVVSENQRLKV-371
      ATF6β    323-KLLKRQQRMIKNRESACQSRKKKK EYLQGLEARLQAVLADNQQLRRENAALRRRLEALLAENSELKL-389

      Zta      171-CDSELEIKRYKNRVASRKCRAKFK QLLQHYREVAAAKSSENDRLRLLLKQMCP-223
      K-bZIP   162-CDQSHSPTRKQGRYGRVSSKAYTR QLQQALEEKDAQLCFLAARLEAHKEQIIFLRDMLMR-221
Viral MEQ       46-EKQKLERRRKRNRDAARRRRRKQT DYVDKLHEACEELQRANEHLRKEIRDLRTECTSLRV-105
      HBZ      132-QERRERKWRQGAEKAKQHSARKEK MQELGIDGYTRQLEGEVESLEAERRKLLQEKEDLMG-191
      NS4B       1-SQHLPYIEQGMMLAEQFKQ KALGLLQTASRQAEVITPAVQTNWQKLEV-48
```

L – heptad repeat dimerization contact residue 'd'

N/**R** – DNA-binding residue

K/R/H – basic residues

A/N – other conserved residues

participate in the formation of AP-1 complexes and prefer to heterodimerize with members of their own family or with ATFs [230,233]. Heterodimer formation not only controls RE recognition and binding affinity, but also affects function. C/EBP/c-Jun heterodimers can bind a hybrid TRE and CAAT box with a higher affinity than C/EBP homodimers. C/EBP/c-Jun and C/EBP/c-Fos heterodimers also potently drive monocyte differentiation in mouse bone marrow mononuclear cells compared to weaker C/EBP homodimers and c-Jun/c-Fos heterodimers [235]. Together, these studies of bZIP complexes have reinforced the idea that heterodimer formation diversifies the transcriptional output of bZIP TFs.

1.7.1 Cross-talk Between the Three Arms of the UPR

The UPR comprises three distinct arms, yet XBP1s, ATF6-N, and ATF4 induce overlapping sets of target genes. For instance, all three transcription factors can drive the expression of UPR target genes *HSPA5* (encoding BiP), homocysteine-inducible ER protein with ubiquitin-like domain 1 (*HERPUD1)*, and *DDIT3* (encoding CHOP) [174,188–192]. This cross-talk can be attributed to the propensity of these TFs for binding similar DNA motifs, as well as the presence of multiple different motifs in a single promoter (Fig. 5). The motifs that facilitate TF binding to most UPR-sensitive targets are well characterized and constitute the 5'-CCAAT-N9-CCACG-3' ERSE-I [188], the 5'-ATTG-N-CCACG-3' ERSE-II [236], the CRE-like 5'-TGACGTG(G/A)-3' UPRE [237], and the ERSE-II-like 5'-ATTG-N-CCGCG-3' UPRE-II [238] (Table 1). The ERSE-I is a bipartite sequence that contains a 5'-CCAAT-3' nuclear factor Y (NF-Y) binding site and a 5'-CCACG-3' ATF6-N and XBP1s binding site separated by a 9 bp spacer. NF-Y binding is required to facilitate ATF6-N and XBP1s binding to the adjacent 5'-CCACG-3' [155,186]. The ERSE-II is similar to the ERSE-I in that it also contains an NF-Y binding site, albeit inverted, and a 5'-CCACG-3' ATF6-N and XBP1s binding site separated by a one nucleotide spacer. ATF6-N and XBP1s induce this ERSE-II by binding the 5'-CCACG-3' portion on one strand, whereas NF-Y presumably binds the 5'-CCAAT-3' portion on the complementary strand [236]. XBP1s is more NF-Y independent than ATF6-N and can bind the ERSE-II and UPRE independently of NF-Y [187]. UPRE-II is nearly identical to ERSE-II and only differs from ERSE-II in that the highly conserved A in the

Figure 5. **Promoters of UPR target genes contain multiple transcription factor binding sites.** The *HSPA5*, *CALR*, *HERPUD1*, and *HYOU1* promoters all contain ERSE-I elements and are ATF6-N- and XBP1s-inducible. The *HERPUD1* and *HYOU1* promoters also contain ATF6-N- and XBP1s-indubible ERSE-II elements. The Additionally, the *HERPUD1* promoter contains an XBP1s binding site, and an AARE that can be bound by ATF4. The *HYOU1* promoter contains a UPRE that can be induced by ATF6-N and XBP1s heterodimers. The *HPSA5* also promoter contains a CRE-like sequence that can be bound by ATF4.

Figure 5. **Promoters of UPR target genes contain multiple transcription factor binding sites.**

HSP A5 (-161)-AGTGACGTTTATTGCGGAGGGGGGCCGCTTCGAATCGGCGGCGGGGCCAGCTTGGTGGCCTGGGCCAATGAACGGGCCTCCAACG

CRE-like   ERSE-I   ERSE-I

AGCAGGGGCCTTCACCAATCGGCGGCGGCCTCCACGACGGGGGCTGGGGGAGGGGTATATAAGCCGAGTAGGCGACGGGTGAGG-(-1)-

ERSE-I   TATA

CALR (-219)-CGCCGTGGTCGACCATCATTGGTCGGTGGTGAGGCCAATAGAAATCGGCCATCTGGGAACCCAGCGTTCCGAGGGCGCAGCCTAA

ERSE-I   ERSE-I

CATAGTGAACCGACGAAGGTCCAATGGAAAAAGACGGCCATAGACCAATGACAAAGTGGCAGGGGGGGCGGGCCCAA-(-55)-

ERSE-I   SP1

HERPUD1 (-180)-GGGTTGCATCAGCCCGTGCCGCCGTGCCGCCACGTGCTCGGTCGGTCCGCCCTCTGCCACCGGATCCGGACGCCGATTGGCCACGTTGGGAG

AARE   XBP1s   ERSE-II

AGTGCCTCGCCTCAGCCAATGGGCGGCAGCCACAGAGCGTTCTGTCCGCAGAGCGGGGCGCGGGGGCTTCTATAAAAGG-(-20)-

ERSE-I   TATA

HIYOU1 (-191)-CGTTGACGTGGTCCAATCCCAGGCCGACGCGCCGGCTGCTTCTGCCAACCGGTGGTCCCTCCGCGCCGCCCATTACAAGGCT

UPRE   ERSE-II   ERSE-I

GGCAAAGGGAGGGGGGCGGGGGGGCCTGGGAGGTGGTCCAATGAGTACCGCGCCGGG-(-52)-

ERSE-I

34

5'-CCACG-3' ATF6-N and XBP1s binding site is substituted for a G. This A to G substitution abolishes ATF6-N binding but permits NF-Y independent XBP1s binding. To date, the *SYVN1* promoter is the only identified mammalian promoter that contains an UPRE-II [238]. The 5'-TGACGTG(G/A)-3' UPRE is an element that only differs from the classical 5'-TGACGTCA-3' CRE in its last two nucleotides but maintains the 5'-TGACGT-3' core sequence. The UPRE was initially discovered through artificial selection of ATF6-N binding sites from a pool of synthetic oligonucleotides [237], but has since been identified in the mammalian promoters of some ERAD genes, such as *EDEM1* [239] (Table 1). XBP1s binds ERSE-II, UPRE, and UPRE-II with a higher affinity than ATF6-N [187] and transactivates a larger pool of genes [174]. By contrast, ATF6-N has a higher affinity for ERSE-I than XBP1s [187] and also responds to lipotoxic stress and induces the expression of lipid metabolism genes besides its classical chaperone targets [175]. ATF6-N has a very low affinity for the UPRE and only binds the UPRE when overexpressed or when heterodimerized with XBP1s [187,239]. Therefore, the primary function of ATF6-N might be the induction of *xbp1*, chaperone genes, and lipid synthesis genes early during ER stress, and may then shift to assisting in the induction of ERAD genes once enough XBP1s has been made to allow for the formation of XBP1s/ATF6-N heterodimers [239,240].

The minimal sequence required to facilitate XBP1s binding to a promoter is 5'-ACGT-3' as identified by chromatin immunoprecipitation sequencing (CHiP-seq) [241]. This sequence constitutes the core of the ERSE-II and UPRE but is also partially present in the ERSE-I and UPRE-II (Table 1, yellow highlights). Such a 5'-ACGT-3' core sequence is contained in the human and mouse promoter of the DnaJ Heat Shock Protein Family (Hsp40) Member B9 (*DNAJB9*) gene (encoding ERdj4) and can be bound and induced by XBP1s to drive optimal gene expression [242]. Interestingly, XBP1s can reactivate KSHV from latency by transactivating the *ORF50* promoter from a 5'-ACGT-3' binding motif located within 200 bp of the ATG start codon [153,243].

ATF4 has not been suggested to bind ERSE-I, ERSE-II, and UPRE-II, but binds CRE elements and may therefore also bind the CRE-like UPRE. Indeed, early research identified a cis-acting element in the rat *HSPA5* promoter that facilitates human ATF4

binding and permits ATF4 to transactivate *HSPA5* expression. In rat, this ATF4 binding element has a sequence of 5'-TGACGTGA-3' and is therefore identical to the UPRE [190]. ATF4 can also induce expression from the human *HSPA5* promoter [192], in which the corresponding sequence is 5'-TGACGTTT-3' (Fig. 5), which retains the 5'-TGACGT-3' core of CRE-like elements [237]. As mentioned, ATF4 is responsive to amino acid starvation in addition to ER stress because the kinase GCN2 is activated in response to nutrient deprivation and, like PERK, phosphorylates eIF2α and leads to the uORF dependent translation of the *ATF4* transcript [244]. To respond to both ER stress and amino acid starvation, ATF4 induces the expression of *DDIT3*, amino acid metabolism genes, such as the *ASNS* gene encoding asparagine synthetase, and genes whose products maintain proteostatic homeostasis, such as the chaperone BiP and protein disulfide isomerases [211]. ATF4 induces expression of some targets, including *HERPUD1*, an ERAD gene, sodium-dependent neutral amino acid transporter-2 *(SNAT2)*, a gene encoding an amino acid transporter, and *DDIT3* by binding amino acid response elements (AAREs) that constitute composite C/EBP/ATF sites with a consensus of 5'-(R/C)TT(R/T)CRTA-3' where R denotes a purine [191,214,245]. Additionally, some promoters, including those found in the *DDIT3*, *SNAT2*, *ATF3*, and asparagine synthetase (*ASNS)* genes, also contain AAREs with a consensus sequence of 5'-TGATG(G/A)(G/A)AH-3', where H denotes any nucleotide that is not a G [215]. These AAREs are functionally and structurally related. The *DDIT3* AAREs have a sequence of 5'-ATTGCATCA-3' and 5'-TGATGCAAT-3', which are complementary to one another and constitute a 5'-TGATG-3' ATF4 half-site and a 5'-CAAT-3' C/EBP half site [215,245]. The affinity with which ATF4 binds AARE sites is altered by heterodimerization or multimeric complex formation with its bZIP binding partners. For instance, the ATF4-mediated induction of the *DDIT3* 5'-ATTGCATCA-3' AARE is increased when ATF2, another bZIP that responds to amino acid starvation, is activated. *DDIT3* expression is therefore higher during amino acid starvation than ER stress [246]. ATF4 heterodimerization with C/EBPα, CHOP, or C/EBPβ liver-enriched activating protein (LAP), a truncated isoform of C/EBPβ derived by alternate splicing, promotes the activation of AARE-containing genes, whereas complex formation with ATF3 or C/EBPβ liver-enriched inhibitory protein (LIP), a truncated and dominant negative

isoform of C/EBPβ, represses or inhibits activation from AAREs. As such, the time-sensitive and stimulus-dependent expression of ATF4 binding partners provides precise and directed transcriptional control in response to ER stress, amino acid depletion, and other stresses that induce ATF4 expression to coordinate a transcriptional response that is tailored to the specific stress pathway [213–215,247].

1.7.2 Viral bZIP TFs and their Functions

The following section 1.7.2 was adapted from the review titled "The bZIP Proteins of Oncogenic Viruses" [161].

Through millennia of co-evolution with their hosts, many viruses have acquired host genes that evolve further when mutations that optimize viral fitness are fixed in the genome [248]. Some viruses have evolved to encode their own bZIP transcription factors. To date, viral bZIPs have been identified in the human oncoviruses EBV, KSHV, human T-lymphotropic virus 1 (HTLV-1), and hepatitis C virus (HCV), as well as in the oncogenic chicken herpesvirus Marek's disease virus (MDV). These bZIPs are BamHI Z EBV replication activator (BZLF1, Zta) [249], K-bZIP [250], HTLV-1 bZIP factor (HBZ) [251], non-structural 4B (NS4B) [252], and MDV Eco Q (MEQ) [253]. MEQ, HBZ, and NS4B are oncoproteins that drive proliferation by different mechanisms, Zta and K-bZIP primarily act as transactivators of the viral lytic cycle and inhibitors of cell proliferation. Most viral bZIP proteins interact with transcription factors to influence viral and host gene expression. Immune evasion and cell cycle control are also common features of these proteins. All viral bZIPs, with the exception of NS4B, have been demonstrated to bind DNA as homodimers and/or heterodimers [161]. Dimerization affects the functions and DNA-binding specificities of cellular bZIPs and viral bZIPs alike. MEQ homodimers recognize a unique 5'-RACACACAY-3' motif [254] and function as repressors, whereas MEQ and Jun heterodimers preferentially bind TREs and CREs and function as transcriptional activators [255]. HBZ, much like the Fos family of bZIPs, exclusively heterodimerizes with cellular bZIPs [256] and selectively activates [257,258] or inhibits [259–262] cellular and viral transcription. By contrast, Zta and K-bZIP do not form heterodimers, but may associate with C/EBPα as higher-order oligomers [263,264]. The ZIP and basic domains of viral bZIPs adhere to the sequence consensus less tightly than

cellular bZIPs (Fig. 4). K-bZIP and HBZ contain atypical basic domains, whereas Zta and NS4B contain atypical ZIP domains. Regardless of these structural abnormalities, most viral bZIPs function as DNA-binding transcription factors. Viral bZIPs recognize unique DNA-binding motifs [254,265], but also classical REs, such as CREs [254,262], TREs [254,266], MAREs [267], and CAAT boxes [85]. Unlike cellular bZIPs, viral bZIPs have evolved to carry out a greater variety of functions that pertain to viral replication and fitness. Not all functions these bZIPs carry out involve their bZIP domains. K-bZIP has small ubiquitin-like modifier (SUMO) E3 ligase activity [268], MEQ contains an N-terminal proline-rich transactivation domain apart from its bZIP domain [269], HBZ has an LXXLL-containing N-terminal transactivation domain [270], and NS4B is primarily a transmembrane protein that re-shapes cellular membranes to allow viral replication compartments to form [271,272].

1.8 Viruses and the UPR

Viruses usurp cellular pathways to facilitate immune evasion or optimize viral replication efficiency. The UPR is an apt target for viral dysregulation because it is potentially pro- and antiviral. UPR activation leads to the production of chaperones that promote the folding of cellular and viral proteins and is therefore proviral. By contrast, UPR activation also leads to increased mRNA and protein turnover and attenuation of global translation and is therefore antiviral. For example, UPR activation reduces influenza A virus (IAV) replication. The viral glycoprotein hemagglutinin (HA) activates IRE1 during infection and is degraded through ERAD following deglycosylation by the mannosidases EDEM1, -2, and ER mannosidase I (ERManI) [273]. Viruses may directly trigger ER stress by overloading the ER folding machinery with viral glycoproteins or by altering ER membrane composition. To harness the proviral effects of the UPR but suppress the antiviral effects, viruses need to dysregulate the UPR. For instance, HCV NS4B induces ROS and disrupts cellular Ca^{2+} signaling and induces the UPR through the NF-κB pathway [274]. In parallel, NS4B prevents the XBP1s-mediated expression of ERAD genes but allows BiP to be synthesized normally [275]. The flavivirus Dengue Virus 2 (DENV-2) inhibits PERK early during infection to reduce eIF2α phosphorylation and avoid global translation attenuation. Late during viral infection, DENV-2 activates CHOP and GADD34 production through the IRE1 pathway and further limits eIF2α

phosphorylation without inducing apoptosis [276]. UPR activation also reduces virion production of the flavivirus Zika virus (ZIKV), which activates the PERK and IRE1 arms during viral infection. ZIKV reduces the antiviral effects of the UPR by downregulating the production of BiP [277]. HSV-1 combats eIF2α phosphorylation and ERAD by inhibiting PERK and IRE1, but not ATF6 [278,279]. The HSV-1 glycoprotein B (gB) associates with the luminal domain of PERK and prevents its activation [278], whereas the viral tegument protein and host shutoff endonuclease unique long 41 (UL41) degrades the *Xbp1* transcript [279]. Other viruses selectively activate the UPR to harness its proviral effects. XBP1s transactivates the KSHV *ORF50* and EBV *BZLF1* promoters from 5'-ACGT-3' binding sites [153,280] and drives expression of the lytic switch proteins KSHV RTA and EBV ZTA to reactivate both viruses from latency [153,281]. HCV infection activates all three UPR sensors and induces autophagy to facilitate innate immune evasion. Expression of autophagy-related genes that encode CHOP, autophagy-related gene 5 (ATG5), and microtubule-associated proteins 1A/1B light chain 3B (LC3B) prevents the expression of IFN-β in response to viral pattern-associated molecular patterns (PAMPs) and allows for efficient HCV RNA replication [282]. The EBV RNA-binding protein and ORF57 homologue EB2 promotes ATF6 processing and leads to the upregulation of BiP production to maximize virion production [283]. XBP1s and ATF6-N activate the major immediate-early promoter (MIEP) of murine cytomegalovirus (MCMV) from a 5'-ACGT-3' DNA motif. In the absence of ER stress or during the resolution phase of ER stress, XBP1u leads to the degradation of XBP1s and ATF6-N and therefore prevents transactivation of the MIEP and impairs MCMV replication. To counter the antiviral effect of XBP1u, MCMV induces the IRE1 arm early during viral replication and drives the cell toward *xbp1* splicing and XBP1s production, which reduces the cellular levels of XBP1u [284]. UPR activation may also promote viral pathogenesis. The HIV-1 transactivator of transcription (Tat) leads to the accumulation of glial fibrillary acidic protein (GFAP) in astrocytes, which triggers ER stress and UPR activation and results in neurotoxicity [285].

1.8.1 KSHV Modulates the UPR during Lytic Replication

KSHV usurps the UPR during lytic replication. Our lab has found that lytic KSHV induces the UPR sensors ATF6, IRE1, and PERK and requires their expression for efficient viral replication and virion production. During lytic replication, ATF6 is properly processed into ATF6-N, *Xbp1* is spliced, and eIF2α is phosphorylated, but ATF6-N and XBP1s targets are not expressed and ATF4 is not produced. XBP1s overexpression reduces viral titers; its inhibition is therefore beneficial to the virus [286]. Our lab is actively pursuing avenues to investigate the KSHV-mediated dysregulation of the UPR. KSHV is a large virus and UPR modulation is likely multi-faceted and requires the concerted action of multiple viral proteins. Several candidate inducers and inhibitors of the UPR have been identified through preliminary screening [287]. K-bZIP shows promise as a candidate inhibitor of the UPR, although it did not score in the initial screen.

1.9 K-bZIP is a Viral Transcription Factor and Repressor

The following section 1.9 and its subsections 1.9.1-1.9.5 were adapted from the review titled "The bZIP Proteins of Oncogenic Viruses" [161].

The viral bZIP TF K-bZIP is expressed early during lytic viral replication from the *K8* gene. The *K8* pre-mRNA contains four exons and three introns that can be differentially spliced and translated to yield up to four different potential protein isoforms (I-IV), the most abundant of which is the 237 aa K-bZIP [250,288,289]. The relative expression levels of these alternatively spliced isoforms during viral replication remain only partially understood. K-bZIP is a functional homolog of the EBV bZIP TF Zta and plays a role as a transactivator and repressor of viral and host genes during lytic KSHV replication. K-bZIP is required for lytic replication and virion production in the KSHV-infected B cell lymphoma cell line BCBL-1 [84,290] and inhibits G_1 cell cycle progression to further aid viral replication [291,292].

K-bZIP contains a classical ZIP domain at its carboxy terminus with only one leucine in the 'd' position replaced by isoleucine (Fig. 4). The DNA-binding domain of K-bZIP is atypical and contains fewer basic aa residues than other cellular and viral bZIPs and lacks conserved arginine and asparagine residues (Fig. 4) [250]. The

transactivation ability of K-bZIP has long been in question because K-bZIP lacks a classical basic domain [293]. The basic domain is an important determinant of DNA binding, but homo- and heterodimerization between bZIPs can likewise affect DNA binding and sequence specificity [230]. An interaction between K-bZIP and DNA may therefore be stabilized by homodimer formation or by association with other proteins, viral or cellular. More recently, several stable K-bZIP/DNA complexes have been identified. For instance, K-bZIP is required for oriLyt-dependent KSHV replication and may act as an origin-binding protein. K-bZIP and RTA bind the oriLyt in concert and potentially recruit the vPIC to initiate viral DNA replication [84,85]. In this model, K-bZIP binds a cluster of CAAT boxes to which it might be recruited by C/EBPα [85].

DNA binding does not warrant transactivation activity. However, Ellison and colleagues showed that K-bZIP can transactivate 21 of 83 KSHV promoters in the absence of RTA. The group also found that K-bZIP modulates RTA transactivation activity to repress expression from RTA-responsive early lytic promoters, including the *K8* promoter, and to enhance expression from RTA-responsive late promoters [83]. Thus, K-bZIP is required to precisely regulate viral gene expression.

K-bZIP, like Zta, co-operates with the immediate early RTA protein to regulate viral gene expression during lytic replication [83,86,87]. Immunostaining and co-immunoprecipitation experiments confirmed that K-bZIP and RTA co-localize in the nuclei of lytic BCBL-1 cells [87], as well as transfected HeLa cells [86] and associate *in vitro*. The interaction between the two proteins is likely multi-faceted. The N-terminal basic domain of K-bZIP is required to associate with RTA in BCBL-1 cells [87], but the ZIP domain is required to associate with and repress RTA in HEK293T cells [86]. To date, no further studies have investigated the nature of the protein-protein interaction between the two proteins. K-bZIP and RTA drive lytic gene expression but can also associate with cellular promoters to transactivate host gene expression [265]. A recent study identified a novel 5'-AAAATGAAAA-3' K-bZIP-binding motif in viral and cellular promoters by ChIP-seq in TREx-BCBL-1-Rta cells. The viral genes containing this motif include all classes of lytic genes (early and late), as well as the *K8* gene. The cellular genes containing the motif encode collagen type IV alpha-3-binding protein (COL4a3BP), an

ER transmembrane transporter of ceramide; deleted in malignant brain tumors 1 protein (DMBT1), a candidate tumor suppressor; melanoma-associated antigen C3 (MAGEC3), a tumor antigen; ubiquitin-protein ligase E3A (UBE3A), a ubiquitin ligase of the proteasomal pathway; cell division cycle 7-related protein kinase (CDC7), a cell cycle regulating kinase; and Rho associated coiled-coil-containing protein kinase 1 pseudogene 1 (ROCK1P1), a pseudogene [265]. K-bZIP can induce transcription from luciferase constructs containing the novel motif, but how K-bZIP affects *de novo* transcription from the above-mentioned genes requires further investigation. It is also not yet known whether other viral bZIP proteins bind this motif.

1.9.1 K-bZIP Stalls Cell Cycle Progression

Like Zta, K-bZIP regulates the cell cycle and causes growth arrest to aid viral replication [292,294] (Fig. 6). K-bZIP delays G_0/G_1 growth phase progression by binding and inhibiting cyclin-dependent kinase 2 (CDK2) in BCBL-1 cells. The interaction between K-bZIP and CDK2 requires the basic domain of K-bZIP [292]. K-bZIP expression also induces C/EBPα and p21 in HeLa cells and stalls G_1 to S phase progression in human diploid fibroblast cells [294]. K-bZIP associates with C/EBPα and p21 in vitro and modulates their activity to affect cell cycle regulation at the post-transcriptional level [264]. K-bZIP, like Zta, binds C/EBPα with its ZIP domain. Glutaraldehyde cross-linking and sodium dodecyl sulfate-polyacrylamide gel electrophoresis (SDS-PAGE) experiments demonstrated that K-bZIP and C/EBPα do not form heterodimers [264], suggesting that they may instead associate via higher-order oligomers. More recent peptide microarray experiments confirmed that K-bZIP prefers homodimerization over heterodimerization and does not heterodimerize with various viral and cellular bZIPs [256].

1.9.2 K-bZIP Facilitates Immune Evasion

During lytic replication, K-bZIP plays a role in immune evasion. Type 1 IFNs are produced in response to viral infection and constitute signaling pathways that induce a range of cellular processes involved in antigen presentation, apoptosis, and inhibition of viral replication and gene expression [295]. Many viruses, including KSHV, have evolved to subvert host cell innate immune responses to facilitate immune evasion and promote ongoing viral replication. K-bZIP assists KSHV by dampening host antiviral type 1 IFN

Figure 6. **K-bZIP inhibits antiviral innate immune signaling and anti-proliferative signaling.** Viral cytosolic dsDNA activates the cGAS/STING pathway, which recruits TBK1 to phosphorylate and activate IRF3. IRF3 transitions to the nucleus to turn on expression of antiviral type 1 IFN genes. The early lytic viral transcription factor K-bZIP prevents IRF3 promoter access to inhibit IFN-β production. K-bZIP inhibits p53 and CDK2 but activates p21 to cause G_0/G_1 cell cycle arrest and prevent apoptosis. K-bZIP also prevents the association of p300/CBP with Smad proteins to inhibit expression of TGF-β-responsive genes in response to TGF-β signaling [161].

Figure 6. **K-bZIP inhibits antiviral innate immune signaling and anti-proliferative signaling.**
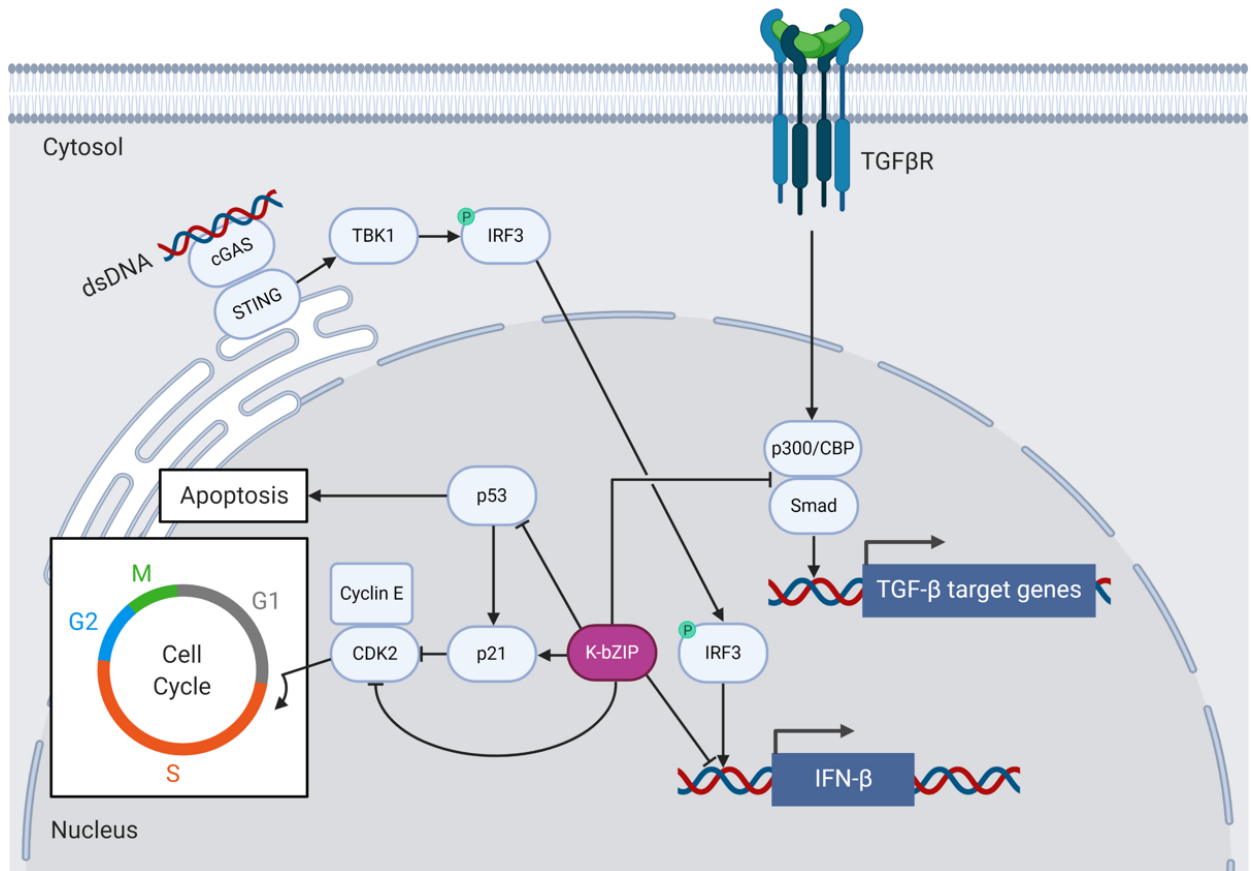
responses [289,296] (Fig. 6). K-bZIP binds and obstructs the IFN-β promoter and prevents IRF3 from binding and activating IFN-β transcription in K-bZIP-expressing 293T cells [296]. Downstream of type 1 IFN expression, K-bZIP interferes with the expression of the IFN-α-responsive genes encoding the antiviral 2'-5' oligoadenylate synthetase (2'-5' OAS) and the cytokine ISG15 [289].

The cellular tumor suppressor proteins p53 and promyelocytic leukemia protein (PML) are also activated in response to type 1 IFN signaling and represent pathways to counter viral infection by inducing cellular senescence and apoptosis [297,298]. The *PML* gene can be activated by IFN-α, IFN-β, and IFN-γ in response to viral infection or cancer [297] and leads to the acetylation, and therefore activation, of p53 and cell cycle arrest [299]. K-bZIP binds and inhibits p53 downstream of IFN signaling, thereby preventing the apoptosis of KSHV-infected cells [120]. An early study showed that co-transfection of a p53-deficient cervical cancer cell line (C33A) with K-bZIP and p53 inhibited gene expression from a p53-dependent luciferase reporter gene. Zta also binds and inhibits p53 [300,301]. Both bZIPs associate with p53 via their ZIP domains [300,302]. A later study also found that K-bZIP recruits p53 to PML bodies in PEL cells [302]. PML-deficient PEL cells displayed reduced viral DNA replication, late gene expression, and virion production, which suggests that PML is important to the viral lytic life cycle. K-bZIP is one of several viral proteins shown to interact with PML [303]. The functional relevance of the localization of p53 to PML bodies during lytic KSHV infection remains to be determined.

1.9.3 K-bZIP is a Multifunctional Interacting Protein

K-bZIP and Zta associate with the histone acetylase and transcriptional co-activator CREB-binding protein (CBP) *in vitro*, but these interactions lead to different outcomes. CPB enhances the Zta-mediated transactivation of lytic EBV promoters [304,305], whereas K-bZIP competes with Smad proteins for CBP binding and prevents assembly of the Smad/CBP complex and activation of Smad-responsive promoters in response to TGF-β signaling (Fig. 6) [306,307]. TGF-β is a cytokine that regulates cellular proliferation. The K-bZIP-mediated inhibition of TGF-β signaling may therefore contribute to KSHV tumorigenesis [307]. K-bZIP also inhibits the function of CBP as a transcription co-factor and represses CBP-dependent gene expression from a TRE-

containing luciferase construct in KSHV/EBV-negative follicular B cell lymphoma (BJAB) cells [306].

K-bZIP co-localizes with HDAC proteins in PML bodies and recruits HDACs to the *ORF50* and oriLyt promoters to epigenetically silence viral gene expression [308]. K-bZIP also interacts with the yeast chromatin remodeling complex subunit sucrose non-fermentable 5 (SNF5) and its human homologue, hSNF5. The interaction between SNF5/hSNF5 and K-bZIP enhance the transactivation activity of K-bZIP in yeast and might assist K-bZIP-mediated viral gene expression [309].

K-bZIP associates with multiple cellular and viral proteins. ORF57 [310] and viral protein kinase (vPK) [311] are viral K-bZIP binding partners. vPK phosphorylates K-bZIP at threonine 111 and relieves the K-bZIP-mediated repression of RTA. The K-bZIP/vPK interaction and subsequent K-bZIP phosphorylation may switch K-bZIP from functioning as a repressor of early gene expression to a transactivator of select early and late genes [311]. Further interactions between K-bZIP and RTA [86] or K-bZIP and ORF57 [310] may establish a feedback mechanism by which these proteins regulate transcription from their own promoters [86,310]. These viral protein-protein interactions may serve to modulate the respective functions of K-bZIP in a timely manner and may represent a mechanism to fine-tune lytic KSHV replication [310,311]. For example, early during lytic replication, the role of K-bZIP may be to inhibit the RTA-mediated expression of early viral genes, such as *ORF57* and *K8*, to assist the transition to late gene expression. Then, later during lytic replication, K-bZIP could assist RTA in the expression of viral structural proteins and other late gene products.

1.9.4 K-bZIP is a SUMO E3 Ligase

In addition to a classical, C-terminal bZIP domain, K-bZIP also contains an N-terminal SUMO interaction motif (SIM). The SIM confers SUMO E3 ligase activity to K-bZIP and allows the protein to bind and covalently attach SUMO-2 and SUMO-3, two of the four different SUMO isoforms, to lysine residues on itself and other viral and cellular proteins [268]. SUMOylation is a reversible PTM that can alter the function of a protein by affecting its ability to bind proteins or DNA or by changing its intracellular location. SUMOylation controls diverse cellular processes including transcription, DNA

replication, DNA damage repair, and cell division. Because many cellular events are regulated by SUMOylation, some viruses, such as HIV-1, IAV, EBV, and KSHV, have evolved mechanisms to manipulate the SUMOylation machinery to aid viral replication and virion production [312]. Many cellular proteins, including the bZIPs Jun/Fos [313], C/EBPβ [314], ATF6 [315], and XBP1s [316], are SUMOylated. SUMOylation negatively or positively affects the transcriptional activity of SUMOylated TFs to provide another layer of transcriptional regulation [317]. How SUMOylation affects bZIP dimer formation and stability remains to be determined.

In the context of KSHV infection, SUMOylation is important for the assembly and disassembly of PML bodies, modulating type 1 IFN responses, and remodeling chromatin during the latent and lytic phases of KSHV infection. At least two viral proteins, K-bZIP and LANA, can be SUMOylated [318]. K-bZIP SUMOylation is required for some of its repressive function, such as repression of IFN-α signaling [289] and repression of the RTA-mediated transactivation of the *ORF57* promoter [288]. K-bZIP-mediated SUMOylation enhances p53 transcriptional activity, and K-bZIP recruitment to p53 target genes is SIM-dependent, which suggests that a SUMO-rich environment stabilizes K-bZIP/p53 interactions [268].

SUMOylation also plays an important role in the regulation of lytic gene expression and virion production. During viral reactivation, SUMOylation of histones occupying the viral chromatin represses gene expression and virion production. Mutation of leucine 75 to alanine abrogates the SUMO E3 ligase activity of K-bZIP and restores viral gene expression and shows that SUMO enrichment of the viral chromatin is dependent on K-bZIP. This suggests that K-bZIP-mediated SUMOylation regulates viral lytic gene expression, which may facilitate immune evasion and efficient viral replication [319].

SUMOylation can also serve as a signal for ubiquitination and proteasomal degradation and can affect the half-life of SUMOylated proteins. SUMO-targeting ubiquitin ligases (STUbLs) target SUMOylated proteins for degradation [320]. The immediate early RTA protein is a SIM-containing viral STUbL that exhibits SUMO2/3 binding and ubiquitinates proteins conjugated with SUMO2/3 [321]. Because K-bZIP is a

viral E3 SUMO ligase that displays SUMO2/3 specificity, and because SUMO2/3 are the preferred substrates for RTA-mediated ubiquitination and subsequent proteasomal degradation, K-bZIP and RTA may work in concert to regulate cellular protein levels during lytic replication to create an optimal environment for KSHV replication. To date, the cellular and viral targets of K-bZIP-mediated SUMOylation are not known, and the extent to which K-bZIP and RTA work in concert to degrade SUMOylated target proteins is not well understood. In future studies, affinity purification and mass spectrometry approaches could be employed to identify cellular and viral protein targets of K-bZIP and their SUMOylation status. Hits from this unbiased approach could be corroborated by bioinformatic analysis (i.e., SIM identification) and in vitro SUMOylation assays [322].

1.9.5 K-bZIP is a Potential Inhibitor of the UPR

K-bZIP is a multifunctional viral repressor and transcriptional co-activator that assists KSHV with viral DNA replication, lytic gene expression, cell cycle arrest, and immune evasion through concerted action with diverse cellular and viral binding partners. The UPR bZIPs ATF6-N and XBP1s and ATF4 and CHOP heterodimerize with one another to transactivate gene expression from RE-containing promoters. Heterodimerization between K-bZIP and the UPR-governing bZIPs has not been documented, because K-bZIP prefers homodimerization [256]. Despite the apparent lack of heterodimerization, many protein-protein interactions between K-bZIP and its binding partners are mediated by the ZIP domain. This suggests that the ZIP domain of K-bZIP may broadly facilitate and/or stabilize protein-protein interactions that allow K-bZIP to partner with a structurally diverse range of cellular and viral proteins and is not limited to bZIP-bZIP interactions. K-bZIP may also associate with cellular bZIPs through oligomerization, as has been observed for C/EBPα [264]. K-bZIP is also a SUMO E3 ligase with SUMO2/3 specificity. XBP1s transactivation activity is negatively regulated by SUMOylation of lysines 276 and 297 with SUMO2 [316] and it is possible that KSHV infection further exacerbates this phenotype.

1.10 Hypotheses and Experimental Approaches

Because K-bZIP is a multifunctional repressor and interacting protein, I hypothesized that K-bZIP assists in the KSHV-mediated repression of UPR-responsive target genes by interaction with and/or modification of the UPR TFs ATF6-N, XBP1s, and ATF4. To test this hypothesis, I transduced a fluorescent hamster cell line with K-bZIP and analyzed IRE1 and PERK signaling, XBP1s expression, and ATF4 expression and transactivation by flow cytometry. I also transduced HEK293A cells with K-bZIP and assessed the expression of the UPR-responsive target genes *HSPA5* (encoding BiP), *DDIT3* (encoding CHOP), *HERPUD1*, *EDEM1*, and *DNAJB9* (encoding ERdj4) by quantitative reverse transcription polymerase chain reaction (RT-qPCR). Lastly, I transfected HEK293T cells and assessed if K-bZIP can inhibit or diminish the ATF6-mediated induction of ERSE-I in co-operation with its known viral interaction partners RTA, ORF57, and vPK.

To show that ATF6-N is functional during lytic KSHV replication, I assessed the nuclear accumulation of ATF6-N in KSHV-infected iSLK.219 and TREx-BCBL-1-RTA cells by nuclear and cytoplasmic fractionation and western blotting. To assess if ATF6-N overexpression is antiviral to KSHV, I transduced iSLK.219 cells with increasing concentrations of ATF6-N and quantified viral titers by flow cytometry.

CHAPTER 2: MATERIALS AND METHODS

2.1 Cell Culture and Chemicals

All cells were cultured in 10 cm dishes or T75 flasks at 37°C and supplied with 5% CO_2. Human embryonic kidney cells HEK293T (ATCC), HEK293A (ThermoFisher), doxycycline-inducible renal carcinoma iSLK.219 cells [323], and Chinese hamster ovarian CHO-KI (ATCC) cells were cultured in Dulbecco's Modified Eagle Medium (DMEM, Gibco) supplemented with 10% heat inactivated fetal bovine serum (FBS, Gibco), 100 U/mL penicillin, 100 µg/mL streptomycin, and 2 mM L-glutamine (ThermoFisher). iSLK.219 cells were cultured in 10 µM puromycin (Gibco) to maintain the recombinant KSHV episome [323]. CHO-7.1 CHOP::GFP XBP1s-mCherry reporter cells (a gift from David Ron, unpublished) (Fig. 7) were cultured in Ham's F12 medium (ThermoFisher) supplied with 10% FetalCycloneII serum (ThermoFisher) and penicillin, streptomycin, and L-glutamine at concentrations described above. Doxycycline-inducible BCBL PEL TREx-BCBL1-RTA cells [324] were cultured in Roswell Park Memorial Institute (RPMI) 1640 medium (Gibco) supplied with 500 µM β-mercaptoethanol (Gibco), as well as FBS, penicillin, streptomycin, and L-glutamine at concentrations described above. All cells were passaged with 0.05% trypsin-ethylenediaminetetraacetic acid (EDTA, Gibco).

2.2 Plasmid Generation

All plasmids used in this study are listed in Table 2.

pLJM1-K8α-puro (Fig. 8B) was generated from pcDNA 3.1 K-bZIP (previously generated in the McCormick lab) by PCR amplification with primers 5'-AATTGCTAGCACCATGCCCAGAATGAAGGACATACC-3' (forward) and 5'-TTAAGAATTCTCAACATGGTGGGAGTGGCG-3' (reverse) to introduce NheI and EcoRI restriction sites as well as a Kozak sequence. The amplicon was digested with NheI and EcoRI and subsequently cloned into pLJM1-B*-puro (previously generated in the McCormick lab) (Fig. 8A) with T4 DNA ligase.

Figure 7. **CHO-7.1 reporter cells express GFP and mCherry during ER stress.** The reporter cell line encodes GFP under the control of a murine CHOP promoter. Following PERK activation in response to ER stress and BiP dissociation, ATF4 is translated from a uORF containing transcript and transactivates GFP expression from the CHOP promoter. The reporter also encodes mCherry fused to XBP1s. Following IRE1 activation in response to stress, IRE1 removes an intron from the Xbp1 transcript by splicing. The spliced transcript is translated into the XBP1s-mCherry fusion protein.

Figure 7. **CHO-7.1 reporter cells express GFP and mCherry during ER stress.**
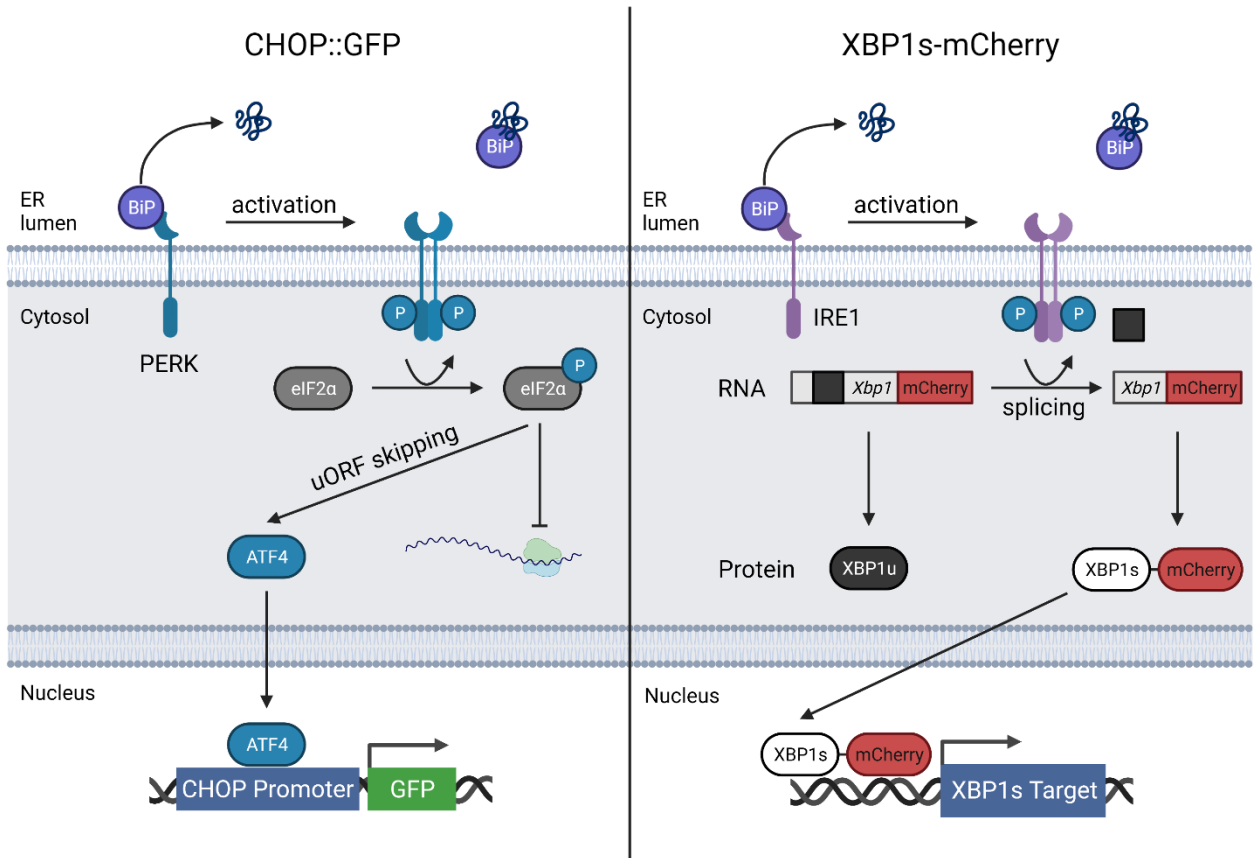
Figure 8. **K-bZIP-encoding plasmids were generated by PCR and restriction cloning.**
(A) pLJM1-B*-puro was previously generated in the McCormick lab and provided the
plasmid background for (B) pLJM1-K8α-puro. (B) pLJM1-K8α-puro was generated from
pcDNA 3.1 K-bZIP by restriction cloning. (C) pcDNA 3.1 (+) K8α was generated from
pLJM1-K8α-puro by restriction cloning.

Figure 8. **K-bZIP-encoding plasmids were generated by PCR and restriction cloning.**
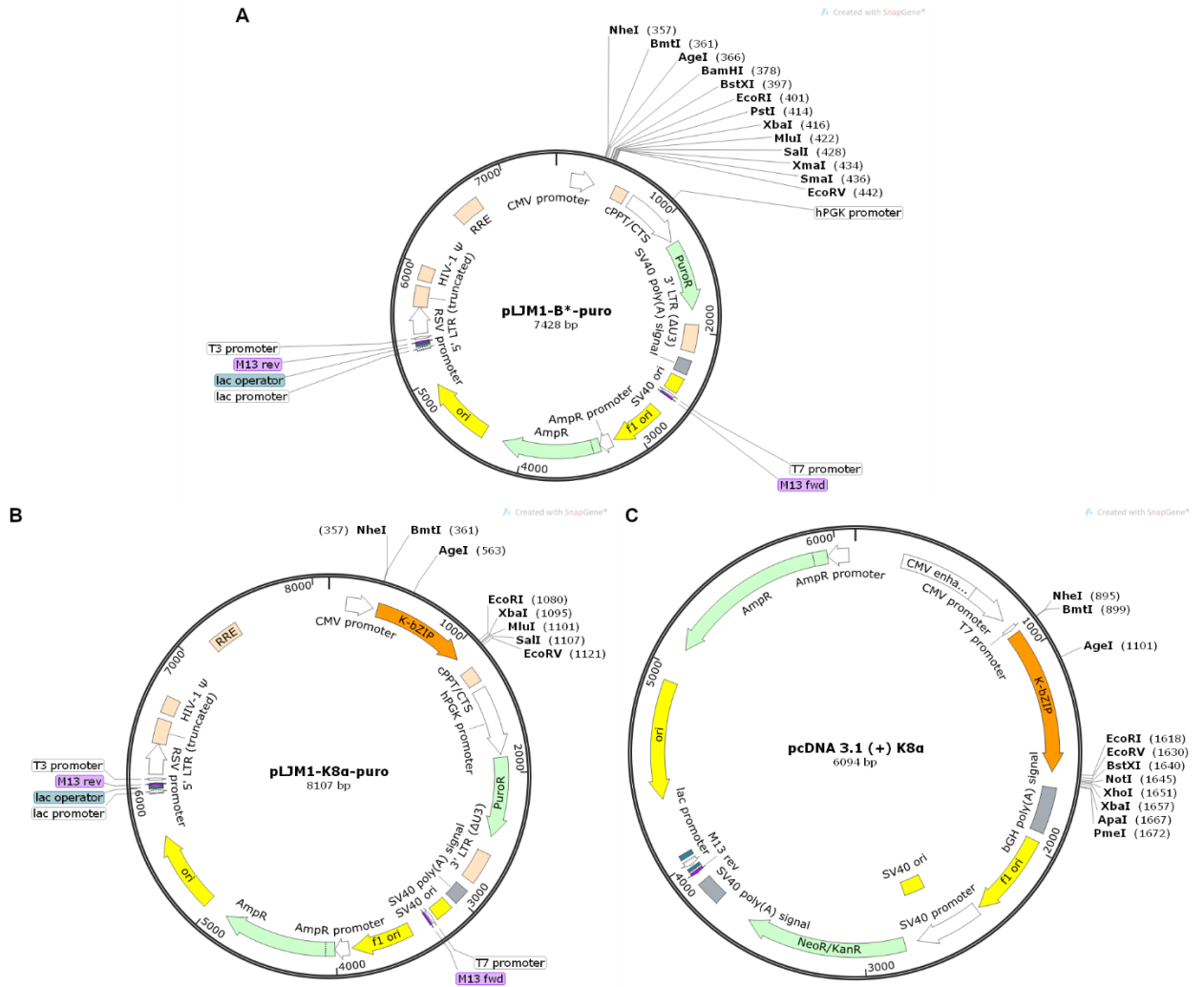
Table 2. Plasmids used in this study

Plasmid Name	Source	Antibiotic Selection Cassette	Mammalian Selection Cassette	Protein Product
pLJM1-B*-puro	McCormick lab	Ampicillin	Puromycin	N/A
pLJM1-B*-blast	McCormick lab	Ampicillin	Blasticidin	N/A
pLJM1-K8α-puro	This study	Ampicillin	Puromycin	K-bZIP
pLJM1-HA-ATF6 BSD	McCormick lab	Ampicillin	Blasticidin	HA-ATF6
pLJM1-HA-ATF6 1-373 BSD	McCormick lab	Ampicillin	Blasticidin	HA-ATF6 1-373
pcDNA3.1(+)	Addgene	Ampicillin	Neomycin	N/A
pcDNA3.1 K-bZIP	McCormick lab	Ampicillin	Neomycin	K-bZIP
pcDNA3.1 K8α	This study	Ampicillin	Neomycin	K-bZIP
pcDNA3 FLAG-RTA	McCormick lab	Ampicillin	Neomycin	FLAG-RTA
pcDNA3.1 HA-ORF36	McCormick lab	Ampicillin	Neomycin	HA-ORF36
pcDNA3.1 HA-ORF57	McCormick lab	Ampicillin	Neomycin	HA-ORF57
pCGN-ATF6	Addgene	Ampicillin	Hygromycin	ATF6
pmCherry-N1	Addgene	Kanamycin	Neomycin	mCherry
pEGFP-C1	Addgene	Kanamycin	Neomycin	EGFP
pEGFP-ATF6N	This study	Kanamycin	Neomycin	EGFP-ATF6 1-373
pGL4.45[*luc2P*/ISRE/Hygro]	Promega	Ampicillin	Hygromycin	FLuc
pMSCV-hygro-STING	Addgene	Ampicillin	Hygromycin	STING
pTRIP-CMV-tagRFP-FLAG-cGAS	Addgene	Ampicillin	N/A	RFP-FLAG-cGAS
pGL4.26 2XERSE	McCormick lab	Ampicillin	Hygromycin	FLuc
pGL4.74[*hRluc*/TK]	Promega	Ampicillin	N/A	RLuc
pGL4.74 promoterless	This study	Ampicillin	N/A	RLuc

pcDNA3.1 K8α (Fig. 8C) was generated from pLJM1-K8α by digestion with NheI and EcoRI, and subsequently ligated into pcDNA3.1(+) (Addgene) with T4 DNA ligase.

pEGFP-ATF6N (Fig. 9A) was generated from pCGN-ATF6 (Addgene) by PCR amplification using primers 5'-AATTAGATCTGGGGAGCCGGCTGGG-3' (forward) and 5'-CGATAAGCTTTAAGGGACTTTAAGCCTCTGGTTCTC-3' (reverse) to amplify the first 724 base pairs of the ORF corresponding to amino acids 1-373 of ATF6. The primer pairs also introduced BglII and HindIII restriction sites. The amplicon was then digested with BglII and HindIII and subsequently cloned into pEGFP-C1 (Clontech) with T4 DNA ligase. The plasmid expresses ATF6-N with an N-terminal EGFP tag.

pGL4.74 promoterless (Fig. 9C) was generated from pGL4.74 (Promega) by digestion with KpnI and HindIII to remove the HSV TK promoter. The resulting 5' and 3' overhangs were filled in with T4 DNA polymerase and the plasmid was re-circularized by blunt-end ligation with T4 DNA ligase.

Enzymes were purchased from New England Biolabs and used in accordance with the manufacturer's instructions. All plasmids were maintained in Stbl3 chemically competent *E. coli* and cultured in liquid Luria broth (LB, Wisent) or on LB agar plates supplemented with 100 μg/mL carbenicillin (Invitrogen) or 50 μg/mL kanamycin (Sigma) prior to plasmid purification. Plasmid DNA was extracted and purified in accordance with the QIAGEN plasmid midi protocol or the QIAGEN spin miniprep protocol.

All plasmid sequences were confirmed by Sanger sequencing through Azenta Life Sciences.

2.3 Lentivirus Generation

HEK293T cells were seeded into 10 cm dishes to achieve 50-60% cell density 24 h later. Prior to transfection, cells were washed with phosphate buffered saline (PBS, Wisent) and supplied with serum-free, antibiotic-free DMEM. Cells were then transfected dropwise with 1 μg pMD2.G (Addgene) VSV-G envelope plasmid, 2 μg pSPAX2 (Addgene) packaging plasmid, and 3 μg pLJM1-B*-puro, pLJM1-K8α-puro, pLJM1-B*

Figure 9. Plasmids used for dual luciferase assays. (A) pEGFP-ATF6N was generated from pCGN-ATF6 by PCR cloning and inserted into a pEGFP-C1 vector by restriction cloning. (B) pGL4.26 2XERSE was cloned from pGL4.26 [luc2/minP/Hygro] by PCR cloning by Taylor Caddell. (C) pGL4.74 promoterless was generated from pGL4.74 [hRluc/TK] through removal of the TK promoter by restriction cloning.

Figure 9. Plasmids used for dual luciferase assays.
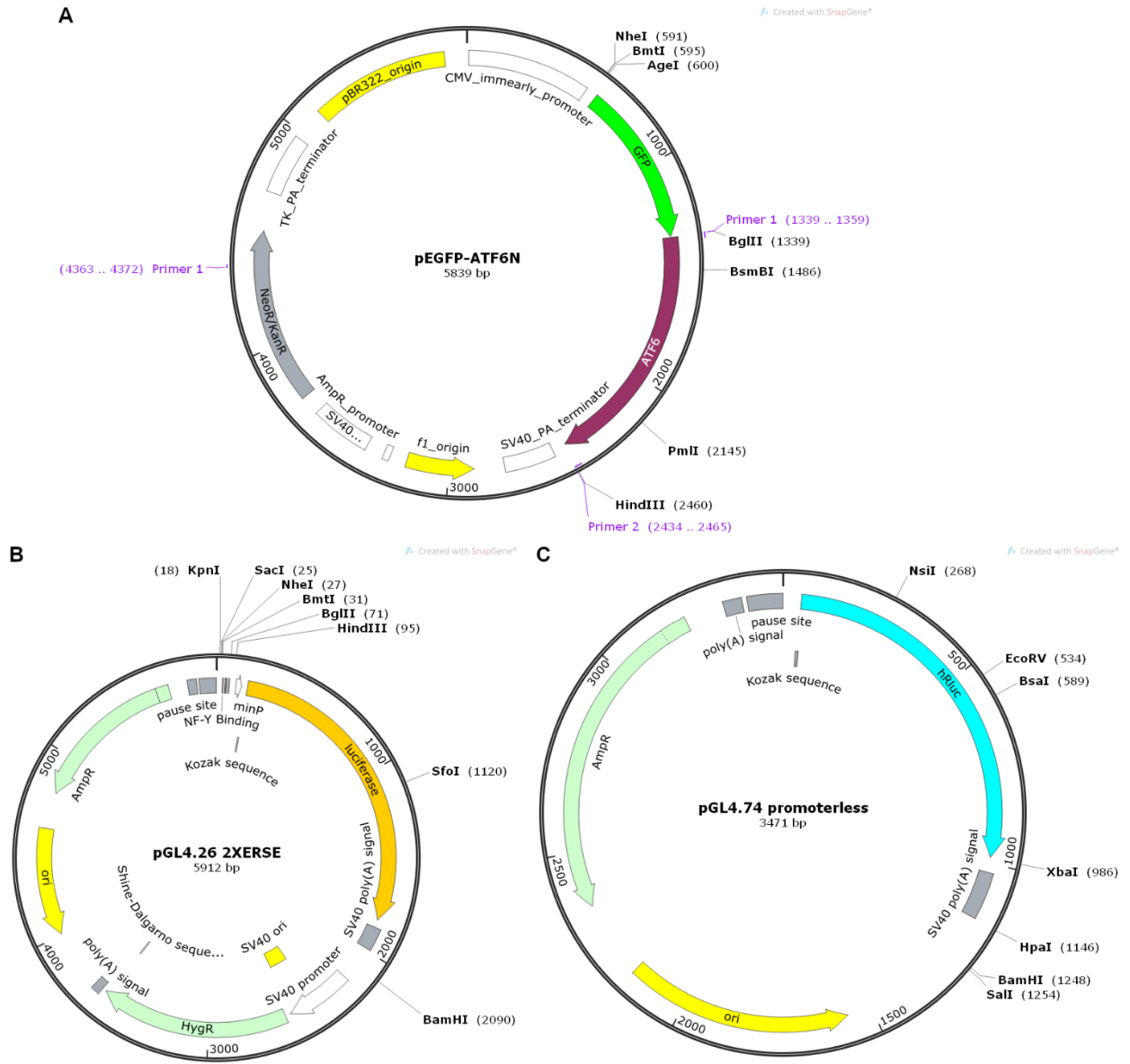
BSD, pLJM1-HA-ATF6 BSD, or pLJM1-HA-ATF6 1-373 BSD per dish using the transfection reagent polyethylenimine (PEI, Polysciences Inc.) diluted in Minimum Essential Medium (Opti-MEM, Gibco). 5 h post-transfection, medium was replaced with DMEM as described in section 2.1. 48 h post-transfection, lentivirus-containing medium was harvested from transfected cells and passed through 0.45 μm sterile polyethersulfone (PES) filters (Sarstedt), and subjected to centrifugation at 500 x g for 5 min. Aliquots were stored at -80°C.

2.4 Lentivirus Transduction

For lentiviral titering, HEK293T, HEK293A, or iSLK.219 cells were seeded into 12-well plates at densities of $10x10^4$, $7.5x10^4$, or $5x10^4$ cells/mL, respectively. The following day, cells were transduced with serially diluted lentivirus and supplemented with DMEM containing 10 μg/mL polybrene (Sigma). Cells were transduced at 37°C for 24h. 24h post-transduction, medium was replaced with fresh DMEM containing 2-5 μg/mL puromycin or 10 μg/mL blasticidin (Gibco) to select for transduced cells. The highest dilution of lentivirus that protected >90% of cells from cell death was designated as a MOI of 1 and was used for all further transductions.

To transduce CHO-7.1 reporter cells with pLJM1-B*-puro or pLJM1-K8α-puro, cells were seeded into 12-well plates at a density of $5x10^4$ cells/mL and incubated at 37°C. The following day, cells were transduced with lentiviruses at a MOI of 10 and supplemented with Ham's F12 medium containing 10 μg/mL polybrene. Cells were incubated at 37°C for 24 h, after which transduced cells were selected for with 8 μg/mL puromycin at 37°C for 48 h.

To transduce HEK293A cells with pLJM1-B*-puro or pLJM1-K8α-puro, cells were seeded into 6-well plates at a density of $5x10^4$ cells/mL and incubated at 37°C. The following day, cells were transduced with lentiviruses at a MOI of 5 and supplemented with DMEM containing 4 μg/mL polybrene. Cells were incubated at 37°C for 48 h prior to harvest.

To transduce iSLK.219 cells with pLJM1-B* BSD, pLJM1-HA-ATF6 BSD, or pLJM1-HA-ATF6 1-373 BSD, cells were seeded into 6-well plates at a density of $5x10^4$

cells/mL and incubated at 37°C. The following day, cells were transduced with lentiviruses at MOIs of 1, 2, 5, 7, or 10 and supplemented with DMEM containing 4 µg/mL polybrene. Cells were incubated at 37°C for 24 h before treatments were administered.

2.5 Flow Cytometry Analysis with CHO-7.1 Reporter Cell Line

CHO-7.1 reporter cells were transduced as described in section 2.5. CHO-K1 cells were seeded into 12-well plates at a density of 5×10^4 cells/mL and incubated at 37°C for 24 h. The following day, cells were washed once with PBS and supplied with serum-free, antibiotic-free DMEM. Cells were then transfected with 500 ng pEGFP-C1 or pmCherry-N1 using 3 µg/mL PEI diluted in Opti-MEM. 5h post-transfection, medium was replaced with DMEM, and cells were incubated at 37°C until harvest. 52 h post-transduction, CHO-7.1 cells were treated with 1 mM thapsigargin (Tg, Sigma) or 0.05% dimethyl sulfoxide (DMSO, Sigma-Aldrich) at 37°C for 20 h. 72h post-transduction or 48h post-transfection, CHO-KI and CHO-7.1 cells were washed once with PBS, lifted off the culture wells with 10 mM EDTA, and collected into 1.5 mL Eppendorf tubes. Samples were then pelleted at 1000 x g for 5 min and washed with PBS twice. Following another spin step at 1000 x g for 5 min, cells were fixed with 4% paraformaldehyde (VWR) at room temperature for 20 min. After fixation, cells were spun at 2000 x g for 2 min and washed with PBS. Supernatant was discarded and pellets were subsequently resuspended in FACS buffer (1% bovine serum albumin (BSA, Bio-Rad or BioShop), 5 mM EDTA in PBS) and transferred to polystyrene tubes (Falcon). Samples were stored at 4°C until use. CHOP::GFP and XBP1s-mCherry fluorescence signals were detected for 10,000 cells per sample on a BD LSRFortessa Flow Cytometer using a 488 nm blue laser (530/30 filter) and a 561 nm yellow/green laser (610/20 filter). Cell populations were visualized using BD FACSDiva (Beckton Dickinson Biosciences). FCSExpress 7 (De Novo) and FlowJo (LLC) were used for data analysis. Samples were gated for live events and single cells and then analyzed for GFP and mCherry expression. All samples were compensated for background GFP and mCherry using transfected CHO-KI cells as the compensation controls. The median fluorescence intensity (MFI) of each sample was normalized to untransduced and untreated (DMSO) CHO-7.1 cells.

2.6 Immunoblotting

All antibodies used in this study are listed in Table 3.

Cells were washed once with PBS, lifted off the culture wells with 10 mM EDTA, and collected into 1.5 mL Eppendorf tubes. Samples were then pelleted at 1000 x g for 5 min and washed with PBS. The supernatant was discarded, and the pellets were lysed with radioimmunoprecipitation assay (RIPA) buffer (50 mM Tris-Cl, 150 mM NaCl, 1 mM EDTA, 1% IPEGAL, 0.1% SDS, 0.5% sodium deoxycholate (all Sigma)) supplemented with cØmplete mini EDTA-free protease inhibitors (Roche) for 20 min on ice. Lysates were spun at 20,000 x g to precipitate debris, and supernatants were stored at -20°C in 4X Laemmli buffer (250 mM Tris-HCl, pH 6.8 (Sigma); 8% SDS (Wisent), 40% glycerol (Wisent), 20% β-mercaptoethanol, 0.004% bromophenol blue (BioShop)) and 50 mM dithiothreitol (DTT, Sigma) until use. Protein concentration was quantified with a DC protein assay (Bio-Rad) using BSA as the standard. Prior to SDS-PAGE, samples were boiled at 95°C for 5 min. 2.4-10 µg per protein sample were loaded onto 8-12.5% polyacrylamide (Bio-Rad) gels and resolved by SDS-PAGE at 80-100 Volts. Proteins were transferred onto polyvinylidene difluoride (PVDF) membranes (Bio-Rad) using a Trans-blot Turbo (Bio-Rad) and blocked in 4% BSA or 5% skim milk powder (Nestle) diluted in Tris-buffered saline (TBS) supplemented with 0.1% Tween 20 (TBST, Fisher) on a table-top shaker at room temperature for 1 h. For protein detection, primary antibodies were diluted in 4% BSA diluted in TBST, and membranes were incubated on a table-top shaker at 4°C overnight. Following incubation, membranes were washed three times with TBST for 5 min each and membranes were incubated with HRP-linked anti-mouse or anti-rabbit antibodies in 4% BSA diluted in TBST on a table-top shaker at room temperature for 1h. Following another set of wash steps, membranes were developed with Clarity or Clarity Max Western ECL substrate (Bio-Rad) and imaged on a Bio-Rad ChemiDoc Imaging System using the chemiluminescence and Ponceau S settings.

Table 3. Antibodies used in this study.

Target	Source	Catalog Number	Dilution Used At
Anti-rabbit IgG HRP-linked	Cell Signaling	#7074	1:5000
Anti-mouse IgG HRP-linked	Cell Signaling	#7076	1:5000
β-actin HRP-linked	Cell Signaling	#5125	1:5000
α-tubulin	Cell Signaling	#2144S	1:2000
GFP	Cell Signaling	#2555S	1:2000
HA-tag	Cell Signaling	#2367	1:1000
FLAG-tag	Cell Signaling	#8146	1:1000
K-bZIP	Santa Cruz	sc-69797	1:2000
ORF57	Santa Cruz	sc-135746	1:1000
ORF65	Shou-Jiang Gao (gift)	N/A	1:1000
XBP1 (s + u)	Cell Signaling	#12782	1:2000
BiP	Cell Signaling	#3177	1:1000
Lamin A/C	Santa Cruz	sc-7292	1:1000
Calnexin	Cell Signaling	#2679	1:1000
Calreticulin	Cell Signaling	#12238	1:1000
Histone H3	Cell Signaling	#4499	1:1000

2.7 Quantitative Reverse Transcription PCR (RT-qPCR)

All primer sets used for RT-qPCR are listed in Table 4.

HEK293A or iSLK.219 cells were transduced as described section 2.5. 24 h post-transduction, iSLK.219 cells were reactivated with 1 μg/mL doxycycline (Sigma) or 0.0005% DMSO for 44 h. 44 h post-transduction or 44 h post-doxycycline addition, cells were treated with 150 nM Tg or 0.00015% DMSO at 37°C for 4h. Following the 4 h treatment, cells were washed once with PBS and lysed with RLT plus buffer (QIAGEN). Lysates were passed through 21-gauge syringes or vortexed for 30 seconds to reduce viscosity, transferred to 1.5 mL Eppendorf tubes, and stored at -80°C until use. Cellular RNA was extracted and purified from lysates in accordance with the QIAGEN RNeasy Plus Mini protocol and eluted with dH_2O. RNA integrity was assessed by agarose gel electrophoresis using a 1% agarose bleach gel [325]. cDNA was synthesized from 250 ng RNA per sample using Maxima H Minus reverse transcriptase (Thermo Scientific) in accordance with the manufacturer's instructions. cDNA was diluted 1:10 or 1:40 with nuclease-free dH_2O. 2 μM per primer were diluted 1:6 with GoTaq RT qPCR Master Mix (Promega) and combined with cDNA into clear-bottom 96-well qPCR plates (Bio-Rad) for a final concentration of 200 nM per primer per reaction. RT-qPCR was then performed using a CFX Connect Real Time System (Bio-Rad) at an annealing temperature of 60°C. Fold changes in target gene mRNA levels were calculated using the ΔΔCt method. For samples harvested from HEK293A cells, *GAPDH* was used as the reference gene for normalization. For samples harvested from iSLK.219 cells, 18S rRNA was used as the reference gene.

2.8 Dual Luciferase Assays

Validation of K-bZIP Functionality Using pGL4.45 ISRE

HEK293T cells were reverse-transfected with 200-900 ng pcDNA3.1(+), 400 ng pcDNA3.1 K8α, 150 ng pMSCV-hygro-STING, 150 ng pTRIP-CMV-tagRFP-FLAG-cGAS, 100 ng pGL4.45[*luc2P*/ISRE/Hygro], and 20 ng pGL4.74 promoterless using 3 μg/mL PEI diluted in Opti-MEM. Transfection reagents were added to 24-well plates and HEK293T cells were seeded into transfection reagents at a density of $4x10^5$ cells/mL.

Table 4. **Primer Sets Used For RT-qPCR.**

Target Transcript	Forward Primer 5'-3'	Reverse Primer 5'-3'	Efficiency
GAPDH	GAGTCAACGGATTTGGT CGT	TTGATTTTGGAGGGATC TCG	N/A
18S	TTCGAACGTCTGCCCTA TCAA	GATGTGGTAGCCGTTTC TCAGG	86%
HSPA5	GCCTGTATTTCTAGACC TGCC	TCCATCTTGCCAGCCAG TTG	99%
HERPUD1	AACGGCCATGTTTTGCA TCTG	GGGGAAGAAAGGTTCC GAAG	106%
DDIT3	ATGAACGGCTCAAGCA GGAA	GGGAAGGTGGGTAGT GTGG	89%
EDEM1	TTGACAAAGATTCCACC GTCC	TGTGAGCAGAAAGGAG GCTTC	88%
DNAJB9	CGCCAAATCAAGAAGG TTC	CAGCATCCGGGCTCTTA TTTT	115%
K8	CGAAAGCAAGGCAGAT ACG	CATCAGCATGTCGCGAA G	103%
Native RTA	CCGAGACTGAAGTGTTC GCA	AACGGAGGAAATACCA CCCC	N/A
Trans RTA	ACTGTACCAGCTGCACC AAT	GGGAGGGGCAAACAAC AGAT	N/A
ORF57	TCCAGTTTTGCTCCCCA CTG	TTCTGCCGTATTGTAGG CGG	N/A
ORF11	ACATTTGACAACACGCA CCG	AAAATCAGCACGCTCGA GGA	N/A
ORF59	CACCAGGCTTCTCCTCT GTG	TCGCTGACAGACACAGT CAC	N/A
ORF45	TGATGAAATCGAGTGGG CGG	CTTAAGCCGCAAAGCAG TGG	N/A
ORF26	CAGTTGAGCGTCCCAGA TGA	GGAATACCAACAGGAG GCCG	N/A
K9 (vIRF1)	GTCATTGACTGGGGTCG GTT	CTACGCAAGGCCGATGA GAT	N/A
K8.1	AGATACGTCTGCCTCTG GGT	AAAGTCACGTGGGAGG TCAC	N/A
ORF65	TGGCTCGCATGAATACC CTG	CTGCAGATGATCCCGCC TTT	N/A
ORF71 (vFLIP)	CAGTCACGTCCCCAAGA GC	CAGGTTCTCCCATCGAC GAC	N/A
ORF73 (LANA)	TCCCACAGTGTTCACAT CCG	GAGGTAAAGGTGTTGCG GGA	N/A

Cells were supplied with antibiotic-free DMEM and incubated at 37°C. 48h post-transfection, cells were washed once with PBS, lysed with 100 μL passive lysis buffer (Promega) per well, and incubated on a Belly Dancer orbital shaker (Stovall) at room temperature for 15 min. Lysates were collected into 1.5 mL Eppendorf tubes and firefly and *Renilla* luciferase relative light units (RLU) were subsequently measures on a GloMax 20/20 luminometer (Promega) in accordance with the Promega Dual Luciferase Reporter Assay protocol. Firefly luciferase signal was normalized to *Renilla* luciferase signal using the following formula:

Ratio (firefly luciferase to *Renilla* luciferase) = firefly luciferase RLU / *Renilla* luciferase RLU

2.9 Assessment of ATF6-N Transcriptional Activity Using pGL4.26 2XERSE

HEK293T cells were reverse-transfected with 300 ng pEGFP-C1, pEGFP-ATF6N, or pCGN ATF6, 300-600 ng pcDNA3.1(+), 300 ng pcDNA3 FLAG-RTA, pcDNA3.1 HA-ORF37, and/or pcDNA3.1 HA-ORF57, and/or pcDNA3.1 K8α, 100 ng pGL4.26 2XERSE (Fig. 9B), and 20 ng pGL4.74 promoterless using 5 μg/mL PEI diluted in Opti-MEM. Transfection reagents were added to 24-well plates and HEK293T cells were seeded into transfection reagents at a density of 4×10^5 cells/mL. Cells were supplied with antibiotic-free DMEM and incubated at 37°C for 48 h. 48 h post-transfection, cells were harvested for dual luciferase assays as in section 2.8.

2.10 Nuclear and Cytoplasmic Fractionation of iSLK.219 and TREx-BCBL1-RTA Cells

Nuclear and cytoplasmic fractionation was performed in accordance with the Lyse & Wash protocol [326].

To assess the subcellular localization and relative protein abundance of transiently expressed HA-ATF6 and HA-ATF6 1-373, iSLK.219 cells were transduced with lentiviruses at MOIs of 7 as described in section 2.4. 24 h post-transduction, latent rKSHV.219 was reactivated using 1 μg/mL doxycycline and 1 mM NaB (Sigma) or 0.001% DMSO (control) at 37°C for 48 h.

To assess the subcellular localization and relative protein abundance of endogenous ATF6, iSLK.219 or TREx-BCBL1-RTA cells were seeded at a density of 5×10^4 cells/mL or 2.5×10^5 cells/mL, respectively, and incubated at 37°C for 24 h. After 24 h, latent KSHV was reactivated using 1 µg/mL doxycycline and 1 mM NaB or 0.001% DMSO (control) at 37°C for 44 h. After 44 h, cells were treated with 150-250 nM Tg or 0.00015-0.00025% DMSO (control) for 4 h.

At the point of harvest, adherent cells were washed once with PBS and lifted off the plates with 0.05% trypsin-ethylenediaminetetraacetic acid. Trypsinized cells were diluted with 800 µL ice-cold DMEM to quench the trypsin, collected into 1.5 mL Eppendorf tubes and pelleted at 500 x g at 4°C for 4 min. Suspension cells were directly collected into 2 mL Eppendorf tubes and pelleted as described. Pellets were subsequently washed with 500 µL ice-cold PBS and pelleted as before. Pellets were re-suspended in 150 µL ice-cold hypotonic buffer (20 mM Tris-HCl, 10 mM KCl, 2 mM MgCl$_2$, 1 mM EGTA (all Sigma), 1 tablet of cØmplete mini EDTA-free protease inhibitors) and incubated on ice for 3 min to separate the ER from the nuclei. Cells were then lysed with 0.1% Nonidet P 40 substitute (Fluka) and incubated for an additional 3 min on ice. After incubation, lysates were spun at 1,000 x g at 4°C for 5 min to separate nuclei (pellet) from all other cellular components (supernatant). Supernatants containing cytoplasmic proteins were centrifuged at 15,000 x g at 4°C for 3 min to precipitate any remaining nuclei and debris, collected into fresh 1.5 mL Eppendorf tubes, and 50 µL 4X Laemmli buffer containing 0.5 mM DTT were added. Pellets containing nuclei were re-suspended in 200 µL isotonic buffer (20 mM Tris-HCl, 150 mM KCl, 2 mM MgCl$_2$, 1 mM EGTA, 1 tablet of cØmplete mini EDTA-free protease inhibitors) and incubated for 5-10 min on ice. Following incubation, nuclei were precipitated at 1,000 x g at 4°C for 3 min and the supernatants were discarded. Pellets were lysed with 200 µL 2X Laemmli buffer (6.25 mM Tris-HCl, pH 6.8; 2.35% SDS, 10% glycerol, 1 mM EDTA) and samples were homogenized, and genomic DNA was sheared by passing lysates through 21-gauge syringes. Finally, 0.001% bromophenol blue and 0.5 mM DTT were added to nuclear lysates. Nuclear and cytoplasmic lysates were stored at -20°C until SDS-PAGE as described in section 2.6.

*2.11 Flow Cytometry Assessment of ATF6-N Antiviral Activity*

For assessing the potential antiviral activity of ATF6-N, iSLK.219 cells were transduced with pLJM1-B* BSD or pLJM1-HA-ATF6 1-373 BSD at MOIs of 1, 2, 5, and 10 as described in section 2.4. 24 h post-transduction, latent rKSHV.219 was reactivated using 1 µg/mL doxycycline and 1 mM NaB for 96 h, after which virus-containing supernatants were collected, spun at 3,300 x g for 5 min, and stored at -80°C until use. For spinoculation, HEK293A cells were seeded into 12-well plates at a density of $1x10^5$ cells/mL to produce a confluent monolayer 48 h later. Virus-containing supernatants were diluted two-fold (1/2 - 1/64) with DMEM containing 3 µg/mL polybrene and 25mM N-2-hydroxyethylpiperazine-N-2-ethane sulfonic acid (HEPES, Gibco) and spinoculated onto HEK293A cells at 800 x g and 30°C for 2 h. Following spinoculation, cells were supplied with fresh DMEM and incubated for 20 h at 37°C. After 20 h, cells were washed once with PBS, lifted off the culture wells with 100 µL trypsin-ethylenediaminetetraacetic acid, and collected into 1.5 mL Eppendorf tubes. At the point of harvest, cell counts were also obtained from uninfected HEK293A cells. Samples were then pelleted at 1000 x g for 5 min and washed with PBS twice. Following another spin step at 1000 x g for 5 min, cells were then fixed with 4% paraformaldehyde at room temperature for 20 min. After fixation, cells were spun at 2000 x g for 2 min and washed with PBS. Supernatant was discarded and pellets were subsequently resuspended in FACS buffer and transferred to polystyrene tubes. Samples were stored at 4°C until use. GFP signal was detected for 50,000 cells per sample on a BD FACSCelesta Flow Cytometer using a 488 nm blue laser (530/30 filter). Cell populations were visualized using BD FACSDiva (Beckton Dickinson Biosciences). FCSExpress 7 (De Novo) was used for data analysis. Samples were gated for live events and single cells and then analyzed for GFP expression (Fig. 10). GFP positive events were determined by comparison with uninfected HEK293A cells. Virus titer was calculated as IU/mL using the following formula:

Virus titer (IU/mL) = (% GFP positive events * total cell count as determined at the time of harvest) / dilution factor

Figure 10. **Flow cytometry gating strategy for GFP-expressing HEK293A cells.** Live cells were gated based on side scatter (SSC) and forward scatter (FSC) (A). Single cells were further gated using FSC-A and FSC-H (B). GFP signal was measured using a 488nm blue laser (530/30 filter) (FITC-channel). GFP-positive, single-cell populations were defined to the exclusion of autofluorescent GFP signal from unstained HEK293A cells (C).

Figure 10. **Flow cytometry gating strategy for GFP-expressing HEK293A cells.**
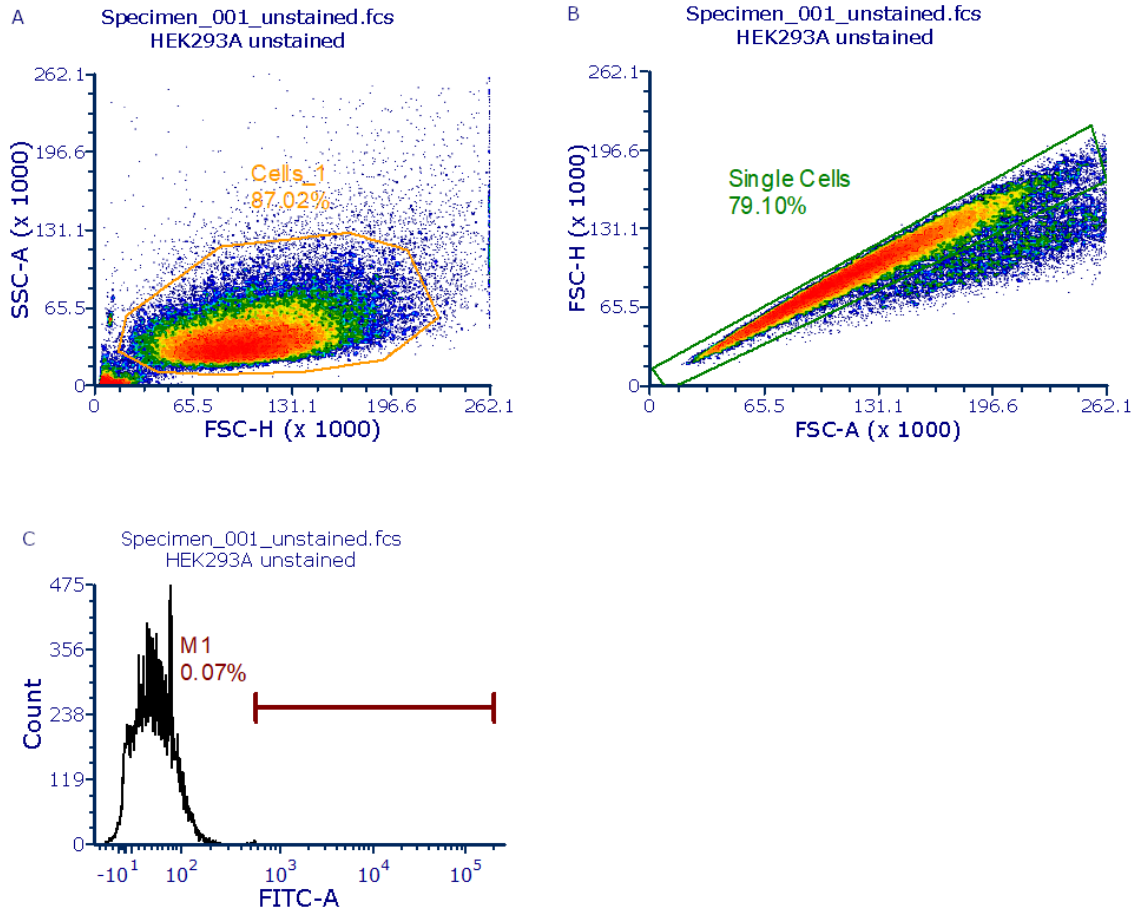
Only titers obtained from samples displaying 1-30% GFP positivity were considered for statistical analysis.

2.12 Statistical Analysis

Statistical analysis was performed using Prism 9 (GraphPad). Statistical significance between two different groups was determined with unpaired, two-tailed Student's t-tests. Statistical significance between three or more different groups was determined with two-way ANOVAs using Tukey's test for correction. A p value of < 0.05 was considered statistically significant. Significance was denoted as follows: **, p value < 0.01; ***, p value < 0.001; ****, p value < 0.0001.

CHAPTER 3: RESULTS

3.1 K-bZIP Expressed from Plasmids and Lentiviral Vectors is Functional

The predominant and transcriptionally active isoform of K8 is the 237 aa, bZIP-containing K8α or K-bZIP [250]. For my experiments, I generated K-bZIP-encoding plasmids by PCR cloning from an intronless parent plasmid amplified from viral cDNA. To confirm that the pLJM1-K8α-puro and pcDNA3.1 K8α plasmids used in this study produce a functional K-bZIP protein, I performed immunoblots and luciferase assays. HEK293A cells transduced with pLJM1-K8α-puro or HEK293T cells transfected with pcDNA3.1 K8α express a K-bZIP of about 35-40 kDa in size (Fig. 13B, Fig. 16), which is consistent with previous observations [87,288,311]. K-bZIP has been reported to facilitate immune evasion by disrupting IFN signaling prior to and following type I IFN production [289,296]. Upstream of type I IFN production, K-bZIP binds the ISRE located on the *IFNB1* and C-C Motif Chemokine Ligand 5 (*CCL5*) promoters and prevents the IFN-β inducer IRF3 from binding [296]. Downstream of type I IFN production, K-bZIP represses the expression of ISGs, such as that encoding 2', 5' OAS, by a mechanism that is not understood [289]. IRF3 is responsive to phosphorylation and activated as part of cellular pathogen sensing pathways. The cellular PRR cGAS activates the stimulator of interferon genes (STING) upon sensing cytosolic dsDNA [327]. STING then activates TANK-binding kinase 1 (TBK1), which is one of the kinases that phosphorylate and activate IRF3 [328,329]. To recapitulate K-bZIP-mediated repression of ISRE-containing genes, I assessed firefly luciferase production by an ISRE-containing luciferase plasmid in HEK293T cells. I artificially induced the type I IFN signaling pathway by co-transfection with cGAS and STING. I decided against treatment with IFN-α because I wanted to stimulate the signaling pathway upstream of IFN production. I Initially induced type 1 IFN production with the IRF3 agonist polyinosinic:polycytidylic acid (poly I:C) [330,331], but co-transfection with poly I:C was inefficient and only minimally induced ISRE-driven luciferase production. By contrast, ectopic cGAS and STING expression induced luciferase production from the ISRE-containing luciferase plasmid almost 1,400-fold (Fig. 11). This increase was reduced roughly 50% or 600-fold in cells that were also

expressing K-bZIP. My data shows that pLJM1-K8α-puro and pcDNA3.1 K8α encode a ~40 kDa K-bZIP that represses gene expression from ISRE and is therefore functional.
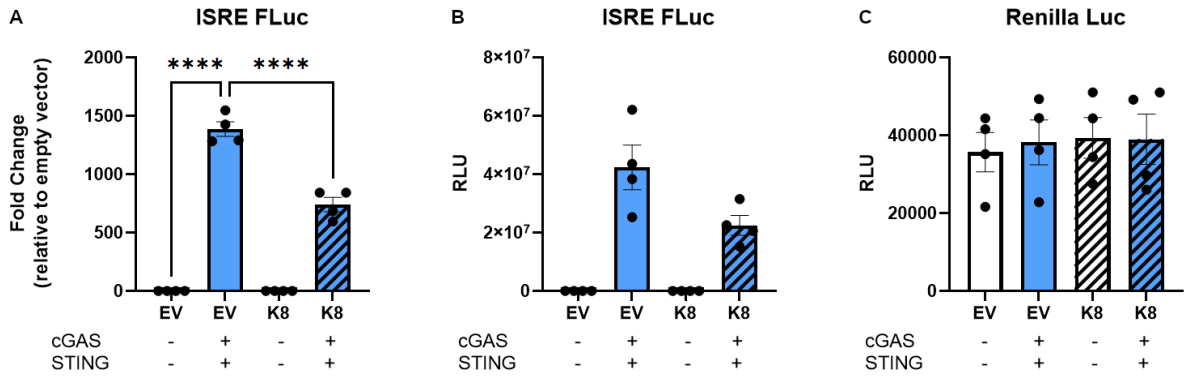
3.2 K-bZIP Does Not Affect the PERK and IRE1 Arms of the UPR in CHO-7.1 Reporter Cells

To test the hypothesis that K-bZIP inhibits the UPR, I investigated UPR activation with ectopic K-bZIP expression using a Chinese hamster ovary reporter cell line. The CHO-7.1 CHOP::GFP/XBP1s-mCherry reporter cell line expresses GFP under the control of the mouse *DDIT3* promoter and expresses mCherry fused to XBP1s (Fig. 7). *DDIT3* expression is induced by ATF4 following PERK stimulation and GFP signal therefore provides a quantitative measure of PERK activation and ATF4 expression and transcriptional activity. XBP1s is produced in response to IRE1-mediated *xbp1* splicing and mCherry signal therefore provides a measure of IRE1 activation and *Xbp1* splicing and expression. The cell line does not allow us to monitor the ATF6 arm of the UPR. To assess if K-bZIP inhibits the PERK and IRE1 arms of the UPR, I performed flow cytometry analysis of GFP and mCherry signals in CHO-7.1 cells transduced with pLJM1-K8α-puro-carrying lentiviruses in the presence of acute ER stress induced by the sarco/endoplasmic reticulum Ca^{2+} ATPase (SERCA) inhibitor thapsigargin [332]. As expected, 20 h treatment with 1 mM Tg increased GFP and XBP1s-mCherry signal, which indicates that Tg activates the PERK and IRE1 arms of the UPR and leads to the production of ATF4 and XBP1s, respectively (Fig. 12). GFP and XBP1s-mCherry were similarly induced in K-bZIP-expressing cells with no observable difference in fluorescence intensity compared to untransduced control cells (Fig. 12B). These results show that ectopic expression of K-bZIP does not affect GFP and XBP1s-mCherry expression in the CHO-7.1 model, which suggests that K-bZIP does not inhibit PERK and IRE1 activation, ATF4 expression and/or activity, and *Xbp1* splicing.

I questioned the validity of CHO cells as a model for studying UPR activation in the presence of KSHV-encoded protein products. KSHV is a human herpesvirus that is restricted to humans and only infects a limited range of human cells. KSHV does not naturally infect cells derived from other animals and cannot productively infect murine cells [333]. However, the UPR is conserved across mammalian cells and constitutes

72

Figure 11. **K-bZIP inhibits cGAS and STING-mediated induction of luciferase from an ISRE-containing promoter.** HEK293T cells were transfected with plasmids encoding K-bZIP, RFP-FLAG-cGAS, and STING for 48 h and firefly (B) and *Renilla* luciferase (C) relative light units (RLU) were measured using a luminometer. Data shown for four independent experiments. Error bars represent SEM. (A) Fold changes in luciferase expression between cells expressing K-bZIP alone or co-expressing RFP-FLAG-cGAS and STING were measured. Fold changes were normalized to empty vector (EV) cells not expressing cGAS and STING. A two-way ANOVA was done to determine statistical significance (*, p value < 0.05; **, p value < 0.01; ***, p value < 0.001; ****, p value < 0.0001).

Figure 11. **K-bZIP inhibits cGAS and STING-mediated induction of luciferase from an ISRE-containing promoter.**

Figure 12. **K-bZIP does not inhibit the PERK and IRE1 arms of the UPR.** Flow cytometry analysis of dual reporter CHO-7.1 cell line expressing GFP under the ATF4-responsive CHOP promoter or expressing an XBP1s-mCherry fusion protein. CHO-7.1 cells were transduced with empty vector (EV) or K-bZIP (K8) expressing lentiviruses for 72 hours and selected for with puromycin. Cells were then left untreated (DMSO) or treated with 1 mM Thapsigargin (Tg) to induce ER stress for 20 h. CHOP::GFP and XBP1s-mCherry signal was measured by flow cytometry on 10,000 cells per sample. (A) Tg treatment induces mCherry and GFP expression indicative of PERK and IRE1 activation (DMSO, orange; 1 mM Tg, blue). (B) K-bZIP does not reduce CHOP::GFP and XBP1s-mCherry expression in untreated and Tg-treated CHO-7.1 cells. Data shown for one independent experiment.

Figure 12. **K-bZIP does not inhibit the PERK and IRE1 arms of the UPR.**
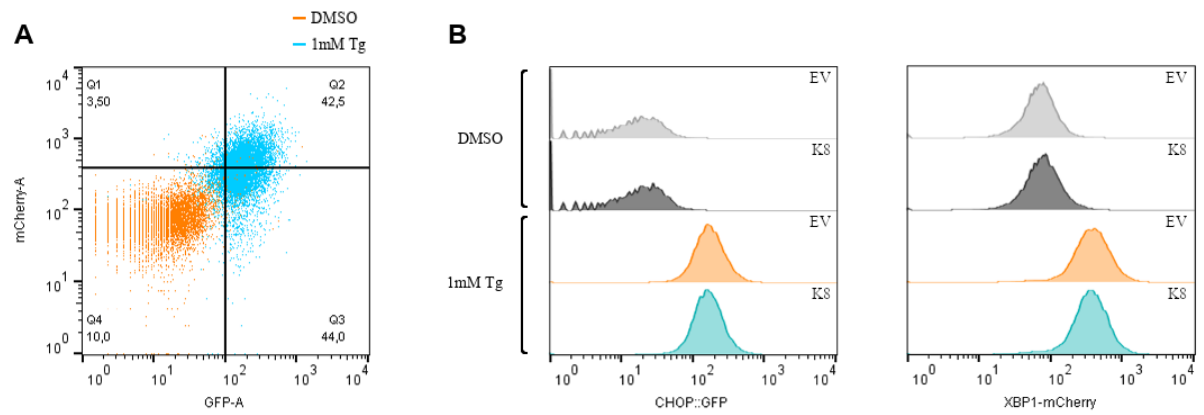
homologous sensors and effector molecules in human and other mammals [334]. Basic Local Alignment Search Tool (BLAST) analysis shows that human and Chinese hamster ATF4 share 87.5% aa sequence identity, human and Chinese hamster PERK share 90% aa identity, and human and Chinese hamster IRE1 share 94% aa identity. By contrast, mouse and human ATF4, PERK, and IRE1 share 86-92% aa sequence identity. Based on these similarities, Chinese hamster represents a model organism for studying the UPR in mammalian systems. Protein-protein and protein-DNA interactions often require recognition of specific binding sites and motifs that can vary between species due to nucleotide substitutions in gene promoters or amino acid differences between homologous proteins. Another limitation of the CHO-7.1 reporter cell line is that it does not allow us to measure ATF6 activation and transcriptional activity and XBP1s activity. I therefore decided to assess the expression levels of multiple UPR-responsive transcripts representative of all three arms of the UPR in human embryonic kidney HEK293A cells.

3.3 K-bZIP Does Not Affect the PERK, IRE1, and ATF6 Arms of the UPR in human (HEK293A) Cells

To test the hypothesis that K-bZIP inhibits the UPR in human cells, I assessed transcript levels of multiple UPR targets by RT-qPCR. I harvested RNA from HEK293A cells that were transduced with empty vector or K-bZIP and treated with 150 nM Tg for 4 h. I measured the fold changes in expression of the UPR-responsive target genes *HSPA5* (BiP), *HERPUD1*, *DDIT3* (CHOP), *EDEM1*, and *DNAJB9* (ERdj4) by RT-qPCR (Fig. 13A). *HSPA5*, *HERPUD1*, and *DDIT3* are transactivated by ATF6-N, XBP1s, and ATF4 to varying degrees [174,188–192]. *DNAJB9* and *EDEM1* are induced by XBP1s alone or ATF6-N/XBP1s heterodimers [174,187,239]. Tg induced the levels of all transcripts 2-40-fold compared to untreated cells (Fig. 13A) and increased the accumulation of XBP1s and BiP protein (Fig. 13B). *HERPUD1* and *DDIT3* transcript levels displayed the greatest induction with roughly 40-fold increase in levels following Tg treatment. *HSPA5* levels were induced 15-fold, whereas *EDEM1* and *DNAJB9* levels were only mildly induced by 2- and 7-fold, respectively.

As expected, Tg treatment did not affect the accumulation of K-bZIP protein (Fig. 13A). Ectopic expression of K-bZIP did not significantly reduce or increase the transcript

Figure 13. **K-bZIP does not inhibit the UPR**. HEK293A cells were transduced with empty vector (EV) or K-bZIP-expressing lentiviruses for 72 hours. Cells were then left untreated (DMSO) or treated with 150nM thapisgargin (Tg) to induce ER stress for 4 h and lysates were harvested for (A) RT-qPCR and (B) immunoblot analysis. (A) Expression of the ATF6-N-induced gene *HSPA5*, the ATF6-N- and XBP1s-induced genes *HERPUD1* and *EDEM1*, the PERK-induced gene *DDIT3*, and the XBP1s-induced gene *DNAJB9* were measured by RT-qPCR. Data shown for three independent experiments. Error bars represent SEM. Data was normalized to *GAPDH* mRNA and changes in fold expression were determined using the ΔΔCT method. A two-way ANOVA was done to determine statistical significance (*, p value < 0.05; **, p value < 0.01; ***, p value < 0.001; ****, p value < 0.0001). (B) Immunoblot analysis of K-bZIP (K8) and UPR markers BiP and XBP1s was performed. α-tubulin and β-actin were used as loading controls.

Figure 13. **K-bZIP does not inhibit the UPR**.
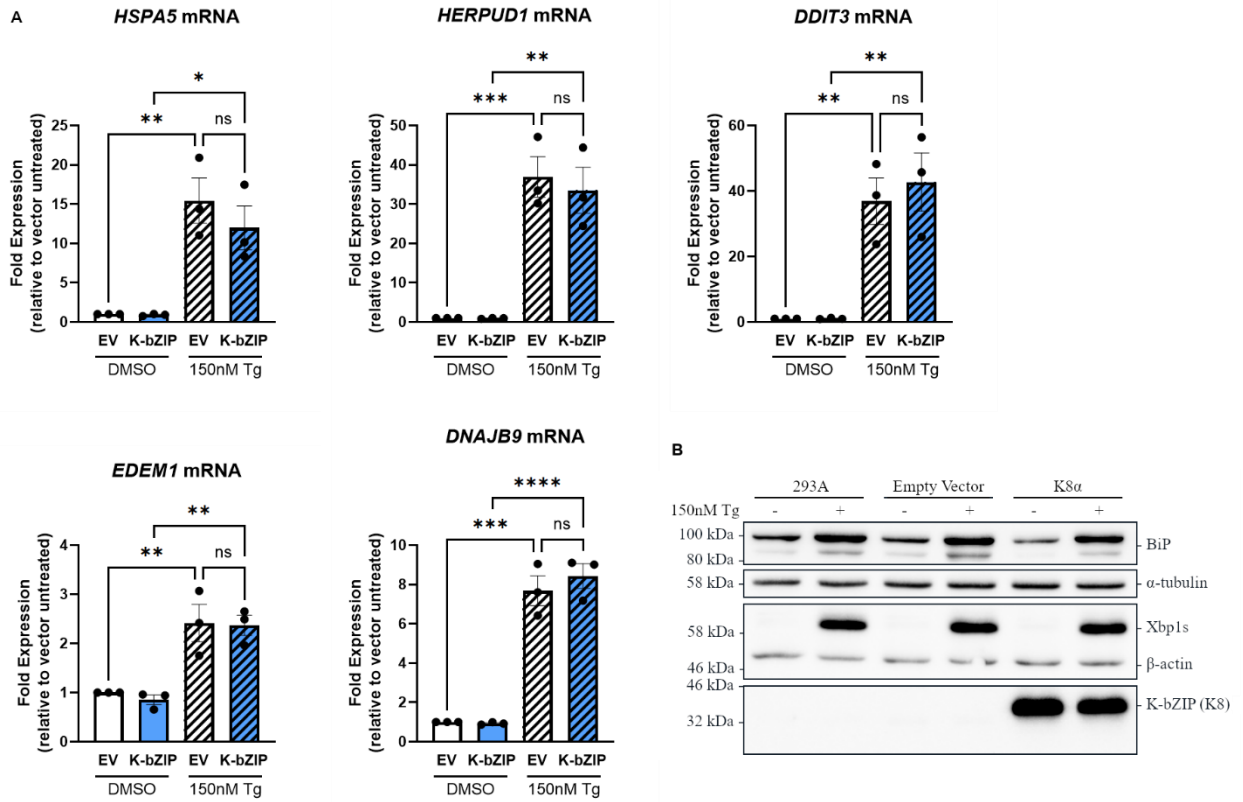
levels of any of the assessed UPR targets regardless of treatment (Fig. 13A). K-bZIP also did not reduce the accumulation of XBP1s and BiP protein (Fig. 13B), which suggests that K-bZIP does not interfere with the transcription and translation of BiP, as well as *Xbp1* splicing and translation. My RT-qPCR data and immunoblots therefore show that K-bZIP has no significant effect on the expression of UPR target genes. It is unclear if K-bZIP does not interact with the cellular bZIPs ATF4, ATF6-N, and XBP1s, or if a potential interaction with these transcription factors does not affect their ability to transactivate UPR targets. A lack of interaction is supported by data from other groups that previously showed that the bZIP domain of K-bZIP forms strong homodimers, but not heterodimers [256]. The interaction of K-bZIP with the cellular bZIP C/EBPα is also through the formation of higher-order oligomers rather than heterodimerization [264]. An interpretation of the qPCR data is limited by the small range of UPR targets I picked. I only assessed expression of five UPR-induced target genes, but the pool of UPR-induced genes is much larger and contains more than 50 different genes [174]. Furthermore, during authentic viral replication, the expression kinetics and repressive activity of K-bZIP are in part regulated by other viral proteins, including the serine/threonine protein kinase vPK [311] and ORF57 [94]. Ectopic expression of K-bZIP in isolation of other viral proteins does therefore not account for potential combinatorial effects. A more comprehensive approach to study the potential, K-bZIP-mediated inhibition of UPR target expression would be to perform RNA-sequencing in KSHV-infected cell lines using K-bZIP mutants that lack diverse functional domains. The phosphorylation- and SUMOylation-deficient T111A [311] and K158R [288] mutants, or the SIM-deficient L75A mutant [268] are well characterized.

3.4 EGFP-ATF6-N is Functional and Induces Luciferase Expression From ERSE-I

UPR TFs transactivate UPR-sensitive target genes by binding DNA motifs, such as the ERSEs. Contrary to assessing the expression levels of select targets, the transcriptional activity of ATF6-N, XBP1s, and ATF4 can also be studied by assessing transcription from a single DNA-binding motif. The best studied UPR-responsive motif is the 5'-CCAAT-N9-CCACG-3' ERSE-I that can be bound by ATF6-N and XBP1s [188]. We have a pGL4.26 firefly luciferase plasmid, pGL4.26 2XERSE, that contains a

minimal promoter and two back-to-back copies of the ERSE-I immediately upstream of the luciferase coding frame (Fig. 9B). Although ERSE elements in naturally occurring promoters, such as the *HSPA5* promoter, are separated by >10 bp spacers and never back-to-back, a single ERSE-I is enough to drive ATF6-N-specific expression of *xbp1*. As such, even if one of the ERSE-I motifs in pGL4.26 2XERSE would not be functional, the downstream luciferase gene could still be induced. pGL4.26 2XERSE does not contain any additional ERSEs or CRE-like consensus sites that allow ATF6-N, XBP1s, or ATF4 to bind. ATF6-N transactivates ERSE-I more strongly than XBP1s [174] because it has a higher affinity for ERSE-I than XBP1s [187]. To induce pGL4.26 2XERSE, I designed pEGFP-ATF6-N, a plasmid that encodes the first 373 aas of ATF6 that correspond to the proteolytically processed, 50 kDa bZIP ATF6-N. The N-terminal EGFP tag allows me to detect the transgene directly without detecting endogenous ATF6. ATF6-N can transactivate *xbp1*, but not mediate its splicing and translation to the transcriptionally active XBP1s [155]; in the absence of UPR stimulators, such as Tg, pEGFP-ATF6N and pGL4.26 2XERSE might therefore provide a means of studying the transactivation activity of ATF6-N separately from the IRE1 and PERK arms.

To confirm that EGFP-ATF6-N, the protein product of pEGFP-ATF6-N, can induce expression of its UPR targets, I harvested protein from HEK293A cells that were transfected with EGFP-ATF6-N or full-length ATF6 and treated with 150 nM Tg for 4 h and compared protein expression by immunoblotting (Fig. 14). EGFP-ATF6-N induced BiP protein accumulation regardless of Tg treatment, whereas full-length ATF6 only induced BiP expression following Tg treatment. EGFP-ATF6-N was able to induce XBP1u accumulation, and therefore *Xbp1* transcription, but was not able to elevate intracellular levels of the spliced product XBP1s. These results are consistent with previous findings that ATF6-N alone is not sufficient to direct *Xbp1* splicing in the absence of IRE1 activation [155]. Co-induction of ERSE-I by baseline XBP1s is probably minimal in the EGFP-ATF6-N/pGL4.26 2XERSE system.

To assess if EGFP-ATF6-N is sufficient to induce gene expression from ERSE-I in the absence of ER stress and UPR activation, I performed dual luciferase assays and measured firefly luciferase production from pGL4.26 2XERSE in HEK293T cells

Figure 14. **EGFP-ATF6-N induces UPR target gene expression in the absence of ER stress.** HEK293A cells were transfected with plasmids encoding EGFP, EGFP-ATF6-N, or full-length HA-ATF6 for 48 h. 4 h prior to harvesting lysates, cells were treated with 150 nM thapsigargin (Tg) or DMSO. Immunoblot analysis of exogenous ATF6 and UPR markers BiP and XBP1s/XBP1u was performed. α-tubulin and β-actin were used as loading controls.

Figure 14. **EGFP-ATF6-N induces UPR target gene expression in the absence of ER stress.**
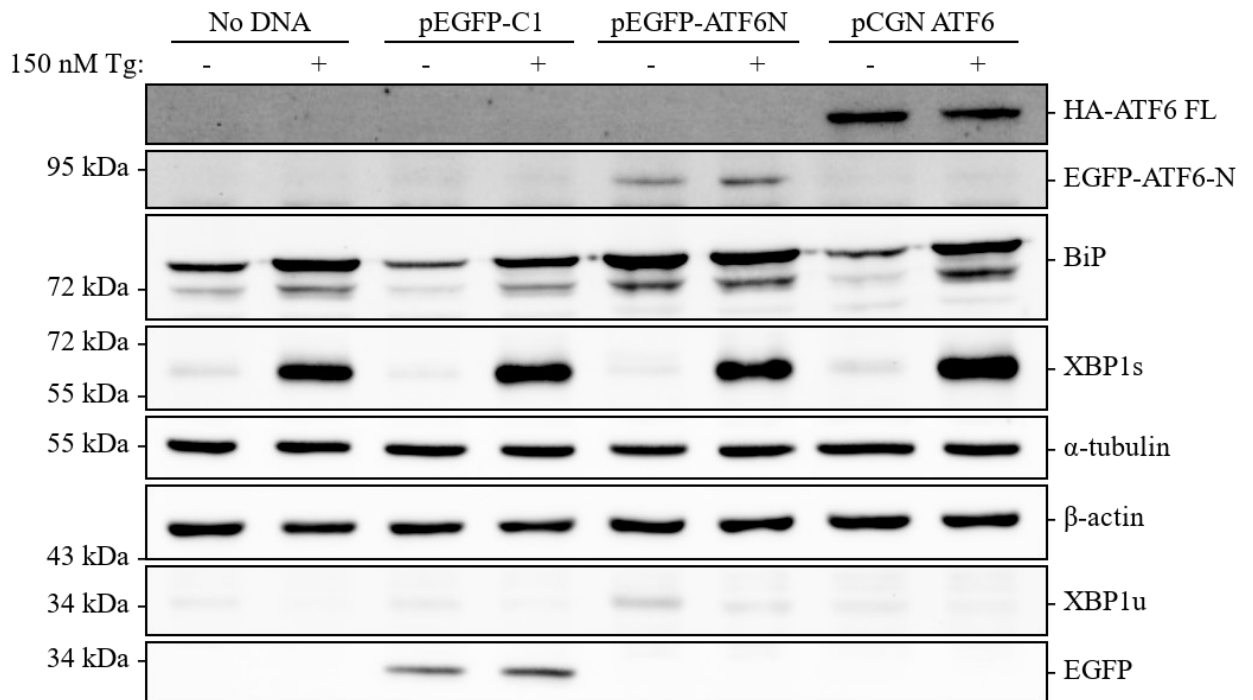
transfected with EGFP-ATF6-N. As a transfection control, I co-transfected a promoterless pGL4.74 *Renilla* luciferase plasmid (Fig. 9C). The pGL4.74 parent plasmid drives *Renilla* luciferase expression from the HSV TK promoter, but HSV TK and CMV promoters contain multiple 5'-TGAC-3' CRE half-sites that are ATF6-N-inducible. Removal of the HSV TK promoter from pGL4.74 reduced ATF6-N sensitivity (Fig. 17B). EGFP-ATF6-N induced firefly luciferase expression from ERSE-I ~20-fold compared to EGFP (Fig. 15A). These findings confirm that EGFP-ATF6-N is a functional, constitutively active transcription factor that can be used to induce ERSE-I in the absence of ER stress.

3.5 K-bZIP Does Not Affect the ATF6 Arm in HEK293T Cells

During lytic KSHV infection, viral proteins assemble into functional complexes. K-bZIP localizes to the nucleus in lytically infected cells and interacts with the viral proteins RTA [83,84,86,87], ORF36/vPK [311], and ORF57 [310]. K-bZIP regulates the transactivation activity of RTA to exert precise, temporal control over lytic gene expression [87] and is itself regulated by ORF36-mediated phosphorylation [311]. ORF57 might further assist K-bZIP with fine-tuning RTA-mediated gene expression [310]. I sought to assess the combined effects of K-bZIP and known viral interaction partners on the transactivation ability of ATF6-N. To this end, I co-transfected HEK293T cells with EGFP-ATF6-N and a combination of K-bZIP with RTA, ORF36, or ORF57 and assessed BiP protein levels by immunoblotting (Fig. 16) or measured firefly luciferase expression in cells also expressing pGL4.26 2XERSE (Fig. 15B). K-bZIP did not reduce EGFP-ATF6-N and BiP protein accumulation alone or in combination with RTA, ORF36, or ORF57. Likewise, K-bZIP did not reduce firefly luciferase expression from ERSE-I alone or in combination with ORF36 or ORF57. These findings are consistent with my flow cytometry and RT-qPCR data and collectively show that K-bZIP is not an inhibitor of the UPR.

The effect of RTA expression on ATF6-N transactivation could not be assessed, because RTA consistently induced *Renilla* luciferase expression above background (Fig. 17B). RTA might be able to induce *Renilla* expression because pGL4.74[*hRluc*/TK] contains RTA-responsive elements (RREs). These RREs have a consensus of

Figure 15. **K-bZIP does not inhibit ATF6-N transcriptional activity alone or in combination with known viral interaction partners**. HEK293T cells were transfected with plasmids encoding EGFP, EGFP-ATF6-N, K-bZIP (K8), FLAG-RTA, HA-ORF36, and HA-ORF57 for 48 h and firefly and *Renilla* luciferase relative fluorescent units (RFU) were measured using a luminometer. (A) Exogenous EGFP-ATF6-N induces an ATF6-responsive tandem (2X) ER stress response element (ERSE) luciferase construct. The ERSE constitutes the CCAAT-N(9)-CCACG upstream activating sequence that facilitates binding to ATF6-N, but not XBP1s. (B) K-bZIP does not affect ATF6-N-mediated transcription of firefly luciferase alone or in combination with viral proteins, but ORF57 alone significantly increases firefly luciferase production. Data shown for four independent experiments. Error bars represent SEM. Fold changes in luciferase expression were normalized to (A) EGFP and (B) EGFP-ATF6-N (EV). A two-way ANOVA (B) or Student's t-test (A) was done to determine statistical significance (*, p value < 0.05; **, p value < 0.01; ***, p value < 0.001; ****, p value < 0.0001).

Figure 15. **K-bZIP does not inhibit ATF6-N transcriptional activity alone or in combination with known viral interaction partners**.
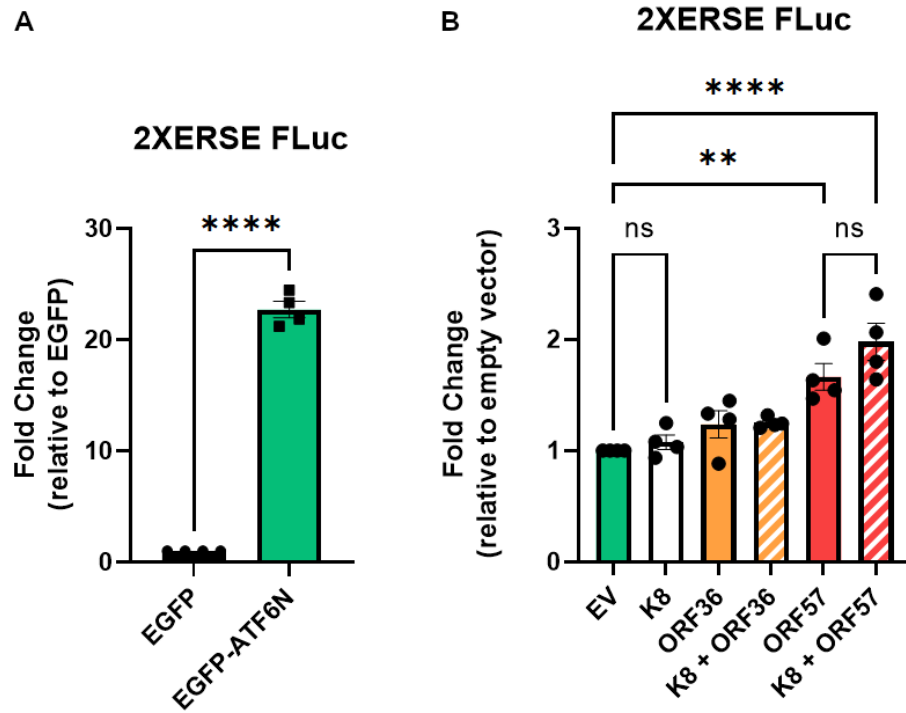
5'-CC-N$_9$-GG-3' and are found in multiple viral promoters, including those of the genes encoding ORF57 and PAN [335]. Several of these RRE consensus sequences are also present on pGL4.26 2XERSE. RTA alone did not increase BiP accumulation (Fig. 16), suggesting that RTA does not transactivate BiP and does not modulate the transactivation activity of ATF6-N.

ORF57 enhanced EGFP-ATF6-N-mediated luciferase expression from ERSE-I 0.6-fold (Fig. 15B, Fig. 18). Although the change in firefly luciferase expression was statistically significant, it was subtle. Co-expression with K-bZIP did not further augment firefly luciferase expression, suggesting that this increase is dependent on ORF57 and not K-bZIP (Fig. 15B). ORF57 is an RNA-binding protein that enhances the translation of viral RNAs by facilitating their nuclear export [89–91,336], protecting them from RNA decay [92,93], and promoting their splicing by interaction with the spliceosome [94]. Indeed, ORF57 enhanced K-bZIP protein levels when both viral proteins were co-expressed but did not increase the accumulation of cellular proteins (Fig. 16). ORF57-mediated post-transcriptional regulation has not been identified for cellular transcripts, and, unlike RTA, ORF57 only increased firefly but not *Renilla* luciferase expression (Fig. 18B & C). Furthermore, ORF57 required concurrent EGFP-ATF6-N expression to enhance firefly luciferase expression, suggesting that ORF57 increases the transactivation activity of EGFP-ATF6-N (Fig. 18B). ORF57 is not a transcription factor but has been shown to assist RTA in activating RRE-containing viral promoters, including those encoding PAN and ORF59 [337,338]. In several lymphoma cell lines, ORF57 only enhanced RTA-mediated transactivation, but was not able to induce promoters on its own [338]. My data similarly shows that ORF57 was not able to induce expression from ERSE-I on its own and required co-expression of EGFP-ATF6-N (Fig. 18B). Previous research also shows that in some select cell lines, including HEK293 cells, ORF57 can induce viral promoters independently of RTA [338]. This might explain why ORF57 augmented transactivation of ERSE-I in the absence of RTA but does not explain the dependence on EGFP-ATF6-N. Co-immunoprecipitation or GST-pull-down experiments could identify a potential interaction between ORF57 and ATF6-N to assess if the mechanism by which ORF57 enhances ATF6-N activity is through direct interaction.

Figure 16. **K-bZIP does not inhibit BiP expression alone or in combination with known viral interaction partners.** HEK293T cells were transfected with plasmids encoding EGFP, EGFP-ATF6-N, K-bZIP (K8), FLAG-RTA, HA-ORF36, and HA-ORF57 for 48 h and lysates were harvested for immunoblot analysis for EGFP-ATF6-N, UPR marker BiP, and viral proteins. α-tubulin and β-actin were used as loading controls.

Figure 16. **K-bZIP does not inhibit BiP expression alone or in combination with known viral interaction partners.**
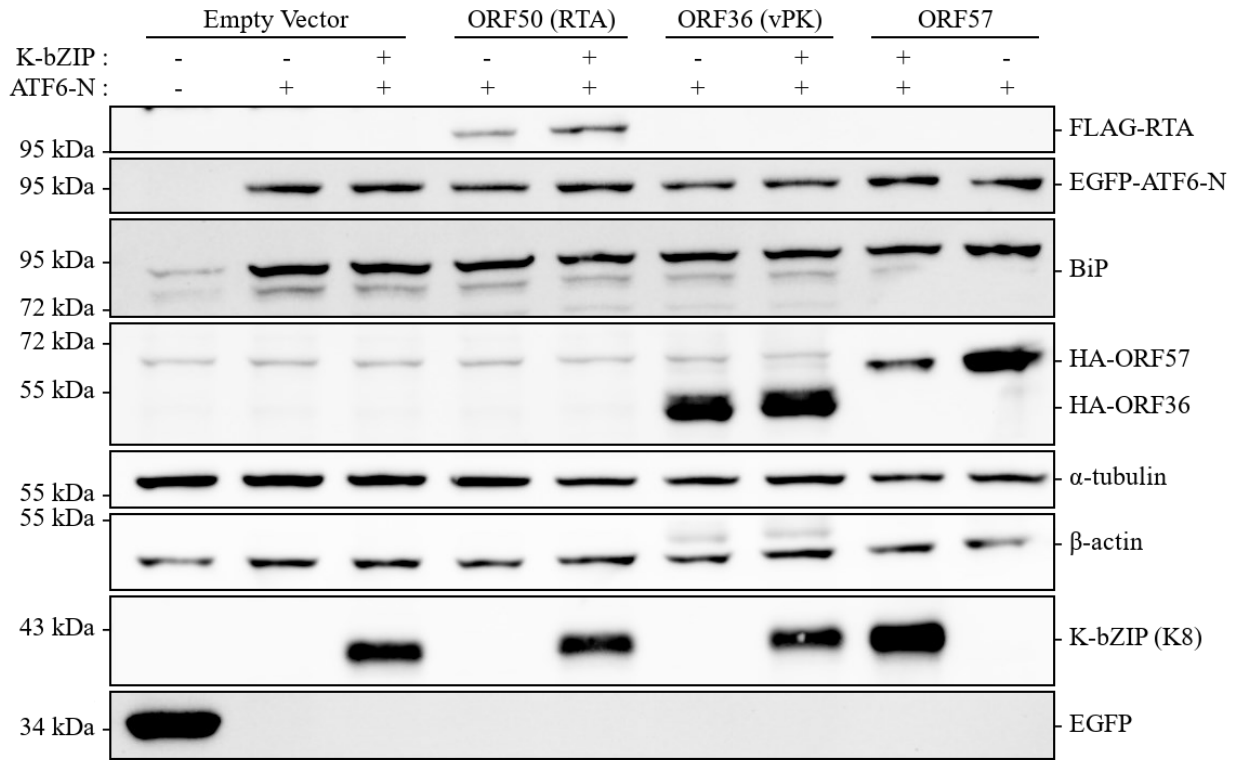
Figure 17. **RTA induces pGL4.26 2XERSE firefly and pGL4.74 *Renilla* luciferase plasmids.** HEK293T cells were transfected with plasmids encoding EGFP, EGFP-ATF6-N, K-bZIP (K8), FLAG-RTA, HA-ORF36, and HA-ORF57 for 48 h and firefly and *Renilla* luciferase relative fluorescent units (RFU) were measured using a luminometer. (A) RTA and ORF57 induce an ATF6-responsive 2XERSE luciferase construct in the presence of exogenous ATF6-N. (B) RTA induces luciferase expression from the promoterless pGL4.74 *Renilla* internal control plasmid. Data shown for three out of four independent experiments. Error bars represent SEM.

Figure 17. **RTA induces pGL4.26 2XERSE firefly and pGL4.74 *Renilla* luciferase plasmids.**
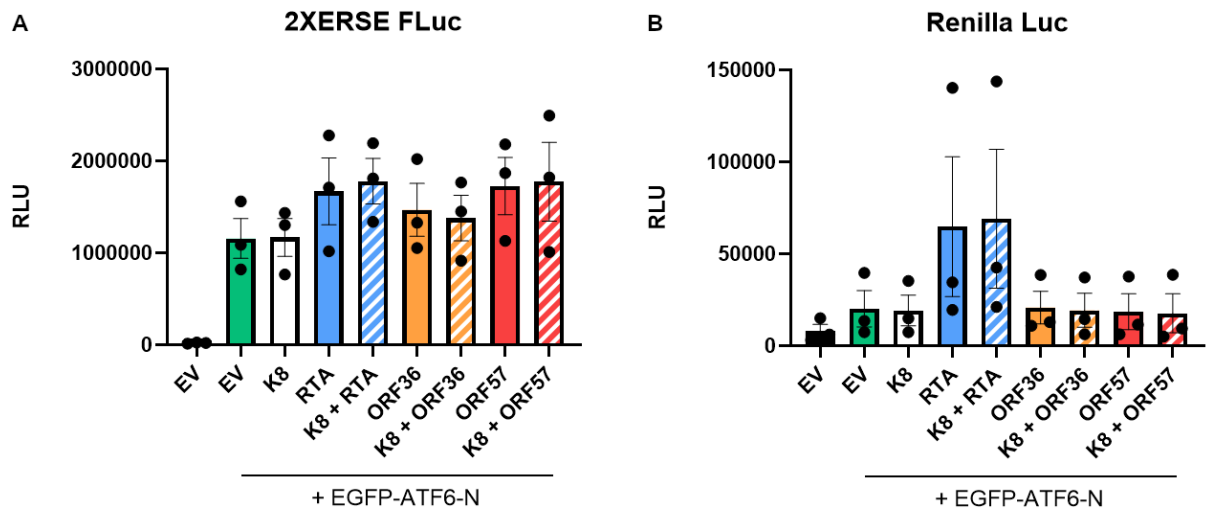
Figure 18. **ORF57 enhances the ATF6-N-mediated activation of luciferase from an ERSE-containing promoter.** HEK293T cells were transfected with plasmids encoding EGFP, EGFP-ATF6-N, and HA-ORF57 for 48 h and firefly (B) and *Renilla* luciferase (C) relative light units (RLU) were measured using a luminometer. Data shown for four independent experiments. Error bars represent SEM. (A) Fold changes in luciferase expression between cells expressing EGFP-ATF6-N alone or co-expressing EGFP-ATF6-N and ORF57 were measured. Fold changes were normalized to EGFP-ATF6-N. Student's t-test (A), or two-way ANOVA (B & C) was done to determine statistical significance (*, p value < 0.05; **, p value < 0.01; ***, p value < 0.001; ****, p value < 0.0001).

Figure 18. **ORF57 enhances the ATF6-N-mediated activation of luciferase from an ERSE-containing promoter.**
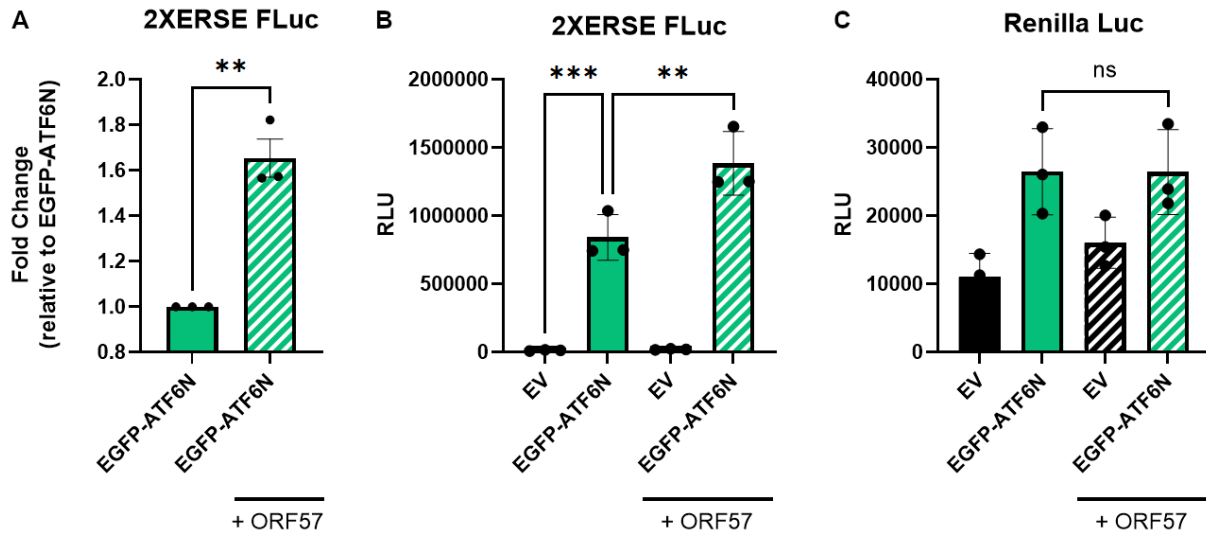
3.6 ATF6-N Localizes to the Nuclei of KSHV-infected Cells

Lytic KSHV replication activates the ATF6, IRE1, and PERK sensors of the UPR, but suppresses the expression of UPR-responsive target genes by preventing the accumulation of the UPR-governing TFs ATF4, XBP1s, and CHOP. ATF6-N activation and cleavage are not affected by lytic replication, but despite its proper proteolytic processing, the expression of its canonical target BiP is suppressed by an unknown mechanism [286]. My RT-qPCR and luciferase experiments assumed a transcriptionally active ATF6-N, but we do not know whether ATF6-N retains its transactivation activity in KSHV-infected cells. ATF6-N, like all transcription factors, requires nuclear import to access DNA. It is currently unknown if ATF6-N properly localizes to the nuclei of KSHV-infected cells. If ATF6-N nuclear import were impaired in KSHV-infected cells, this would explain why ATF6-N targets fail to accumulate during lytic replication.

To assess if ATF6-N localizes to the nuclei of KSHV-infected cells, I used a nuclear and cytoplasmic fractionation protocol that separates the ER from the nuclei and allows me to distinguish between the ER-resident ATF6 and the nuclear ATF6-N [326]. We have two KSHV-infected cell lines, renal carcinoma iSLK.219 cells and B-cell lymphoma PEL TREx-BCBL1-RTA cells, that contain a chromosomal RTA transgene under the control of the tetracycline operator from which KSHV reactivation can be controlled by addition of doxycycline [323,324]. I assessed the nuclear accumulation of ATF6-N in doxycycline-treated iSLK.219 and TREx-BCBL1-RTA cells that were treated with Tg for 4 h and analyzed the accumulation of ATF6-N targets BiP and calreticulin by immunoblotting (Fig. 20 & 21). Expression of endogenous ATF6 is very low in iSLK.219 cells despite Tg treatment (Fig. 20). I therefore also fractionated iSLK.219 cells that were transduced with full-length ATF6 or ATF6-N prior to reactivation with doxycycline (Fig. 19). The ~70 kDa ATF6-N accumulated in the nuclear fraction of iSLK.219 and TREx-BCBL1-RTA cells regardless of treatment (Fig. 19, 20 & 21), which suggests that KSHV does not interfere with the proper nuclear localization of ATF6-N. As expected, ATF6 was not processed into ATF6-N in the absence of ER stress and UPR induction (Fig. 19). Protein levels of ectopically expressed full-length and N-terminal ATF6 were significantly higher in iSLK.219 cells undergoing lytic KSHV replication

Figure 19. **Lytic KSHV replication diminishes BiP accumulation but does not affect the nuclear localization of ectopically expressed ATF6-N in iSLK.219 cells.** iSLK.219 cells were transduced with lentiviruses encoding empty vector (EV), HA-ATF6 full-length (FL), or HA-ATF6-N at MOIs of 7 for 24 h. Cells were then left untreated (DMSO) or reactivated with 1 μg/mL doxycycline for 48 h and lysates were harvested for immunoblot analysis of HA-ATF6, UPR markers BiP and calreticulin, and viral proteins. α-tubulin (cytoplasmic), calnexin (ER), LaminA/C (nuclear), and histone H3 (nuclear) were used as loading controls.

Figure 19. **Lytic KSHV replication diminishes BiP accumulation but does not affect the nuclear localization of ectopically expressed ATF6-N in iSLK.219 cells.**
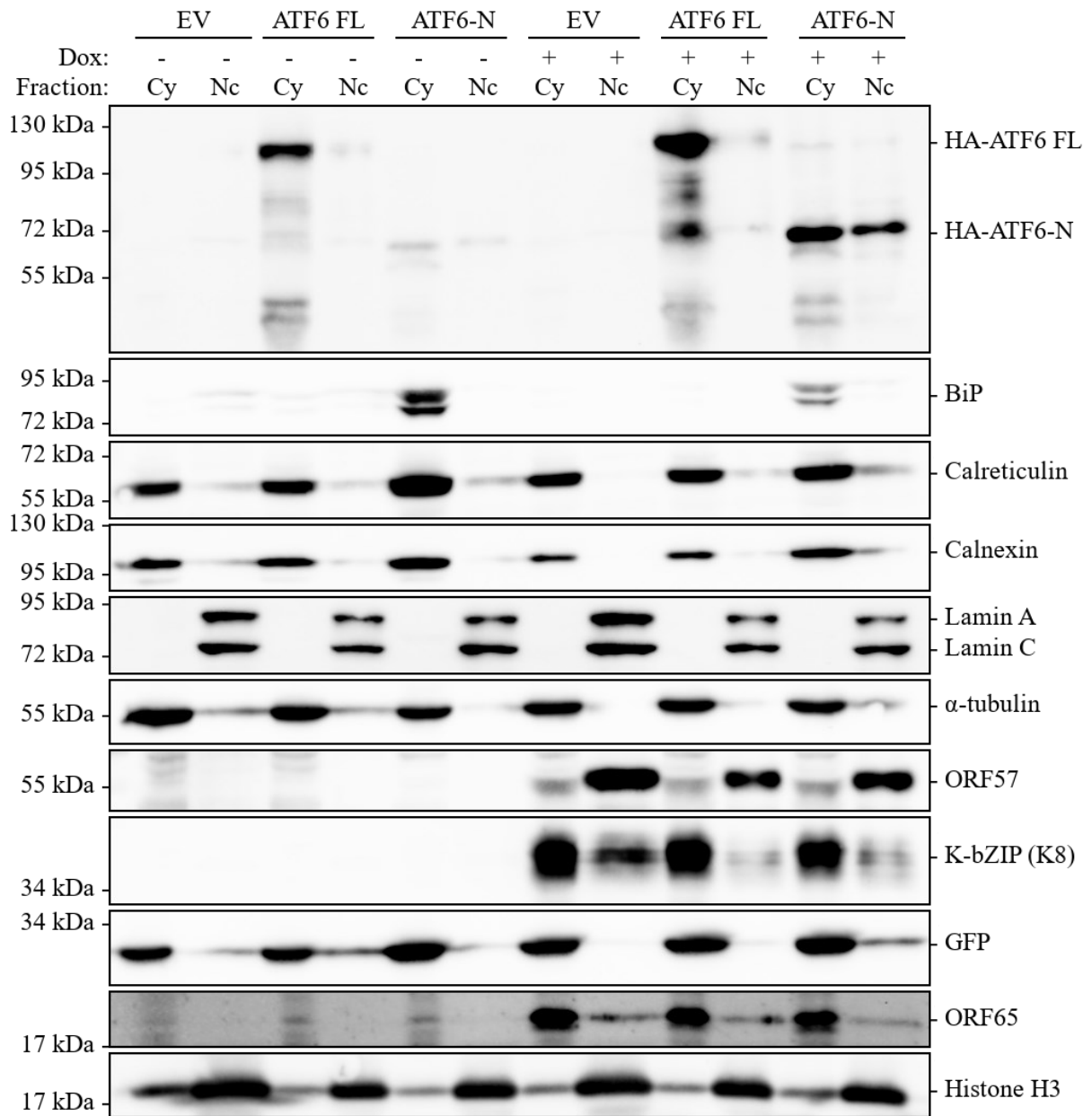
Figure 20. **Lytic KSHV replication diminishes BiP accumulation but does not affect the nuclear localization of stress-induced ATF6-N in iSLK.219 cells.** iSLK.219 cells were left untreated (DMSO) or reactivated with 1 μg/mL doxycycline for 44 h. After 44 h, cells were left untreated (DMSO) or treated with 150 nM thapsigargin for 4h and lysates were harvested for immunoblot analysis of ATF6, UPR markers BiP and calreticulin, and viral proteins. α-tubulin (cytoplasmic), calnexin (ER), LaminA/C (nuclear), and histone H3 (nuclear) were used as loading controls.

Figure 20. **Lytic KSHV replication diminishes BiP accumulation but does not affect the nuclear localization of stress-induced ATF6-N in iSLK.219 cells.**
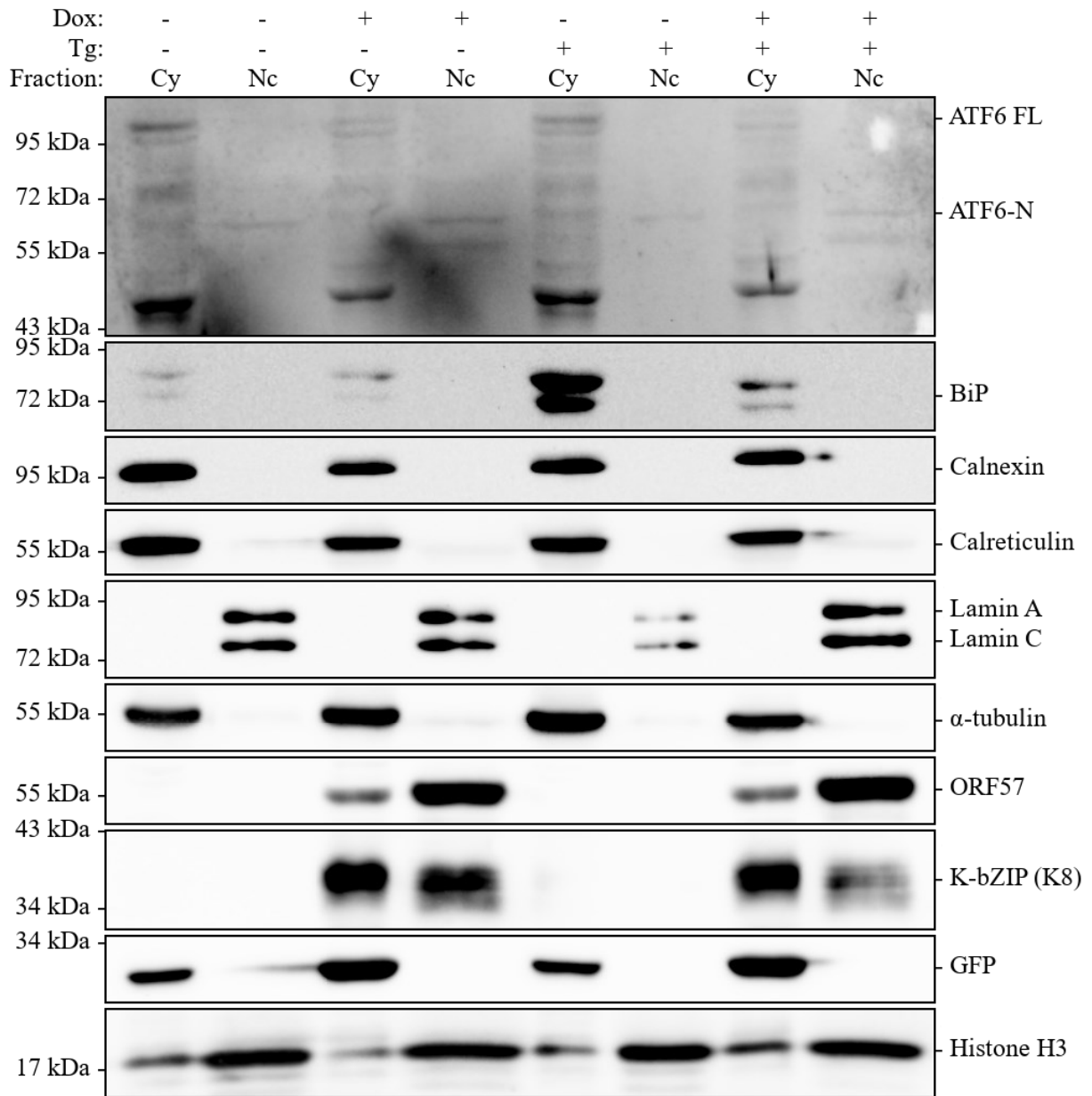
Figure 21. **Lytic KSHV replication does not affect the nuclear localization of stress-induced ATF6-N in TREx-BCBL1-RTA cells.** TREx-BCBL1-RTA cells were left untreated (DMSO) or reactivated with 1 μg/mL doxycycline and 1 mM sodium butyrate for 44 h. After 44 h, cells were left untreated (DMSO) or treated with 250 nM thapsigargin for 4h and lysates were harvested for immunoblot analysis of ATF6, UPR markers BiP and calreticulin, and viral proteins. α-tubulin (cytoplasmic), calnexin (ER), LaminA/C (nuclear), and histone H3 (nuclear) were used as loading controls.

Figure 21. **Lytic KSHV replication does not affect the nuclear localization of stress-induced ATF6-N in TREx-BCBL1-RTA cells.**
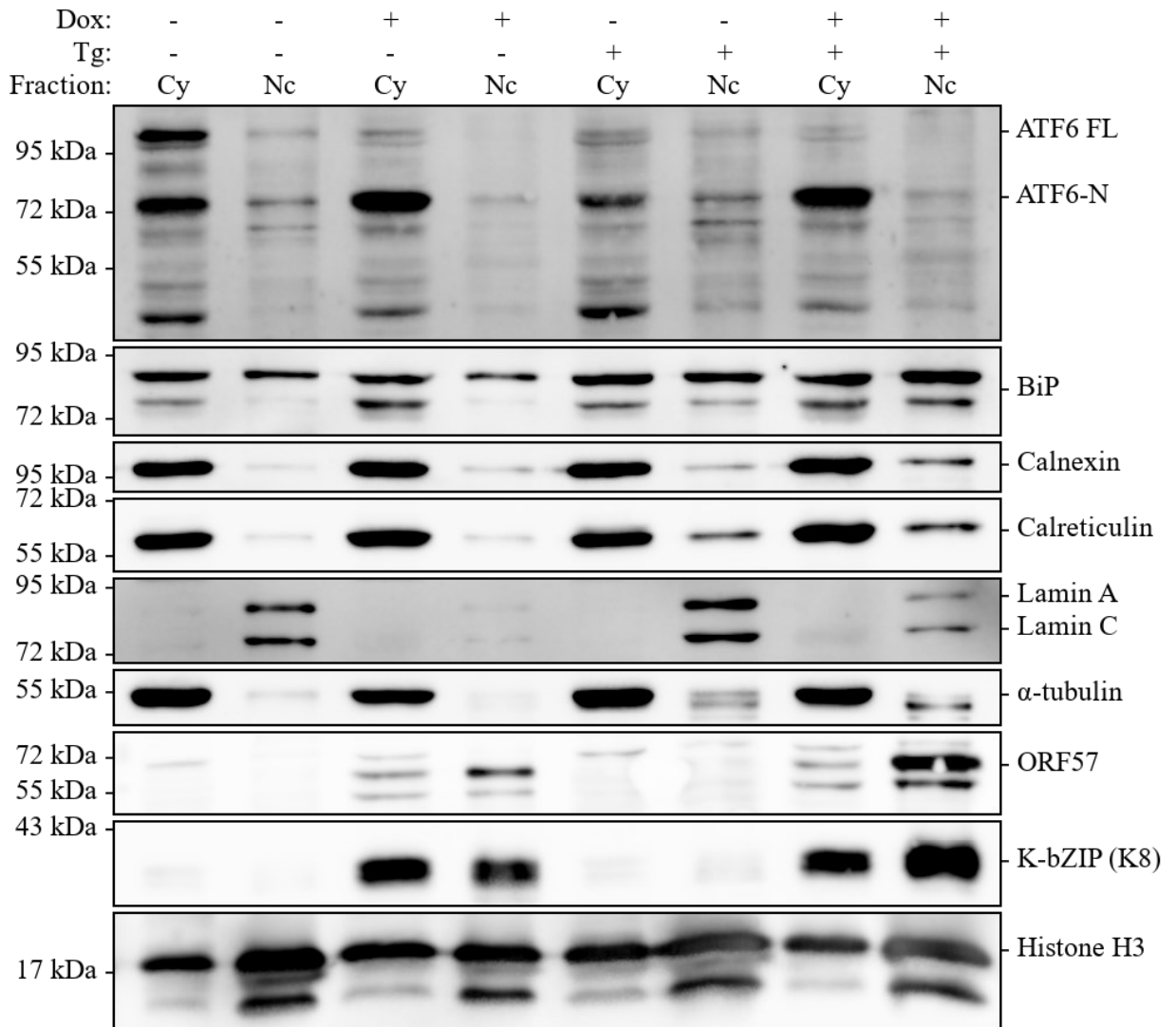
than in latently infected cells (Fig. 19). In this experiment, ATF6 was expressed from the CMV promoter, which contains an RRE sequence and may therefore be RTA-inducible. As such, RTA might have upregulated full-length ATF6 and ATF6-N expression in cells undergoing lytic replication, but not in latently infected cells lacking RTA. Consistent with previous observations, protein levels of the ATF6-N target BiP were enriched in latently infected iSLK.219 cells but were diminished upon reactivation with doxycycline (Fig. 19 & 20). Transiently expressed ATF6-N accumulated to high levels in reactivated iSLK.219 cells, most likely because viral transcription factors can enhance the expression of ATF6-N from the CMV promoter. Despite the elevated concentration of ATF6-N in cells undergoing lytic replication, BiP protein levels were markedly reduced under these conditions. By comparison, BiP accumulated to higher levels in latently infected iSLK.219 cells in which ATF6-N concentrations were lower than in the lytic populations (Fig. 19). Accumulation of the ER-resident chaperone and ATF6-N target calreticulin was only increased when ATF6-N was overexpressed and was not reduced during lytic replication (Fig. 16). The *CALR* promoter contains three ERSE-I sequences that allow for ATF6-N and XBP1s binding [188] (Fig. 5), but contains additional binding elements for other transcription factors, including Sp1 and adaptor protein complex 2 (AP-2) [339] and is responsive to intracellular calcium concentrations and heat shock [340]. Calreticulin expression is therefore augmented by, but not dependent on, ER stress and UPR activation.

TREx-BCBL1-RTA cells displayed different protein expression patterns than iSLK.219 cells. 250 nM Tg did not visibly increase BiP accumulation in TREx-BCBL1-RTA cells (Fig. 21), whereas 150 nM Tg were sufficient to upregulate BiP expression in iSLK.219 cells (Fig. 20). Interpretation of the TREx-BCBL1-RTA immunoblots is limited by significant spill-over of cytosolic and ER-resident proteins into the nuclear fraction (Fig. 21). It is therefore possible that Tg treatment enhanced BiP accumulation, but loss of BiP from the cytosolic fraction may have perturbed this phenotype. It is also possible that BCBL cells are more refractory to Tg treatment than SLK cells. Research shows that myeloid differentiation and tumorigenesis affect expression of SERCA isoforms, which are produced from three different genes (SERCA 1, 2, and 3) by alternative splicing. SERCA isoforms are differentially expressed across cell types and

multiple isoforms can be expressed concurrently [341,342]. SERCA expression kinetics and levels may therefore differ between TREx-BCBL1-RTA and iSLK.219 cells and may result in different Tg-sensitivities. Viral protein levels were also differently affected in the two cell lines. Endogenous and exogenous expression of ATF6-N reduced nuclear but not cytosolic accumulation of K-bZIP in iSLK.219 cells. By contrast, ATF6-N did not reduce the nuclear accumulation of ORF57 (Fig. 19 & 20). Conversely, Tg treatment increased nuclear but not cytosolic accumulation of K-bZIP and ORF57 in TREx-BCBL1-RTA cells, but this phenotype could be a result of the loss of cytosolic protein and spill-over into the nuclear fraction during fractionation (Fig. 21). At this point, I cannot conclude whether UPR activation indeed increases viral protein levels in TREx-BCBL1-RTA cells. Diminished accumulation of K-bZIP in the nuclear fraction was, however, consistently observed in ATF6-N-expressing iSLK.219 cells (Fig. 19 & 20). Whole protein levels of K-bZIP were not decreased by ATF6-N overexpression, suggesting that ATF6-N interferes with the nuclear import of K-bZIP and not its expression (Fig. 23). This is further supported by RT-qPCR data that shows that ATF6-N overexpression does not affect the accumulation of the K8α transcript in iSLK.219 cells (Fig. 24). K-bZIP contains a classical nuclear localization signal (NLS) with a sequence similar to the NLS of the SV40 large T antigen [306,343] and utilizes the importin family of proteins for nuclear import. Because ATF6-N and its targets have not been implicated in the regulation of nuclear import, it is unlikely that they interfere with the nuclear import of K-bZIP by interacting with the nuclear import machinery. A recent study demonstrated that nuclear import of RTA can be impaired by phosphoribosylformyl-glycinamidine synthetase (PFAS) mediated deamidation of asparagine residues critical to the nuclear localization of RTA [344]. It is possible that PTM of K-bZIP could likewise mask its NLS and inhibit or slow import. Compared to K-bZIP, ORF57 localized to the nuclei of iSLK.219 cells normally regardless of ATF6-N overexpression or UPR induction (Fig. 19 & 20), but ORF57 also contains three NLS and may be more refractory to NLS masking [345]. Further studies are required to determine if UPR activation interferes with the nuclear import of additional viral proteins.

3.7 ATF6-N Inhibits rKSHV.219 in a Dose-Dependent Manner

K-bZIP is indispensable for efficient viral DNA replication and virion production [290] and directs viral lytic gene expression by modulating RTA transactivation [83,87]. Because the functions of K-bZIP require proper nuclear localization, it is possible that ATF6-N-mediated reduction of K-bZIP nuclear accumulation is detrimental to virion production. ATF6-N may therefore be antiviral to KSHV in iSLK.219 cells. To assess if ATF6-N has antiviral activity, I transduced iSLK.219 cells with ATF6-N at increasing MOIs (1, 2, 5 & 10; Fig. 23) and maximized viral reactivation and virion production by 96 h treatment with doxycycline and the HDAC inhibitor sodium butyrate. rKSHV.219 constitutively expresses GFP under control of the elongation factor 1-α (EF-1-α) promoter [346]; GFP expression from rKSHV.219-infected cells therefore directly correlates with viral titers. I subsequently infected HEK293A cells with virus-containing supernatants and quantified viral titers by flow cytometry. ATF6-N overexpression reduced viral titers in a dose-dependent manner, suggesting that ATF6-N is antiviral to rKSHV.219 (Fig. 22). At MOI 10 of ATF6-N, viral titers were reduced 0.6-fold over cells transduced with an empty control construct at the same MOI (Fig. 22A). This data contradicts previous findings that ATF6 inhibition with the selective ATF6 inhibitor Ceapin-A7 reduces viral titers from iSLK.219 cells [286]. Johnston and colleagues observed this pro-viral effect at steady-state levels of ATF6 in cells not experiencing ER stress, whereas I observed an antiviral effect at higher than physiological concentrations of ATF6-N. It is therefore possible that ATF6-N is pro-viral at low concentrations and antiviral at high concentrations. Interestingly, Johnston and colleagues also found that XBP1s overexpression reduces viral titers of rKSHV.219 in a dose-dependent manner. ATF6-N and XBP1s can both induce gene expression from ERSE-I and ERSE-II and share multiple target genes as a result [174,187]. As such, high concentrations of ATF6-N and XBP1s protein might reduce rKSHV.219 virion production by similar mechanisms. Because ATF6-N and XBP1s can also synergistically activate UPR-responsive target genes as heterodimers [174,239], assessing rKSHV.219 titers from cells co-expressing ATF6-N and XBP1s at various concentrations could help determine if ATF6-N and XBP1s act in concert to reduce the efficiency of virion production from iSLK.219 cells. I do not assume that ATF6-N overexpression would reduce virion production from

Figure 22. **ATF6-N inhibits KSHV production in a dose-dependent manner.**
iSLK.219 cells were transduced with lentiviruses encoding empty vector (EV) or HA-ATF6-N at MOIs of 1, 2, 5, or 10 for 24 h. After 24 h, cells were treated with 1 μg/mL doxycycline and 1 mM sodium butyrate to reactivate rKSHV.219 for 96 h, and virus-containing supernatants were harvested. Supernatants were serially diluted (1/2 - 1/64 or 1/8 - 1/512) and HEK293A cells were spinoculated with diluted supernatants at 800 x g at 30°C for 2 h and subsequently incubated for 20h. Infected cells were then fixed with 4% formaldehyde and GFP signal was measured by flow cytometry on 50,000 events per sample. Fold changes represent the ratio of virus titer in IU/mL of empty vector (EV) to HA-ATF6-N at the same MOI. A two-way ANOVA was done to determine statistical significance (*, p value < 0.05; **, p value < 0.01; ***, p value < 0.001; ****, p value < 0.0001).

Figure 22. **ATF6-N inhibits KSHV production in a dose-dependent manner.**
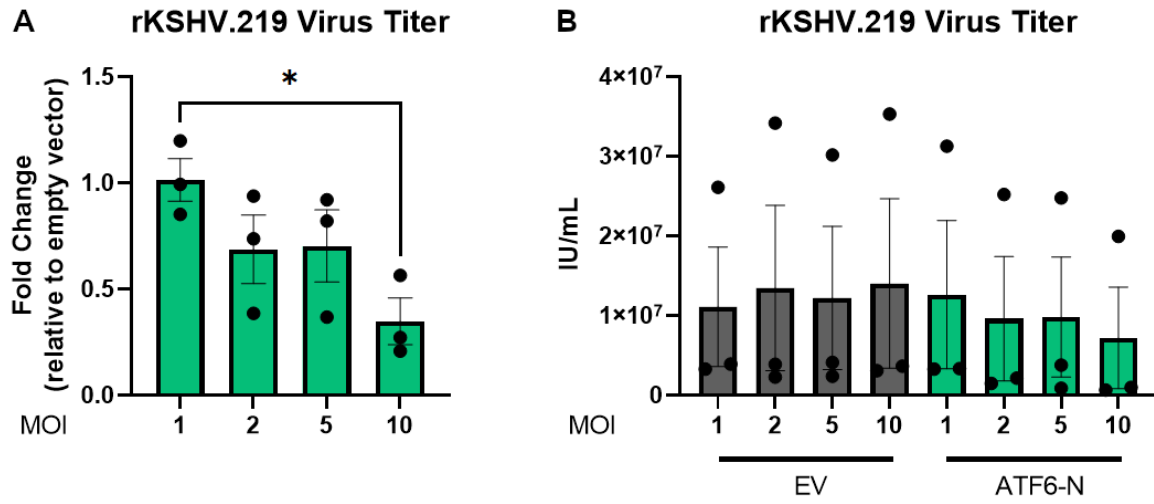
Figure 23. **Ectopic expression of ATF6-N does not affect total protein levels of K-bZIP.** iSLK.219 cells were transduced with lentiviruses encoding empty vector (EV) or HA-ATF6-N at MOIs of 1, 2, 5, or 10 for 24 h. After 24 h, cells were left untreated (DMSO) or reactivated with 1 μg/mL doxycycline and 1 mM sodium butyrate for 48 h and lysates were harvested for immunoblot analysis of HA-ATF6-N, BiP, and viral targets. α-tubulin was used as the loading control.

Figure 23. **Ectopic expression of ATF6-N does not affect total protein levels of K-bZIP.**
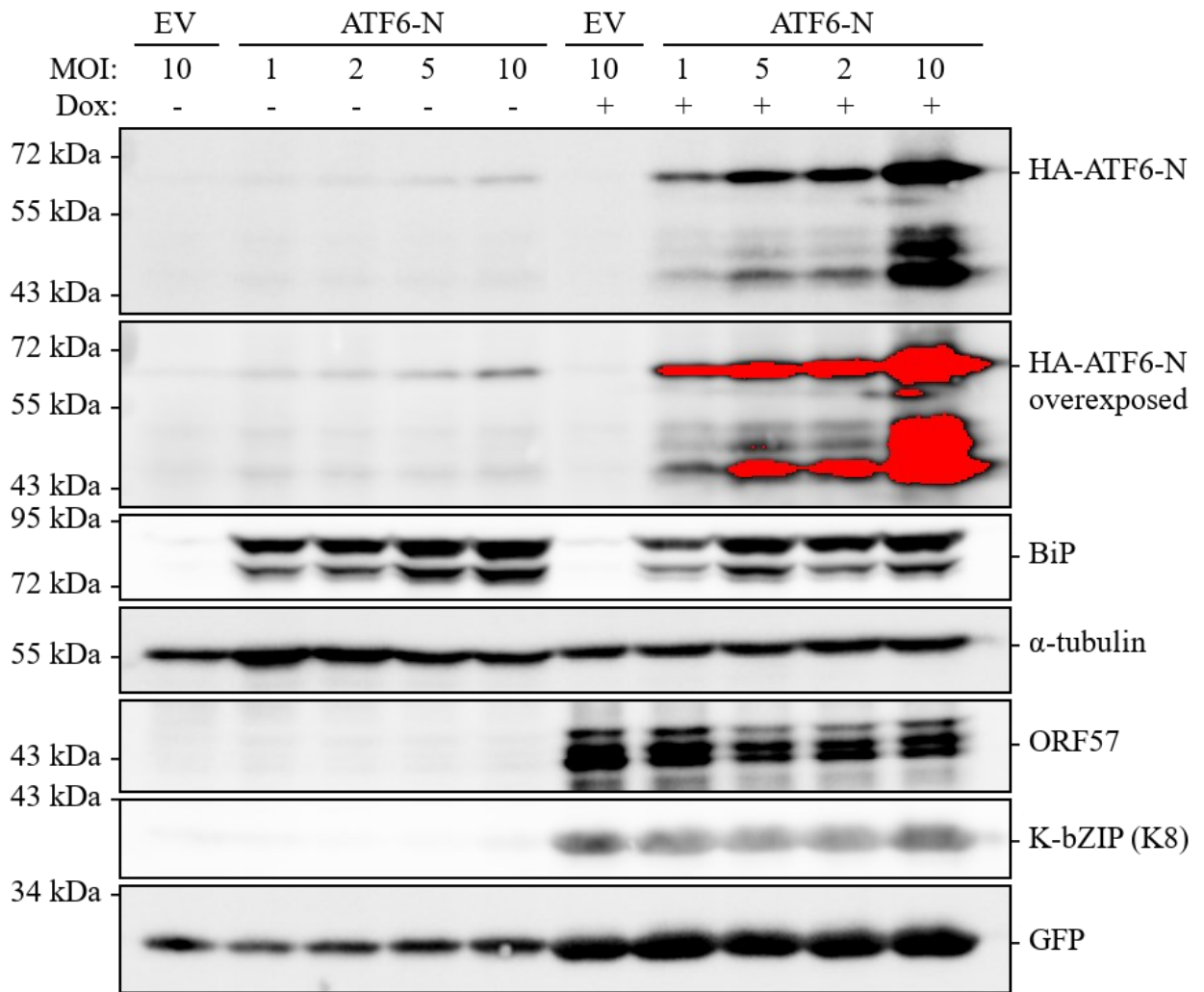
Figure 24. **Ectopic expression of ATF6-N does not reduce viral transcript levels.** iSLK.219 cells were left untransduced or transduced with lentiviruses encoding empty vector or HA-ATF6-N at MOIs of 1 or 10 for 24 h. After 24 h, cells were treated with 0.2% DMSO or reactivated with 1 μg/mL doxycycline for 44 h (untransduced cells) or 48 h (transduced cells). Untransduced cells were left untreated (DMSO) or treated with 150 nM thapsigargin (Tg) to induce ER stress for 4 h prior to harvest. 48h post-reactivation, cells were harvested, and expression of viral transcripts was measured by RT-qPCR. Data shown for one independent experiments. Data was normalized to *18S* rRNA and changes in fold expression were determined using the ΔΔCT method. Fold changes were calculated relative to control cells, empty vector of the same MOI for transduced cells, or relative to untreated (DMSO) for drug-treated samples. Expression of the indicated target transcripts in control cells were set to 1, as indicated by the dashed line.

Figure 24. **Ectopic expression of ATF6-N does not reduce viral transcript levels.**
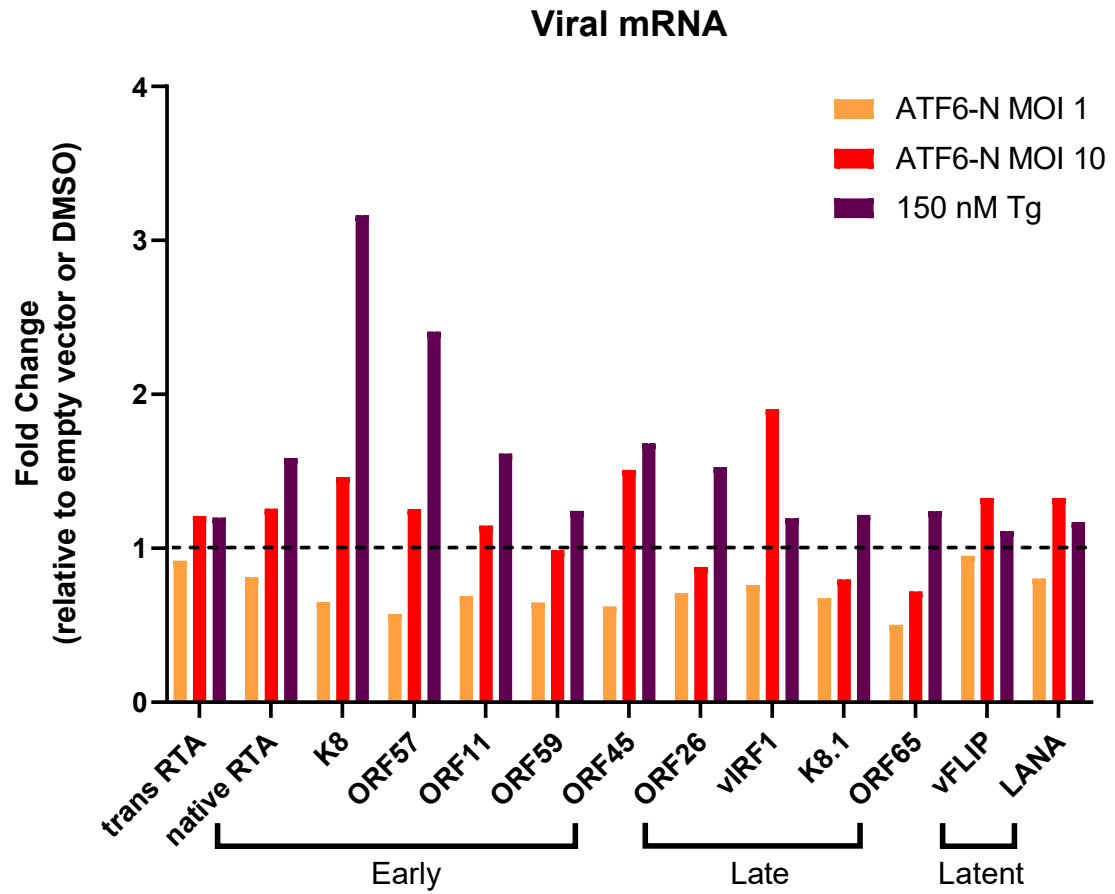
TREx-BCBL1-RTA cells, because I did not observe any changes in viral protein accumulation in this cell line (Fig. 21). The cell line-specific differences between iSLK.219 and TREx-BCBL1-RTA are also supported by data from Johnston and colleagues showing that the antiviral effect of XBP1s overexpression was specific to iSLK.219 cells and could not be reconstituted in TREx-BCBL1-RTA cells [286].

The mechanism by which high concentrations of ATF6-N reduce viral titers from iSLK.219 cells is currently unknown and cannot be delineated solely by quantitating viral titers. During ER stress, the primary function of ATF6-N is that of a transcriptional activator and it is possible that ATF6-N or its products negatively affect viral gene expression. To determine if ATF6-N has a direct effect on the expression of viral genes, I transduced iSLK.219 cells with low (MOI 1) or high (MOI 10) concentrations of ATF6-N, induced viral gene expression with doxycycline, and quantified viral transcripts by RT-qPCR. ATF6-N overexpression changed the levels of select viral early, late, and latent transcripts by less than 1-fold compared to the controls and therefore does not affect viral gene expression (Fig. 24). These results are unsurprising, because the KSHV episome does not contain ERSE-I or ERSE-II sequences in the promoter regions of viral genes that could facilitate ATF6-N binding. My immunoblots further show that ATF6-N did not reduce the accumulation of nuclear and cytoplasmic ORF57 (Fig. 19 & 20) or K-bZIP total protein (Fig. 23). I therefore conclude that ATF6-N exerts an antiviral effect on iSLK.219 cells without reducing viral gene expression and protein accumulation.

CHAPTER 4: DISCUSSION

4.1 K-bZIP is Not an Inhibitor of the UPR

K-bZIP is a multifunctional transcriptional co-factor and repressor, but inhibition of UPR sensor signaling or suppression of UPR-sensitive target gene expression are not among its functions. I showed by flow cytometry that K-bZIP does not perturb IRE1 and PERK signaling in CHO reporter cells (Fig. 12B), I showed by RT-qPCR that K-bZIP does not inhibit the expression of select UPR target genes in HEK293A cells (Fig. 13), and I showed by luciferase assays that K-bZIP does not prevent ATF6-N-mediated transactivation of ERSE-I containing promoters in HEK293T cells (Fig. 15B). As such, K-bZIP is not an inhibitor of the UPR. K-bZIP shares some of its functions and cellular binding partners with EBV ZTA. K-bZIP and ZTA are functional, but not structural, homologues and share no significant aa sequence identity. Furthermore, KSHV and EBV are the only mammalian herpesviruses that encode bZIP TFs [161]. ZTA, like K-bZIP, prefers homodimerization over heterodimerization [256] and the only cellular bZIP K-bZIP and ZTA are known to associate with is C/EBPα [263,264]. UPR modulation has not been documented for ZTA to date. My experiments show that K-bZIP most likely does not interact with the cellular bZIPs ATF6-N, XBP1s, and ATF4 and does not contribute to the KSHV-mediated dysregulation of the UPR.

4.2 ORF57 is a Weak Activator of ATF6-N Transactivation Activity

ORF57 is a RNA-binding protein that supports the KSHV lytic cycle primarily by mediating the nuclear export of viral transcripts and promoting their translation [89,336]. I assessed the transactivation activity of ATF6-N in the presence of various viral proteins and showed by luciferase assays that ORF57 enhanced the ATF6-N-mediated expression of firefly luciferase from an ERSE-I containing promoter by ~0.6 fold over empty vector (Fig. 15B, Fig. 18). ORF57 is a structural and functional homologue of the HSV-1 protein infected cell culture polypeptide 27 (ICP27) together with human cytomegalovirus (HCMV) UL69, EBV EB2, Varicella-Zoster virus (VZV) ORF4, and herpesvirus saimiri (HVS) ORF57 [347]. EBV EB2, which shares 23% aa sequence homology with ORF57, also mediates the nuclear export of viral mRNAs, promotes the translation of spliced transcripts, and is essential to efficient viral DNA replication and

virion production [348–351]. A recent study conducted by Chen and colleagues investigated BiP expression from the *HSPA5* promoter in various cell lines and found that EB2 enhances BiP production in an ATF6-dependent manner. The group investigated firefly luciferase production from the ERSE-I-containing *HSPA5* promoter in HEK293T cells and showed that ectopic expression of EB2 and ATF6 induced luciferase production ~50 fold. The group also showed that KSHV ORF57 did not induce luciferase production in the same model [283]. In my experiment, however, ORF57 weakly induced luciferase expression from ERSE-I (Fig. 15B, Fig. 18). Chen and colleagues co-transfected HEK293T cells with 200 ng of an EB2- or ORF57-encoding plasmid and 50 ng of an ATF6-encoding plasmid for their luciferase experiments and stimulated UPR induction with tunicamycin or thapsigargin [283]. By contrast, I co-transfected 300 ng of ORF57-encoding plasmid and 300 ng of an ATF6-N-encoding plasmid and did not chemically induce ER stress. The higher concentrations of transfected ORF57 and ATF6-N might explain why I observed weak luciferase production from ERSE-I, whereas Chen and colleagues did not. Chen and colleagues also investigated the potential mechanism by which EB2 increases ATF6 activity and showed that EB2 enhances the nuclear translocation of ATF6 in the EBV-infected B-cell lymphoma cell line P3HR1 and that the EB2 C-terminal zinc-binding domain is required to enhance ATF6-dependent BiP production [283]. ORF57 also contains a C-terminal zinc-binding domain that is important for protein stability [352]. Sequence-specific differences between the zinc-binding domains of EB2 and ORF57 could explain why EB2 is a more potent ATF6 activator than ORF57. I did not assess the nuclear localization of ATF6-N in the presence of ORF57, but nuclear and cytoplasmic fractionation or immunofluorescence experiments could allow us to investigate if ORF57, like EB2, enhances the nuclear localization of ATF6-N. The value of further investigating the ORF57-mediated increase in ATF6-N activity is in question, because ATF6-N-mediated gene expression is inhibited during lytic viral replication in iSLK.219 and TREx-BCBL1-RTA cells [286].

4.3 EGFP-ATF6-N and pGL4.26 are Tools to Study TF Activity in the Presence of Viral Proteins

In my experiments, EGFP-ATF6-N significantly induced luciferase expression from ERSE-I in the absence of ER stress and UPR activation (Fig. 15A) and therefore represents a tool to study RE-specific ATF6-N transactivation activity in isolation of XBP1s and ATF4. Using this system, I was able to show that ORF57 is a weak activator of ATF6-N (Fig. 15B, Fig. 18). We can further use this tool to screen individual KSHV ORFs for potential activators or inhibitors of ATF6-N. The assay can be scaled down from a 24-well format to a 96-well format and permit investigation of multiple viral proteins in parallel. CMV-driven plasmids encoding various KSHV ORFs were previously generated in the lab [287] and can be easily transfected into HEK293T cells. Because the system allows for co-transfections, we can also assess if viral protein complexes can modulate ATF6-N activity through concerted action. Potential hits can then be further validated by various molecular techniques, mutational analysis, and single gene knockdowns or knockouts in iSLK.219 and/or TREx-BCBL1-RTA cell lines. We can likewise clone XBP1s- and ATF4-encoding plasmids and generate 5'-ACGT-3', UPRE-, CRE- and AARE-driven firefly luciferase plasmids to identify viral activators and inhibitors of XBP1s and ATF4. Identifying candidate activators or inhibitors of ATF6-N, XBP1s, and ATF4 will allow us to gain a better understanding of the multifaceted, KSHV-mediated dysregulation of the UPR during lytic viral replication. The biggest limitation of these luciferase-based assays is that they are quantitative and cannot provide a mechanistical explanation for how a given viral protein modulates TF activity. Furthermore, viral proteins, such as RTA, that enhance or inhibit expression of *Renilla* luciferase from the transfection control plasmid are not compatible with these assays and will result in a false positive or false negative hit. Overexpression experiments in isolation of viral infection are also not representative of the complex viral protein expression kinetics and protein-protein interaction networks that take place in a timely and spatially coordinated fashion during lytic viral replication. It is therefore important to follow up on potential hits with appropriate molecular techniques in relevant cell lines.

4.4 ATF6-N Impairs Nuclear Import of K-bZIP During Lytic KSHV Replication in iSLK.219 Cells

I assessed the subcellular localization of select viral and cellular targets in dox-induced iSLK.219 cells transduced with ATF6-N-carrying lentiviruses or treated with Tg to induce ER stress and UPR activation. My nuclear and cytoplasmic fractionation experiments showed that Tg treatment and transient overexpression of ATF6-N reduced the accumulation of K-bZIP in the nuclei of lytically replicating iSLK.219 cells (Fig. 19 & 20) without reducing total K-bZIP protein levels (Fig. 23). Because ATF6-N overexpression was sufficient to reduce nuclear levels of K-bZIP (Fig. 20), I concluded that ATF6-N expression interferes with the proper nuclear localization of K-bZIP. Proteins need to cross the nuclear envelope to translocate into and out of the nucleus. Import and export take place across the nuclear pore complex (NPC), a transmembrane channel consisting of up to 100 different proteins that allows for the bi-directional traffic of cargoes. The shuttling β-karyopherins importin-β and importin-α form a complex that recognizes and binds NLS-containing polypeptides and ferries them across the NPC by interaction with the nucleoporins that form the hydrophobic channel of the NPC. Inside the nucleus, the GTP-bound GTPase ras-related nuclear protein (Ran-GTP) binds importin-β and triggers a confirmational change that destabilizes the interaction between importin-β and importin-α and causes them to release their cargo. The importins are then shuttled back to the cytoplasm [353]. Nuclear export also utilizes β-karyopherin proteins and Ran-GTP and functions similarly to nuclear import [354]. UPR activation is not known to alter the nuclear import and export machinery. Indeed, most UPR-responsive genes encode ER-resident proteins that carry out proteostatic functions. I therefore conclude that the mechanism by which ATF6-N expression impairs the nuclear import of K-bZIP is not through inhibition of the nuclear import machinery. In my experiment, only the nuclear accumulation of K-bZIP, but not that of the viral ORF57, was diminished. I did not assess if K-bZIP is the only target whose nuclear import is impaired in the presence of ATF6-N. Nuclear and cytoplasmic fractionation of ATF6-N-expressing, dox-reactivated iSLK.219 cells and detection of multiple, nuclear viral proteins by immunoblotting could help determine if ATF6-N expression impairs the nuclear translocation of additional viral proteins.

Post-translational modifications can alter the nuclear localization of proteins. For instance, phosphorylation of IRF3 and the MAP kinases ERK1 and ERK2 promotes their nuclear translocation [355–357]. O-glycosylation permits the nuclear translocation of the heavy subunit of the macrophage iron-storage protein ferritin (H-ferritin) [358], polyubiquitination is required for the nuclear translocation of neurotrophin receptor interacting factor (NRIF) [359], and SUMOylation retains nuclear factor of activated T cells (NFAT) in the nucleus [360]. As mentioned previously, deamidation of asparagine residues adjacent to the NLS of RTA disrupts the interaction between RTA and importin-β and impairs the nuclear import of RTA [344]. K-bZIP contains a classical, SV40 large T antigen-like NLS with an amino acid sequence of TRRSKRRLHRKF that is located between aas 124 and 135 [343]. Furthermore, K-bZIP is a substrate for phosphorylation and SUMOylation, both of which regulate its repressive function. Phosphorylation of threonine 111 reduces the ability of K-bZIP to repress RTA-mediated transactivation of target promoters and is therefore a negative regulator of K-bZIP activity and function [311]. SUMOylation of lysine 158 is required for the K-bZIP-mediated repression of RTA transactivation activity [288] and for the K-bZIP-mediated inhibition of gene expression from ISRE-containing promoters during type I IFN signaling [289] and is therefore a positive regulator of K-bZIP function. The role of phosphorylation and SUMOylation in the nuclear translocation of K-bZIP and its interaction with the nuclear import/export machinery has not been investigated to date. Furthermore, the target genes of ATF6-N primarily encode chaperones and protein disulfide isomerases [174] and do not include kinases, E3 ligases, phosphatases, or deconjugating enzymes that could alter the phosphorylation and SUMOylation status of K-bZIP. Other PTMs of K-bZIP have not been identified to date. The ATF6-N-dependent reduction of K-bZIP nuclear localization warrants further research. For instance, we can analyze the subcellular localization of K-bZIP in ATF6-N-expressing iSLK.219 cells by immunofluorescence to assess how ATF6-N expression affects the cellular distribution of K-bZIP. Because ATF6-N and XBP1s induce overlapping transcriptional programs [174,189,239], and because the two TFs heterodimerize to co-operatively drive ERAD, we can co-express ATF6-N and XBP1s and investigate if their combined action impairs the nuclear translocation of K-bZIP more strongly than ATF6-N alone. The K-bZIP T111A mutant that cannot be phosphorylated

[311] or the K158R mutant that cannot be SUMOylated [288] are well characterized and could aid in determining if PTMs play a role in directing the nuclear localization of K-bZIP.

4.5 High Concentrations of ATF6-N are Antiviral to rKSHV.219

I quantified viral titers of rKSHV.219 harvested from doxycycline-induced iSLK.219 cells transduced with increasing concentrations of ATF6-N and showed that ATF6-N overexpression reduced viral titers in a dose-dependent manner and is therefore antiviral (Fig. 22). The ATF6-N-mediated reduction of viral titers was subtle and required a significant concentration of protein to reduce viral titers by 0.6-fold compared to empty vector (Fig. 22A). Endogenous ATF6 expression and protein accumulation is low in iSLK.219 cells despite UPR induction with Tg (Fig. 20). Overexpression of ATF6-N at a MOI of 10 results in protein accumulation multiple times the physiological protein level and is not representative of the concentration of ATF6-N that would accumulate in the nuclei of iSLK.219 cells during ER stress. ATF6-N overexpression at a MOI of 1 was not able to reduce viral titers (Fig. 22A), I therefore conclude that ATF6-N expression at levels comparable to those achieved during ER stress and UPR activation would not reduce rKSHV.219 titers.

The mechanism by which high concentrations of ATF6-N reduce viral titers is currently unknown. I showed by RT-qPCR that ATF6-N expression does not affect the accumulation of various viral transcripts accumulating during lytic and latent KSHV replication is iSLK.219 cells (Fig. 24). Therefore, it is unlikely that ATF6-N exhibits its antiviral effect by inducing or inhibiting the expression of select viral genes. KSHV gene promoters also do not contain any ERSE-I, ERSE-II, and UPRE elements that ATF6-N would be able to bind and transactivate. Because the primary function of ATF6-N is that of a transcriptional activator of UPR-responsive genes, ATF6-N might exert its antiviral effect through induction or upregulation of one or multiple effectors. Further studies can be aimed at determining if the transactivation activity of ATF6-N is required to carry out its antiviral function. Our lab has obtained plasmids encoding ATF6β, a homologue of ATF6. ATF6 and ATF6β are encoded from different genes located on different chromosomes and share only 43% aa sequence identity. In response to ER stress, both

116

proteins translocate to the Golgi and are proteolytically processed to produce transcription factors with N-terminal bZIP domains. The bZIP domains of ATF6 and ATF6β share 63% aa sequence identity and bind the ERSE-I in the presence of NF-Y [361]. The transactivation domain of ATF6β differs from that of ATF6 and is not able to induce expression from the *HSPA5* promoter and inhibits ATF6-N transactivation of *HSPA5* when both proteins are co-expressed [362]. As such, ATF6β is an inhibitor of ATF6. Because ATF6β is activated during ER stress and can recognize and bind the same REs as ATF6, but cannot transactivate target gene expression, we can use ATF6β-N to determine if the transactivation activity of ATF6-N is required to reduce rKSHV.219 titers. If ATF6β-N cannot reduce rKSHV.219 titers, the antiviral effect of ATF6-N is likely mediated through induction of an ATF6-N-responsive target.

ATF6-N might be able to reduce rKSHV.219 viral titers by inducing apoptosis through transactivation of *DDIT3*, which encodes CHOP [192,363]. I did not assess whether iSLK.219 cells transduced with increasing concentrations of ATF6-N are actively undergoing apoptosis. As such, it is possible that the dose-dependent reduction of viral titers is a result of premature cell death. To determine if ATF6-N overexpression induces apoptosis in iSLK.219 cells, we can detect apoptotic markers, such as cleaved caspase-3 and cleaved poly ADP-ribose polymerase 1 (PARP-1), by immunoblotting or stain with annexin V and detect apoptotic cells by flow cytometry. We can also directly assess CHOP production in iSLK.219 cells transduced with ATF6-N by western blotting or RT-qPCR. KSHV lytic replication inhibits the accumulation of UPR-responsive targets, including BiP and CHOP [286]. However, a high nuclear concentration of ATF6-N might be able to produce sufficient effectors to interfere with viral replication and reduce viral titers. This might explain why I only observed a significant reduction of viral titers at a MOI of 10 of ATF6-N, but not at lower concentrations.

ATF6-N might also reduce viral titers through induction of autophagy in response to IFN-γ signaling during infection or in tumors [364]. IFN-γ signaling leads to the ERK1/2-dependent phosphorylation and activation of the bZIP C/EBPβ, which induces expression of the pro-apoptotic death-associated protein kinase 1 (DAPK1) from a CRE-like element with a core sequence of 5'-GACG-3' contained in the *dapk1* promoter in

mouse embryonic fibroblasts (MEFs) [365]. The core of this CRE-like element is similar to the 5'-CCACG-3' binding site of the ERSE-I and ERSE-II (Table 1). Indeed, IFN-γ signaling induces ATF6 cleavage and promotes the formation of ATF6-N/C/EBPβ heterodimers that work in concert to transactivate *dapk1* expression from the CRE-like site in MEFs [364]. DAPK1 plays a role in autophagy and ATF6 knockout leads to reduced autophagy and significant mortality of mice in response to infection with *Bacillus anthracis* and *Salmonella typhimurium* [364]. Autophagy can also play a role in antiviral defense by triggering the degradation of viral and host proteins that promote efficient viral replication. Much like the UPR, autophagy can be pro- and antiviral [366]. Lytic KSHV replication induces autophagy and autophagosome formation, possibly to facilitate intracellular transport via autophagosomes [367], but prevents autophagosome maturation [368] and fusion with the lysosome in PEL cells [367]. Multiple viral proteins mediate the regulation of autophagy during KSHV infection. The viral B-cell lymphoma 2 (Bcl-2)-homologue vBcl-2, the lytic K7, and the latent vFLIP inhibit autophagy by different mechanisms [368–370]. It is possible that ATF6 activation in response to IFN signaling and KSHV infection may help to partially overcome the KSHV-mediated dysregulation of autophagy. We can assess if DAPK1 plays a role in the ATF6-N-mediated reduction of viral titers by co-expressing or knocking down C/EBPβ in ATF6-N-expressing, dox-reactivated iSLK.219 cells.

ATF6-N overexpression and Tg treatment impair the nuclear accumulation of K-bZIP in iSLK.219 cells (Fig. 19 & 20). The primary functions of K-bZIP require access to DNA and therefore depend on proper nuclear import. K-bZIP modifies the transactivation activity of RTA to direct viral gene expression [83,87] and binds the viral oriLyt to license DNA replication [84,85]. Impaired nuclear accumulation of K-bZIP might reduce the efficiency of viral gene expression and DNA replication, which might result in reduced iSLK.219 titers. ATF6-N might therefore be antiviral to rKSHV.219 by impairing the nuclear translocation of K-bZIP. K-bZIP overexpression reduces viral DNA replication in BCBL-1 cells [87] and can likely not be used to attempt to re-constitute viral titers in reactivated, ATF6-N-overexpressing iSLK.219 cells. However, nuclear translocation of K-bZIP was not impaired in reactivated, ATF6-N-overexpressing TREx-BCBL1-RTA cells (Fig. 21). We can quantify the viral titers of rKSHV recovered

from reactivated TREx-BCBL1-RTA cells transduced with increasing concentrations of ATF6-N to investigate the antiviral properties of ATF6-N across different cell lines. CHiP-seq can also be used to study how lytic viral replication affects the ATF6-N-mediated transactivation of cellular target genes.

4.6 Conclusion

I investigated K-bZIP as a potential inhibitor of the UPR based on the hypothesis that K-bZIP is a multifunctional, interacting bZIP TF and repressor that might interact with the UPR-governing bZIP TFs ATF6-N, XBP1s, and ATF4 and inhibit their function. I assessed UPR activation and signaling in K-bZIP-transfected or -transduced CHO, HEK293A, and HEK293T cells and showed by flow cytometry, RT-qPCR, and luciferase assays that K-bZIP does not perturb UPR signaling. I developed a luciferase-based assay that can be used to identify viral candidate activators and inhibitors of ATF6-N in HEK293T cells, and, using this assay, found that ORF57 is a weak activator of ATF6-N transactivation activity. The luciferase assay assesses ATF6-N and viral protein function in the absence of viral infection and assumes proper ATF6 processing and nuclear localization during lytic viral replication. I confirmed that ATF6-N properly localizes to the nuclei of KSHV-infected, reactivated iSLK.219 and TREx-BCBL1-RTA cells by nuclear and cytoplasmic fractionation. I discovered that ATF6-N expression in reactivated iSLK.219 cells impaired nuclear import of K-bZIP, but not other viral protein tested. Because K-bZIP is required for efficient lytic gene expression and DNA replication, and because ATF6-N impairs the nuclear translocation of K-bZIP in iSLK.219 cells, I hypothesized that ATF6-N might be antiviral to KSHV. I quantified viral titers of rKSHV.219 harvested from reactivated iSLK.219 cells expressing ATF6-N at various concentrations and found that ATF6-N reduces viral titers in a dose-dependent manner and is therefore antiviral. The mechanism by which ATF6-N reduces viral titers is currently unknown and requires further investigation.

References

1. McGeoch, D. J., Gatherer, D., & Dolan, A. (2005). On phylogenetic relationships among major lineages of the Gammaherpesvirinae. *Journal of General Virology*, *86*(2), 307–316. https://doi.org/10.1099/vir.0.80588-0

2. Goncalves, P. H., Ziegelbauer, J., Uldrick, T. S., & Yarchoan, R. (2017). Kaposi sarcoma herpesvirus-associated cancers and related diseases. *Current Opinion in HIV and AIDS*, *12*(1), 47–56. https://doi.org/10.1097/COH.0000000000000330

3. Vega, F., Miranda, R. N., & Medeiros, L. J. (2020). KSHV/HHV8-positive large B-cell lymphomas and associated diseases: a heterogeneous group of lymphoproliferative processes with significant clinicopathological overlap. *Modern Pathology*, *33*(1), 18–28. https://doi.org/10.1038/s41379-019-0365-y

4. Chang, P.-J., Yang, Y.-H., Chen, P.-C., Chen, L.-W., Wang, S.-S., Shih, Y.-J., Chen, L.-Y., Chen, C.-J., Hung, C.-H., & Lin, C.-L. (2017). Diabetes and risk of Kaposi's sarcoma: effects of high glucose on reactivation and infection of Kaposi's sarcoma-associated herpesvirus. *Oncotarget*, *8*(46), 80595–80611.

5. Mariggiò, G., Koch, S., & Schulz, T. F. (2017). Kaposi sarcoma herpesvirus pathogenesis. *Philosophical Transactions of the Royal Society B: Biological Sciences*, *372*(1732), 20160275. https://doi.org/10.1098/rstb.2016.0275

6. Gonçalves, P. H., Uldrick, T. S., & Yarchoan, R. (2017). HIV-associated Kaposi sarcoma and related diseases. *AIDS*, *31*(14), 1903–1916. https://doi.org/10.1097/QAD.0000000000001567

7. Carbone, A., Cesarman, E., Gloghini, A., & Drexler, H. G. (2010). Understanding pathogenetic aspects and clinical presentation of primary effusion lymphoma through its derived cell lines. *AIDS*, *24*(4), 479–490. https://doi.org/10.1097/QAD.0b013e3283365395

8. Aneja, K. K., & Yuan, Y. (2017). Reactivation and lytic replication of Kaposi's sarcoma-associated herpesvirus: an update. *Frontiers in Microbiology*, *8*, 613. https://doi.org/10.3389/fmicb.2017.00613

9. Giffin, L., & Damania, B. (2014). KSHV: Pathways to tumorigenesis and persistent infection. In *Advances in Virus Research* (Vol. 88, pp. 111–159). Elsevier. https://doi.org/10.1016/B978-0-12-800098-4.00002-7

10. Manners, O., Murphy, J. C., Coleman, A., Hughes, D. J., & Whitehouse, A. (2018). Contribution of the KSHV and EBV lytic cycles to tumourigenesis. *Current Opinion in Virology*, *32*, 60–70. https://doi.org/10.1016/j.coviro.2018.08.014

11. Schneider, J. W., & Dittmer, D. P. (2017). Diagnosis and treatment of Kaposi sarcoma. *American Journal of Clinical Dermatology*, *18*(4), 529–539. https://doi.org/10.1007/s40257-017-0270-4

12. Narkhede, M., Arora, S., & Ujjani, C. (2018). Primary effusion lymphoma: current perspectives. *OncoTargets and Therapy*, *11*, 3747–3754. https://doi.org/10.2147/OTT.S167392

13. Lurain, K., Yarchoan, R., & Uldrick, T. S. (2018). Treatment of Kaposi sarcoma herpesvirus–associated multicentric Castleman disease. *Hematology/Oncology Clinics of North America*, *32*(1), 75–88. https://doi.org/10.1016/j.hoc.2017.09.007

14. Minhas, V., & Wood, C. (2014). Epidemiology and transmission of Kaposi's sarcoma-associated herpesvirus. *Viruses*, *6*(11), 4178–4194. https://doi.org/10.3390/v6114178

15. Mantina, H., Kankasa, C., Klaskala, W., Brayfield, B., Campbell, J., Du, Q., Bhat, G., Kasolo, F., Mitchell, C., & Wood, C. (2001). Vertical transmission of Kaposi's sarcoma-associated herpesvirus. *International Journal of Cancer*, *94*(5), 749–752. https://doi.org/10.1002/ijc.1529

16. Malope, B. I., Pfeiffer, R. M., Mbisa, G., Stein, L., Ratshikhopha, E. M., O'Connell, D. L., Sitas, F., MacPhail, P., & Whitby, D. (2007). Transmission of Kaposi sarcoma-associated herpesvirus between mothers and children in a South African population. *JAIDS Journal of Acquired Immune Deficiency Syndromes*, *44*(3), 351–355. https://doi.org/10.1097/QAI.0b013e31802f12ea

17. Boshoff, C., Schulz, T. F., Kennedy, M. M., Graham, A. K., Fisher, C., Thomas, A., McGee, J. O., Weiss, R. A., & O'Leary, J. J. (1995). Kaposi's sarcoma-associated herpesvirus infects endothelial and spindle cells. *Nature Medicine*, *1*(12), 1274–1278.

18. Mesri, E. A., Cesarman, E., Arvanitakis, L., Rafii, S., Moore, M. A. S., Posnett, D. N., Knowles, D. M., & Asch, A. S. (1996). Human herpesvirus-8/Kaposi's sarcoma-associated herpesvirus is a new transmissible virus that infects B cells. *Journal of Experimental Medicine*, *183*, 2385–2390.

19. Rappocciolo, G., Jenkins, F. J., Hensler, H. R., Piazza, P., Jais, M., Borowski, L., Watkins, S. C., & Rinaldo, C. R. (2006). DC-SIGN Is a receptor for human herpesvirus 8 on dendritic cells and macrophages. *The Journal of Immunology*, *176*(3), 1741–1749. https://doi.org/10.4049/jimmunol.176.3.1741

20. Akula, S. M., Pramod, N. P., Wang, F.-Z., & Chandran, B. (2001). Human herpesvirus 8 envelope-associated glycoprotein B interacts with heparan sulfate-like moieties. *Virology*, *284*(2), 235–249. https://doi.org/10.1006/viro.2001.0921

21. Li, M., MacKey, J., Czajak, S. C., Desrosiers, R. C., Lackner, A. A., & Jung, J. U. (1999). Identification and characterization of Kaposi's sarcoma-associated herpesvirus K8.1 virion glycoprotein. *Journal of Virology*, *73*(2), 1341–1349. https://doi.org/10.1128/JVI.73.2.1341-1349.1999

22. Wang, F.-Z., Akula, S. M., Pramod, N. P., Zeng, L., & Chandran, B. (2001). Human herpesvirus 8 envelope glycoprotein K8.1A interaction with the target cells involves heparan sulfate. *Journal of Virology*, *75*(16), 7517–7527. https://doi.org/10.1128/JVI.75.16.7517-7527.2001

23. Hahn, A., Birkmann, A., Wies, E., Dorer, D., Mahr, K., Stürzl, M., Titgemeyer, F., & Neipel, F. (2009). Kaposi's sarcoma-associated herpesvirus gH/gL: Glycoprotein export and interaction with cellular receptors. *Journal of Virology*, *83*(1), 396–407. https://doi.org/10.1128/JVI.01170-08

24. Akula, S. M., Pramod, N. P., Wang, F.-Z., & Chandran, B. (2002). Integrin α3β1 (CD 49c/29) is a cellular receptor for Kaposi's sarcoma-associated herpesvirus (KSHV/HHV-8) entry into the target cells. *Cell*, *108*, 407–419.

25. Garrigues, H. J., Rubinchikova, Y. E., DiPersio, C. M., & Rose, T. M. (2008). Integrin αvβ3 binds to the RGD motif of glycoprotein B of Kaposi's sarcoma-associated herpesvirus and functions as an RGD-dependent entry receptor. *Journal of Virology*, *82*(3), 1570–1580. https://doi.org/10.1128/JVI.01673-07

26. Hahn, A. S., Kaufmann, J. K., Wies, E., Naschberger, E., Panteleev-Ivlev, J., Schmidt, K., Holzer, A., Schmidt, M., Chen, J., König, S., Ensser, A., Myoung, J., Brockmeyer, N. H., Stürzl, M., Fleckenstein, B., & Neipel, F. (2012). The ephrin receptor tyrosine kinase A2 is a cellular receptor for Kaposi's sarcoma–associated herpesvirus. *Nature Medicine*, *18*(6), 961–966. https://doi.org/10.1038/nm.2805

27. Akula, S. M., Naranatt, P. P., Walia, N.-S., Wang, F.-Z., Fegley, B., & Chandran, B. (2003). Kaposi's sarcoma-associated herpesvirus (human herpesvirus 8) infection of human fibroblast cells occurs through endocytosis. *Journal of Virology*, *77*(14), 7978–7990. https://doi.org/10.1128/JVI.77.14.7978-7990.2003

28. Dutta, D., Chakraborty, S., Bandyopadhyay, C., Valiya Veettil, M., Ansari, M. A., Singh, V. V., & Chandran, B. (2013). EphrinA2 regulates clathrin mediated KSHV endocytosis in fibroblast cells by coordinating integrin-associated signaling and c-Cbl directed polyubiquitination. *PLoS Pathogens*, *9*(7), e1003510. https://doi.org/10.1371/journal.ppat.1003510

29. Raghu, H., Sharma-Walia, N., Veettil, M. V., Sadagopan, S., & Chandran, B. (2009). Kaposi's sarcoma-associated herpesvirus utilizes an actin polymerization-dependent macropinocytic pathway to enter human dermal microvascular endothelial and human umbilical vein endothelial cells. *Journal of Virology*, *83*(10), 4895–4911. https://doi.org/10.1128/JVI.02498-08

30. Pertel, P. E. (2002). Human herpesvirus 8 glycoprotein B (gB), gH, and gL can mediate cell fusion. *Journal of Virology*, *76*(9), 4390–4400. https://doi.org/10.1128/JVI.76.9.4390-4400.2002

31. Kaleeba, J. A. R., & Berger, E. A. (2006). Kaposi's Sarcoma-Associated herpesvirus fusion-entry receptor: Cystine transporter xCT. *Science*, *311*(5769), 1921–1924. https://doi.org/10.1126/science.1120878

32. Naranatt, P. P., Krishnan, H. H., Smith, M. S., & Chandran, B. (2005). Kaposi's sarcoma-associated herpesvirus modulates microtubule dynamics via rhoA-GTP-diaphanous 2 signaling and utilizes the dynein motors to deliver its DNA to the nucleus. *Journal of Virology*, *79*(2), 1191–1206. https://doi.org/10.1128/JVI.79.2.1191-1206.2005

33. Dünn-Kittenplon, D., Ashkenazy-Titelman, A., Kalt, I., Lellouche, J.-P., Shav-Tal, Y., & Sarid, R. (2021). The portal vertex of KSHV promotes docking of capsids at the nuclear pores. *Viruses*, *13*(4), 597. https://doi.org/10.3390/v13040597

34. Dezube, B. J., Zambela, M., Sage, D. R., Wang, J.-F., & Fingeroth, J. D. (2002). Characterization of Kaposi sarcoma–associated herpesvirus/human herpesvirus–8 infection of human vascular endothelial cells: Early events. *Blood*, *100*(3), 888–896. https://doi.org/10.1182/blood.V100.3.888

35. Lukac, D. M., Renne, R., Kirshner, J. R., & Ganem, D. (1998). Reactivation of Kaposi's sarcoma-associated herpesvirus infection from latency by expression of the ORF 50 transactivator, a homolog of the EBV R protein. *Virology*, *252*(2), 304–312. https://doi.org/10.1006/viro.1998.9486

36. Toth, Z., Brulois, K., Lee, H.-R., Izumiya, Y., Tepper, C., Kung, H.-J., & Jung, J. U. (2013). Biphasic euchromatin-to-heterochromatin transition on the KSHV genome following de novo infection. *PLoS Pathogens*, *9*(12), e1003813. https://doi.org/10.1371/journal.ppat.1003813

37. Günther, T., & Grundhoff, A. (2010). The epigenetic landscape of latent Kaposi sarcoma-associated herpesvirus genomes. *PLoS Pathogens*, *6*(6), e1000935. https://doi.org/10.1371/journal.ppat.1000935

38. Toth, Z., Papp, B., Brulois, K., Choi, Y. J., Gao, S.-J., & Jung, J. U. (2016). LANA-mediated recruitment of host polycomb repressive complexes onto the KSHV genome during de novo infection. *PLOS Pathogens*, *12*(9), e1005878. https://doi.org/10.1371/journal.ppat.1005878

39. Li, Q., He, M., Zhou, F., Ye, F., & Gao, S.-J. (2014). Activation of Kaposi's sarcoma-associated herpesvirus (KSHV) by inhibitors of class III histone deacetylases: Identification of sirtuin 1 as a regulator of the KSHV life cycle. *Journal of Virology*, *88*(11), 6355–6367. https://doi.org/10.1128/JVI.00219-14

40. Chen, J., Ueda, K., Sakakibara, S., Okuno, T., Parravicini, C., Corbellino, M., & Yamanishi, K. (2001). Activation of latent Kaposi's sarcoma-associated herpesvirus by demethylation of the promoter of the lytic transactivator. *Proceedings of the National Academy of Sciences*, *98*(7), 4119–4124. https://doi.org/10.1073/pnas.051004198

41. Rainbow, L., Platt, G. M., Simpson, G. R., Sarid, R., Gao, S. J., Stoiber, H., Herrington, C. S., Moore, P. S., & Schulz, T. F. (1997). The 222- to 234-kilodalton latent nuclear protein (LNA) of Kaposi's sarcoma-associated herpesvirus (human herpesvirus 8) is encoded by orf73 and is a component of the latency-associated nuclear antigen. *Journal of Virology*, *71*(8), 5915–5921. https://doi.org/10.1128/jvi.71.8.5915-5921.1997

42. Dittmer, D. P. (2003). Transcription profile of Kaposi's sarcoma-associated herpesvirus in primary Kaposi's sarcoma lesions as determined by real-time PCR arrays. *Cancer Research*, *63*, 2010–2015.

43. Hu, J., Yang, Y., Turner, P. C., Jain, V., McIntyre, L. M., & Renne, R. (2014). LANA binds to multiple active viral and cellular promoters and associates with the H3K4 methyltransferase hSET1 complex. *PLoS Pathogens*, *10*(7), e1004240. https://doi.org/10.1371/journal.ppat.1004240

44. De Leo, A., Deng, Z., Vladimirova, O., Chen, H.-S., Dheekollu, J., Calderon, A., Myers, K. A., Hayden, J., Keeney, F., Kaufer, B. B., Yuan, Y., Robertson, E., & Lieberman, P. M. (2019). LANA oligomeric architecture is essential for KSHV nuclear body formation and viral genome maintenance during latency. *PLOS Pathogens*, *15*(1), e1007489. https://doi.org/10.1371/journal.ppat.1007489

45. Barbera, A. J., Ballestas, M. E., & Kaye, K. M. (2004). The Kaposi's sarcoma-associated herpesvirus latency-associated nuclear antigen 1 N-terminus is essential for chromosome association, DNA replication, and episome persistence. *Journal of Virology*, *78*(1), 294–301. https://doi.org/10.1128/JVI.78.1.294-301.2004

46. Verma, S. C., Choudhuri, T., Kaul, R., & Robertson, E. S. (2006). Latency-associated nuclear antigen (LANA) of Kaposi's sarcoma-associated herpesvirus interacts with origin recognition complexes at the LANA binding sequence within the terminal repeats. *Journal of Virology*, *80*(5), 2243–2256. https://doi.org/10.1128/JVI.80.5.2243-2256.2006

47. Gupta, N., Thakker, S., & Verma, S. C. (2016). KSHV encoded LANA recruits nucleosome assembly protein NAP1L1 for regulating viral DNA replication and transcription. *Scientific Reports*, *6*(1), 32633. https://doi.org/10.1038/srep32633

48. Stuber, G., Mattsson, K., Flaberg, E., Kati, E., Markasz, L., Sheldon, J. A., Klein, G., Schulz, T. F., & Szekely, L. (2007). HHV-8 encoded LANA-1 alters the higher organization of the cell nucleus. *Molecular Cancer*, *6*(1), 28. https://doi.org/10.1186/1476-4598-6-28

49. Friborg, J., Kong, W., Hottiger, M. O., & Nabel, G. J. (1999). P53 inhibition by the LANA protein of KSHV protects against cell death. *Nature*, *402*(6764), 889–894. https://doi.org/10.1038/47266

50. Di Bartolo, D. L., Cannon, M., Liu, Y.-F., Renne, R., Chadburn, A., Boshoff, C., & Cesarman, E. (2008). KSHV LANA inhibits TGF-β signaling through epigenetic silencing of the TGF-β type II receptor. *Blood*, *111*(9), 4731–4740. https://doi.org/10.1182/blood-2007-09-110544

51. Chang, Y., Moore, P. S., Talbot, S. J., Boshoff, C. H., Zarkowska, T., Godden-Kent, D., Paterson, H., Weiss, R. A., & Mittnacht, S. (1996). Cyclin encoded by KS herpesvirus. *Nature*, *382*(6590), 410–410. https://doi.org/10.1038/382410a0

52. Dittmer, D., Lagunoff, M., Renne, R., Staskus, K., Haase, A., & Ganem, D. (1998). A cluster of latently expressed genes in Kaposi's sarcoma-associated herpesvirus. *Journal of Virology*, *72*(10), 8309–8315. https://doi.org/10.1128/JVI.72.10.8309-8315.1998

53. Thome, M., Schneider, P., Hofmann, K., Fickenscher, H., Meinl, E., Neipel, F., Mattmann, C., Burns, K., Bodmer, J.-L., Schröter, M., Scaffidi, C., Krammer, P. H., Peter, M. E., & Tschopp, J. (1997). Viral FLICE-inhibitory proteins (FLIPs) prevent apoptosis induced by death receptors. *Nature*, *386*, 517–521.

54. Sadler, R., Wu, L., Forghani, B., Renne, R., Zhong, W., Herndier, B., & Ganem, D. (1999). A complex translational program generates multiple novel proteins from the latently expressed kaposin (K12) locus of Kaposi's sarcoma-associated herpesvirus. *Journal of Virology*, *73*(7), 5722–5730. https://doi.org/10.1128/JVI.73.7.5722-5730.1999

55. Li, H., Komatsu, T., Dezube, B. J., & Kaye, K. M. (2002). The Kaposi's sarcoma-associated herpesvirus K12 transcript from a primary effusion lymphoma contains complex repeat elements, is spliced, and initiates from a novel promoter. *Journal of Virology*, *76*(23), 11880–11888. https://doi.org/10.1128/JVI.76.23.11880-11888.2002

56. Cai, X., Lu, S., Zhang, Z., Gonzalez, C. M., Damania, B., & Cullen, B. R. (2005). Kaposi's sarcoma-associated herpesvirus expresses an array of viral microRNAs in latently infected cells. *Proceedings of the National Academy of Sciences*, *102*(15), 5570–5575. https://doi.org/10.1073/pnas.0408192102

57. Cai, X., & Cullen, B. R. (2006). Transcriptional origin of Kaposi's sarcoma-associated herpesvirus microRNAs. *Journal of Virology*, *80*(5), 2234–2242. https://doi.org/10.1128/JVI.80.5.2234-2242.2006

58. Lin, Y.-T., Kincaid, R. P., Arasappan, D., Dowd, S. E., Hunicke-Smith, S. P., & Sullivan, C. S. (2010). Small RNA profiling reveals antisense transcription throughout the KSHV genome and novel small RNAs. *RNA*, *16*(8), 1540–1558. https://doi.org/10.1261/rna.1967910

59. O'Brien, J., Hayder, H., Zayed, Y., & Peng, C. (2018). Overview of microRNA biogenesis, mechanisms of actions, and circulation. *Frontiers in Endocrinology*, *9*(402). https://doi.org/10.3389/fendo.2018.00402

60. Gottwein, E., & Cullen, B. R. (2010). A human herpesvirus microRNA inhibits p21 expression and attenuates p21-mediated cell cycle arrest. *Journal of Virology*, *84*(10), 5229–5237. https://doi.org/10.1128/JVI.00202-10

61. Lei, X., Bai, Z., Ye, F., Xie, J., Kim, C.-G., Huang, Y., & Gao, S.-J. (2010). Regulation of NF-κB inhibitor IκBα and viral replication by a KSHV microRNA. *Nature Cell Biology*, *12*(2), 193–199. https://doi.org/10.1038/ncb2019

62. Moody, R., Zhu, Y., Huang, Y., Cui, X., Jones, T., Bedolla, R., Lei, X., Bai, Z., & Gao, S.-J. (2013). KSHV microRNAs mediate cellular transformation and tumorigenesis by redundantly targeting cell growth and survival pathways. *PLoS Pathogens*, *9*(12), e1003857. https://doi.org/10.1371/journal.ppat.1003857

63. Plaisance-Bonstaff, K., Choi, H., Beals, T., Krueger, B., Boss, I., Gay, L., Haecker, I., Hu, J., & Renne, R. (2014). KSHV miRNAs decrease expression of lytic genes in latently infected PEL and endothelial cells by targeting host transcription factors. *Viruses*, *6*(10), 4005–4023. https://doi.org/10.3390/v6104005

64. Liu, X., Happel, C., & Ziegelbauer, J. M. (2017). Kaposi's sarcoma-associated herpesvirus microRNAs target GADD45B to protect infected cells from cell cycle arrest and apoptosis. *Journal of Virology*, *91*(3), e02045-16. https://doi.org/10.1128/JVI.02045-16

65. Zhi, H., Zahoor, M. A., Shudofsky, A. M. D., & Giam, C.-Z. (2015). KSHV vCyclin counters the senescence/G1 arrest response triggered by NF-κB hyperactivation. *Oncogene*, *34*(4), 496–505. https://doi.org/10.1038/onc.2013.567

66. DiMaio, T. A., Vogt, D. T., & Lagunoff, M. (2020). KSHV requires vCyclin to overcome replicative senescence in primary human lymphatic endothelial cells. *PLOS Pathogens*, *16*(6), e1008634. https://doi.org/10.1371/journal.ppat.1008634

67. Ye, F.-C., Zhou, F.-C., Xie, J.-P., Kang, T., Greene, W., Kuhne, K., Lei, X.-F., Li, Q.-H., & Gao, S.-J. (2008). Kaposi's sarcoma-associated herpesvirus latent gene vFLIP inhibits viral lytic replication through NF-κB-mediated suppression of the AP-1 pathway: A novel mechanism of virus control of latency. *Journal of Virology*, *82*(9), 4235–4249. https://doi.org/10.1128/JVI.02370-07

68. Ballon, G., Chen, K., Perez, R., Tam, W., & Cesarman, E. (2011). Kaposi sarcoma herpesvirus (KSHV) vFLIP oncoprotein induces B cell transdifferentiation and tumorigenesis in mice. *Journal of Clinical Investigation*, *121*(3), 1141–1153. https://doi.org/10.1172/JCI44417

69. Jones, T., Ramos da Silva, S., Bedolla, R., Ye, F., Zhou, F., & Gao, S. (2014). Viral cyclin promotes KSHV-induced cellular transformation and tumorigenesis by overriding contact inhibition. *Cell Cycle*, *13*(5), 845–858. https://doi.org/10.4161/cc.27758

70. Ballon, G., Akar, G., & Cesarman, E. (2015). Systemic expression of Kaposi sarcoma herpesvirus (KSHV) vFLIP in endothelial cells leads to a profound proinflammatory phenotype and myeloid lineage remodeling in vivo. *PLOS Pathogens*, *11*(1), e1004581. https://doi.org/10.1371/journal.ppat.1004581

71. McCormick, C., & Ganem, D. (2005). The kaposin B protein of KSHV activates the p38/MK2 pathway and stabilizes cytokine mRNAs. *Science*, *307*(5710), 739–741. https://doi.org/10.1126/science.1105779

72. Renne, R., Zhong, W., Herndier, B., Mcgrath, M., Abbey, N., Kedes, D., & Ganem, D. (1996). Lytic growth of Kaposi's sarcoma–associated herpesvirus (human herpesvirus 8) in culture. *Nature Medicine*, *2*(3), 342–346. https://doi.org/10.1038/nm0396-342

73. Miller, G., Heston, L., Grogan, E., Gradoville, L., Rigsby, M., Sun, R., Shedd, D., Kushnaryov, V. M., Grossberg, S., & Chang, Y. (1997). Selective switch between latency and lytic replication of Kaposi's sarcoma herpesvirus and Epstein-Barr virus in dually infected body cavity lymphoma cells. *Journal of Virology*, *71*(1), 314–324. https://doi.org/10.1128/jvi.71.1.314-324.1997

74. Liang, Y., Chang, J., Lynch, S. J., Lukac, D. M., & Ganem, D. (2002). The lytic switch protein of KSHV activates gene expression via functional interaction with RBP-Jκ (CSL), the target of the Notch signaling pathway. *Genes & Development*, *16*, 1977–1989.

75. Polstra, A. M., Goudsmit, J., & Cornelissen, M. (2003). Latent and lytic HHV-8 mRNA expression in PBMCs and Kaposi's sarcoma skin biopsies of AIDS Kaposi's sarcoma patients. *Journal of Medical Virology*, *70*(4), 624–627. https://doi.org/10.1002/jmv.10440

76. Myoung, J., & Ganem, D. (2011). Active lytic infection of human primary tonsillar B cells by KSHV and its noncytolytic control by activated CD4+ T cells. *Journal of Clinical Investigation*, *121*(3), 1130–1140. https://doi.org/10.1172/JCI43755

77. Ye, F., Zhou, F., Bedolla, R. G., Jones, T., Lei, X., Kang, T., Guadalupe, M., & Gao, S.-J. (2011). Reactive oxygen species hydrogen peroxide mediates Kaposi's sarcoma-associated herpesvirus reactivation from latency. *PLoS Pathogens*, *7*(5), e1002054. https://doi.org/10.1371/journal.ppat.1002054

78. Grundhoff, A., & Ganem, D. (2004). Inefficient establishment of KSHV latency suggests an additional role for continued lytic replication in Kaposi sarcoma pathogenesis. *Journal of Clinical Investigation*, *113*(1), 124–136. https://doi.org/10.1172/JCI200417803

79. Toth, Z., Maglinte, D. T., Lee, S. H., Lee, H.-R., Wong, L.-Y., Brulois, K. F., Lee, S., Buckley, J. D., Laird, P. W., Marquez, V. E., & Jung, J. U. (2010). Epigenetic analysis of KSHV latent and lytic genomes. *PLoS Pathogens*, *6*(7), e1001013. https://doi.org/10.1371/journal.ppat.1001013

80. Rossetto, C. C., & Pari, G. (2012). KSHV PAN RNA associates with demethylases UTX and JMJD3 to activate lytic replication through a physical interaction with the virus genome. *PLoS Pathogens*, *8*(5), e1002680. https://doi.org/10.1371/journal.ppat.1002680

81. Hiura, K., Strahan, R., Uppal, T., Prince, B., Rossetto, C. C., & Verma, S. C. (2020). KSHV ORF59 and PAN RNA recruit histone demethylases to the viral chromatin during lytic reactivation. *Viruses*, *12*(4), 420. https://doi.org/10.3390/v12040420

82. Strahan, R. C., McDowell-Sargent, M., Uppal, T., Purushothaman, P., & Verma, S. C. (2017). KSHV encoded ORF59 modulates histone arginine methylation of the viral genome to promote viral reactivation. *PLOS Pathogens*, *13*(7), e1006482. https://doi.org/10.1371/journal.ppat.1006482

83. Ellison, T. J., Izumiya, Y., Izumiya, C., Luciw, P. A., & Kung, H.-J. (2009). A comprehensive analysis of recruitment and transactivation potential of K-Rta and K-bZIP during reactivation of Kaposi's sarcoma-associated herpesvirus. *Virology*, *387*(1), 76–88. https://doi.org/10.1016/j.virol.2009.02.016

84. AuCoin, D. P., Colletti, K. S., Cei, S. A., Papousková, I., Tarrant, M., & Pari, G. S. (2004). Amplification of the Kaposi's sarcoma-associated herpesvirus/human herpesvirus 8 lytic origin of DNA replication is dependent upon a cis-acting AT-rich region and an ORF50 response element and the trans-acting factors ORF50 (K-Rta) and K8 (K-bZIP). *Virology*, *318*(2), 542–555. https://doi.org/10.1016/j.virol.2003.10.016

85. Wang, Y., Tang, Q., Maul, G. G., & Yuan, Y. (2006). Kaposi's sarcoma-associated herpesvirus ori-Lyt-dependent DNA replication: Dual role of replication and transcription activator. *Journal of Virology*, *80*(24), 12171–12186. https://doi.org/10.1128/JVI.00990-06

86. Liao, W., Tang, Y., Lin, S.-F., Kung, H.-J., & Giam, C.-Z. (2003). K-bZIP of kaposi's sarcoma-associated herpesvirus/human herpesvirus 8 (KSHV/HHV-8) binds KSHV/HHV-8 Rta and represses Rta-mediated transactivation. *Journal of Virology*, *77*(6), 3809–3815. https://doi.org/10.1128/JVI.77.6.3809-3815.2003

87. Izumiya, Y., Lin, S.-F., Ellison, T., Chen, L.-Y., Izumiya, C., Luciw, P., & Kung, H.-J. (2003). Kaposi's sarcoma-associated herpesvirus K-bZIP is a coregulator of K-Rta: Physical association and promoter-dependent transcriptional repression. *Journal of Virology*, *77*(2), 1441–1451. https://doi.org/10.1128/JVI.77.2.1441-1451.2003

88. Rossetto, C. C., Tarrant-Elorza, M., Verma, S., Purushothaman, P., & Pari, G. S. (2013). Regulation of viral and cellular gene expression by Kaposi's sarcoma-associated herpesvirus polyadenylated nuclear RNA. *Journal of Virology*, *87*(10), 5540–5553. https://doi.org/10.1128/JVI.03111-12

89. Malik, P., Blackbourn, D. J., & Clements, J. B. (2004). The evolutionarily conserved Kaposi's sarcoma-associated herpesvirus ORF57 protein interacts with REF protein and acts as an RNA export factor. *Journal of Biological Chemistry*, *279*(31), 33001–33011. https://doi.org/10.1074/jbc.M313008200

90. Boyne, J. R., Colgan, K. J., & Whitehouse, A. (2008). Recruitment of the complete hTREX complex is required for Kaposi's sarcoma–associated herpesvirus intronless mRNA nuclear export and virus replication. *PLoS Pathogens*, *4*(10), e1000194. https://doi.org/10.1371/journal.ppat.1000194

91. Jackson, B. R., Boyne, J. R., Noerenberg, M., Taylor, A., Hautbergue, G. M., Walsh, M. J., Wheat, R., Blackbourn, D. J., Wilson, S. A., & Whitehouse, A. (2011). An interaction between KSHV ORF57 and UIF provides mRNA-adaptor redundancy in herpesvirus intronless mRNA export. *PLoS Pathogens*, *7*(7), e1002138. https://doi.org/10.1371/journal.ppat.1002138

92. Sahin, B. B., Patel, D., & Conrad, N. K. (2010). Kaposi's sarcoma-associated herpesvirus ORF57 protein binds and protects a nuclear noncoding RNA from cellular RNA decay pathways. *PLoS Pathogens*, *6*(3), e1000799. https://doi.org/10.1371/journal.ppat.1000799

93. Ruiz, J. C., Hunter, O. V., & Conrad, N. K. (2019). Kaposi's sarcoma-associated herpesvirus ORF57 protein protects viral transcripts from specific nuclear RNA decay pathways by preventing hMTR4 recruitment. *PLOS Pathogens*, *15*(2), e1007596. https://doi.org/10.1371/journal.ppat.1007596

94. Majerciak, V., Yamanegi, K., Allemand, E., Kruhlak, M., Krainer, A. R., & Zheng, Z.-M. (2008). Kaposi's sarcoma-associated herpesvirus ORF57 functions as a viral splicing factor and promotes expression of intron-containing viral lytic genes in spliceosome-mediated RNA splicing. *Journal of Virology*, *82*(6), 2792–2801. https://doi.org/10.1128/JVI.01856-07

95. Han, Z., & Swaminathan, S. (2006). Kaposi's sarcoma-associated herpesvirus lytic gene ORF57 is essential for infectious virion production. *Journal of Virology*, *80*(11), 5251–5260. https://doi.org/10.1128/JVI.02570-05

96. Mazewski, C., Perez, R. E., Fish, E. N., & Platanias, L. C. (2020). Type I interferon (IFN)-regulated activation of canonical and non-canonical signaling pathways. *Frontiers in Immunology*, *11*, 606456. https://doi.org/10.3389/fimmu.2020.606456

97. Golas, G., Jang, S. J., Naik, N. G., Alonso, J. D., Papp, B., & Toth, Z. (2020). Comparative analysis of the viral interferon regulatory factors of KSHV for their requisite for virus production and inhibition of the type I interferon pathway. *Virology*, *541*, 160–173. https://doi.org/10.1016/j.virol.2019.12.011

98. Hwang, S.-W., Kim, D., Jung, J. U., & Lee, H.-R. (2017). KSHV-encoded viral interferon regulatory factor 4 (vIRF4) interacts with IRF7 and inhibits interferon alpha production. *Biochemical and Biophysical Research Communications*, *486*(3), 700–705. https://doi.org/10.1016/j.bbrc.2017.03.101

99. Joo, C. H., Shin, Y. C., Gack, M., Wu, L., Levy, D., & Jung, J. U. (2007). Inhibition of interferon regulatory factor 7 (IRF7)-mediated interferon signal transduction by the Kaposi's sarcoma-associated herpesvirus viral IRF homolog vIRF3. *Journal of Virology*, *81*(15), 8282–8292. https://doi.org/10.1128/JVI.00235-07

100. Mutocheluh, M., Hindle, L., Aresté, C., Chanas, S. A., Butler, L. M., Lowry, K., Shah, K., Evans, D. J., & Blackbourn, D. J. (2011). Kaposi's sarcoma-associated herpesvirus viral interferon regulatory factor-2 inhibits type 1 interferon signalling by targeting interferon-stimulated gene factor-3. *Journal of General Virology*, *92*(10), 2394–2398. https://doi.org/10.1099/vir.0.034322-0

101. Zhu, F. X., King, S. M., Smith, E. J., Levy, D. E., & Yuan, Y. (2002). A Kaposi's sarcoma-associated herpesviral protein inhibits virus-mediated induction of type I interferon by blocking IRF-7 phosphorylation and nuclear accumulation. *Proceedings of the National Academy of Sciences*, *99*(8), 5573–5578. https://doi.org/10.1073/pnas.082420599

102. Wu, J., Li, W., Shao, Y., Avey, D., Fu, B., Gillen, J., Hand, T., Ma, S., Liu, X., Miley, W., Konrad, A., Neipel, F., Stürzl, M., Whitby, D., Li, H., & Zhu, F. (2015). Inhibition of cGAS DNA sensing by a herpesvirus virion protein. *Cell Host & Microbe*, *18*(3), 333–344. https://doi.org/10.1016/j.chom.2015.07.015

103. Ishido, S., Wang, C., Lee, B.-S., Cohen, G. B., & Jung, J. U. (2000). Downregulation of major histocompatibility complex class I molecules by Kaposi's sarcoma-associated herpesvirus K3 and K5 proteins. *Journal of Virology*, *74*(11), 5300–5309.

104. Brulois, K., Toth, Z., Wong, L.-Y., Feng, P., Gao, S.-J., Ensser, A., & Jung, J. U. (2014). Kaposi's sarcoma-associated herpesvirus K3 and K5 ubiquitin E3 ligases have stage-specific immune evasion roles during lytic replication. *Journal of Virology*, *88*(16), 9335–9349. https://doi.org/10.1128/JVI.00873-14

105. Lee, H., Patschull, A. O. M., Bagnéris, C., Ryan, H., Sanderson, C. M., Ebrahimi, B., Nobeli, I., & Barrett, T. E. (2017). KSHV SOX mediated host shutoff: The molecular mechanism underlying mRNA transcript processing. *Nucleic Acids Research*, *45*(8), 4756–4767. https://doi.org/doi: 10.1093/nar/gkw1340

106. Glaunsinger, B., & Ganem, D. (2004). Lytic KSHV infection inhibits host gene expression by accelerating global mRNA turnover. *Molecular Cell*, *13*(5), 713–723. https://doi.org/10.1016/S1097-2765(04)00091-7

107. Glaunsinger, B., & Ganem, D. (2004). Highly selective escape from KSHV-mediated host mRNA shutoff and its implications for viral pathogenesis. *Journal of Experimental Medicine*, *200*(3), 391–398. https://doi.org/10.1084/jem.20031881

108. Chandriani, S., & Ganem, D. (2007). Host transcript accumulation during lytic KSHV infection reveals several classes of host responses. *PLoS ONE*, *2*(8), e811. https://doi.org/10.1371/journal.pone.0000811

109. Gaglia, M. M., Rycroft, C. H., & Glaunsinger, B. A. (2015). Transcriptome-wide cleavage site mapping on cellular mRNAs reveals features underlying sequence-specific cleavage by the viral ribonuclease SOX. *PLOS Pathogens*, *11*(12), e1005305. https://doi.org/10.1371/journal.ppat.1005305

110. Covarrubias, S., Gaglia, M. M., Kumar, G. R., Wong, W., Jackson, A. O., & Glaunsinger, B. A. (2011). Coordinated destruction of cellular messages in translation complexes by the gammaherpesvirus host shutoff factor and the mammalian exonuclease Xrn1. *PLoS Pathogens*, *7*(10), e1002339. https://doi.org/10.1371/journal.ppat.1002339

111. Gao, S.-J., Boshoff, C., Jayachandra, S., Weiss, R. A., Chang, Y., & Moore, P. S. (1997). KSHV ORF K9 (vIRF) is an oncogene which inhibits the interferon signaling pathway. *Oncogene*, *15*(16), 1979–1985. https://doi.org/10.1038/sj.onc.1201571

112. Nakamura, H., Li, M., Zarycki, J., & Jung, J. U. (2001). Inhibition of p53 tumor suppressor by viral interferon regulatory factor. *Journal of Virology*, *75*(16), 7572–7582. https://doi.org/10.1128/JVI.75.16.7572-7582.2001

113. Shin, Y. C., Nakamura, H., Liang, X., Feng, P., Chang, H., Kowalik, T. F., & Jung, J. U. (2006). Inhibition of the ATM/p53 signal transduction pathway by Kaposi's sarcoma-associated herpesvirus interferon regulatory factor 1. *Journal of Virology*, *80*(5), 2257–2266. https://doi.org/10.1128/JVI.80.5.2257-2266.2006

114. Wies, E., Mori, Y., Hahn, A., Kremmer, E., Stürzl, M., Fleckenstein, B., & Neipel, F. (2008). The viral interferon-regulatory factor-3 is required for the survival of KSHV-infected primary effusion lymphoma cells. *Blood*, *111*(1), 320–327. https://doi.org/10.1182/blood-2007-05-092288

115. Bais, C., Santomasso, B., Coso, O., Arvanitakis, L., Geras-Raaka, E., Gutkind, J. S., Asch, A. S., Cesarman, E., Gerhengorn, M. C., & Mesri, E. A. (1998). G-protein-coupled receptor of Kaposi's sarcoma-associated herpesvirusisaviraloncogene and angiogenesis activator. *Nature*, *391*, 86–89. https://doi.org/10.1038/42722

116. Cannon, M. L., & Cesarman, E. (2004). The KSHV G protein-coupled receptor signals via multiple pathways to induce transcription factor activation in primary effusion lymphoma cells. *Oncogene*, *23*(2), 514–523. https://doi.org/10.1038/sj.onc.1207021

117. Sodhi, A., Montaner, S., Patel, V., Zohar, M., Bais, C., Mesri, E. A., & Gutkind, J. S. (2000). The Kaposi's sarcoma-associated herpes virus G protein-coupled receptor up- regulates vascular endothelial growth factor expression and secretion through mitogen-activated protein kinase and p38 pathways acting on hypoxia-inducible factor 1α. *Cancer Research*, *60*, 4873–4880.

118. Schwarz, M., & Murphy, P. M. (2001). Kaposi's sarcoma-associated herpesvirus G protein-coupled receptor constitutively activates NF-κB and induces proinflammatory cytokine and chemokine production via a C-terminal signaling determinant. *The Journal of Immunology*, *167*(1), 505–513. https://doi.org/10.4049/jimmunol.167.1.505

119. Medina, M. V., D´Agostino, A., Ma, Q., Eroles, P., Cavallin, L., Chiozzini, C., Sapochnik, D., Cymeryng, C., Hyjek, E., Cesarman, E., Naipauer, J., Mesri, E. A., & Coso, O. A. (2020). KSHV G-protein coupled receptor vGPCR oncogenic signaling upregulation of Cyclooxygenase-2 expression mediates angiogenesis and tumorigenesis in Kaposi's sarcoma. *PLOS Pathogens*, *16*(10), e1009006. https://doi.org/10.1371/journal.ppat.1009006

120. Park, J., Seo, T., Hwang, S., Lee, D., Gwack, Y., & Choe, J. (2000). The K-bZIP protein from Kaposi's sarcoma-associated herpesvirus interacts with p53 and represses its transcriptional activity. *Journal of Virology*, *74*(24), 11977–11982. https://doi.org/10.1128/JVI.74.24.11977-11982.2000

121. Alzhanova, D., Meyo, J. O., Juarez, A., & Dittmer, D. P. (2021). The ORF45 protein of Kaposi sarcoma-associated herpesvirus is an inhibitor of p53 signaling during viral reactivation. *Journal of Virology*, *95*(23), e01459-21. https://doi.org/10.1128/JVI.01459-21

122. AuCoin, D. P., Colletti, K. S., Xu, Y., Cei, S. A., & Pari, G. S. (2002). Kaposi's Sarcoma-associated herpesvirus (human herpesvirus 8) contains two functional lytic origins of DNA replication. *Journal of Virology*, *76*(15), 7890–7896. https://doi.org/10.1128/JVI.76.15.7890-7896.2002

123. Wang, Y., Li, H., Chan, M. Y., Zhu, F. X., Lukac, D. M., & Yuan, Y. (2004). Kaposi's sarcoma-associated herpesvirus oriLyt-dependent DNA replication: Cis-acting requirements for replication and oriLyt-associated RNA transcription. *Journal of Virology*, *78*(16), 8615–8629. https://doi.org/10.1128/JVI.78.16.8615-8629.2004

124. Li, D., Fu, W., & Swaminathan, S. (2018). Continuous DNA replication is required for late gene transcription and maintenance of replication compartments in gammaherpesviruses. *PLOS Pathogens*, *14*(5), e1007070. https://doi.org/10.1371/journal.ppat.1007070

125. Nishimura, M., Watanabe, T., Yagi, S., Yamanaka, T., & Fujimuro, M. (2017). Kaposi's sarcoma-associated herpesvirus ORF34 is essential for late gene expression and virus production. *Scientific Reports*, *7*(1), 329. https://doi.org/10.1038/s41598-017-00401-7

126. Davis, Z. H., Hesser, C. R., Park, J., & Glaunsinger, B. A. (2016). Interaction between ORF24 and ORF34 in the Kaposi's Sarcoma-associated herpesvirus late gene transcription factor complex is essential for viral late gene expression. *Journal of Virology*, *90*(1), 599–604. https://doi.org/10.1128/JVI.02157-15

127. Castañeda, A. F., Didychuk, A. L., Louder, R. K., McCollum, C. O., Davis, Z. H., Nogales, E., & Glaunsinger, B. A. (2020). The gammaherpesviral TATA-box-binding protein directly interacts with the CTD of host RNA Pol II to direct late gene transcription. *PLOS Pathogens*, *16*(9), e1008843. https://doi.org/10.1371/journal.ppat.1008843

128. Davis, Z. H., Verschueren, E., Jang, G. M., Kleffman, K., Johnson, J. R., Park, J., Von Dollen, J., Maher, M. C., Johnson, T., Newton, W., Jäger, S., Shales, M., Horner, J., Hernandez, R. D., Krogan, N. J., & Glaunsinger, B. A. (2015). Global mapping of herpesvirus-host protein complexes reveals a transcription strategy for late genes. *Molecular Cell*, *57*(2), 349–360. https://doi.org/10.1016/j.molcel.2014.11.026

129. Perkins, E. M., Anacker, D., Davis, A., Sankar, V., Ambinder, R. F., & Desai, P. (2008). Small capsid protein pORF65 is essential for assembly of Kaposi's sarcoma-associated herpesvirus capsids. *Journal of Virology*, *82*(14), 7201–7211. https://doi.org/10.1128/JVI.00423-08

130. Dai, X., Gong, D., Lim, H., Jih, J., Wu, T.-T., Sun, R., & Zhou, Z. H. (2018). Structure and mutagenesis reveal essential capsid protein interactions for KSHV replication. *Nature*, *553*(7689), 521–525. https://doi.org/10.1038/nature25438

131. Trus, B. L., Heymann, J. B., Nealon, K., Cheng, N., Newcomb, W. W., Brown, J. C., Kedes, D. H., & Steven, A. C. (2001). Capsid structure of Kaposi's sarcoma-associated herpesvirus, a gammaherpesvirus, compared to those of an alphaherpesvirus, herpes simplex virus type 1, and a betaherpesvirus, cytomegalovirus. *Journal of Virology*, *75*(6), 2879–2890. https://doi.org/10.1128/JVI.75.6.2879-2890.2001

132. Deng, B., O'Connor, C. M., Kedes, D. H., & Zhou, Z. H. (2008). Cryo-electron tomography of Kaposi's sarcoma-associated herpesvirus capsids reveals dynamic scaffolding structures essential to capsid assembly and maturation. *Journal of Structural Biology*, *161*(3), 419–427. https://doi.org/10.1016/j.jsb.2007.10.016

133. Tsurumi, S., Watanabe, T., Iwaisako, Y., Suzuki, Y., Nakano, T., & Fujimuro, M. (2021). Kaposi's sarcoma-associated herpesvirus ORF17 plays a key role in capsid maturation. *Virology*, *558*, 76–85. https://doi.org/10.1016/j.virol.2021.02.009

134. Dünn-Kittenplon, D. (Dana), Kalt, I., Lellouche, J.-P. (Moshe), & Sarid, R. (2019). The KSHV portal protein ORF43 is essential for the production of infectious viral particles. *Virology*, *529*, 205–215. https://doi.org/10.1016/j.virol.2019.01.028

135. Gong, D., Dai, X., Jih, J., Liu, Y.-T., Bi, G.-Q., Sun, R., & Zhou, Z. H. (2019). DNA-packing portal and capsid-associated tegument complexes in the tumor herpesvirus KSHV. *Cell*, *178*(6), 1329-1343.e12. https://doi.org/10.1016/j.cell.2019.07.035

136. Neuber, S., Wagner, K., Goldner, T., Lischka, P., Steinbrueck, L., Messerle, M., & Borst, E. M. (2017). Mutual interplay between the human cytomegalovirus terminase subunits pUL51, pUL56, and pUL89 promotes terminase complex formation. *Journal of Virology*, *91*(12), e02384-16. https://doi.org/10.1128/JVI.02384-16

137. Iwaisako, Y., Watanabe, T., Hanajiri, M., Sekine, Y., & Fujimuro, M. (2021). Kaposi's sarcoma-associated herpesvirus ORF7 is essential for virus production. *Microorganisms*, *9*(6), 1169. https://doi.org/10.3390/microorganisms9061169

138. Gardner, M. R., & Glaunsinger, B. A. (2018). Kaposi's sarcoma-associated herpesvirus ORF68 is a DNA binding protein required for viral genome cleavage and packaging. *Journal of Virology*, *92*(16), e00840-18. https://doi.org/10.1128/JVI .00840-18

139. Didychuk, A. L., Gates, S. N., Gardner, M. R., Strong, L. M., Martin, A., & Glaunsinger, B. A. (2021). A pentameric protein ring with novel architecture is required for herpesviral packaging. *ELife*, *10*, e62261. https://doi.org/10.7554/eLife.62261

140. Mettenleiter, T. C. (2002). Herpesvirus Assembly and Egress. *Journal of Virology*, *76*(4), 1537–1547. https://doi.org/10.1128/JVI.76.4.1537-1547.2002

141. Wang, X., Zhu, N., Li, W., Zhu, F., Wang, Y., & Yuan, Y. (2015). Mono-ubiquitylated ORF45 mediates association of KSHV particles with internal lipid rafts for viral assembly and egress. *PLOS Pathogens*, *11*(12), e1005332. https://doi.org/10.1371/journal.ppat.1005332

142. Zhu, F. X., Chong, J. M., Wu, L., & Yuan, Y. (2005). Virion proteins of Kaposi's sarcoma-associated herpesvirus. *Journal of Virology*, *79*(2), 800–811. https://doi.org/10.1128/JVI.79.2.800-811.2005

143. Sathish, N., Wang, X., & Yuan, Y. (2012). Tegument proteins of Kaposi's sarcoma-associated herpesvirus and related gamma-herpesviruses. *Frontiers in Microbiology*, *3*(98), 1–13. https://doi.org/10.3389/fmicb.2012.00098

144. Nabiee, R., Syed, B., Ramirez Castano, J., Lalani, R., & Totonchy, J. E. (2020). An update of the virion proteome of Kaposi sarcoma-associated herpesvirus. *Viruses*, *12*(12), 1382. https://doi.org/10.3390/v12121382

145. Sathish, N., Zhu, F. X., & Yuan, Y. (2009). Kaposi's sarcoma-associated herpesvirus ORF45 interacts with kinesin-2 transporting viral capsid-tegument complexes along microtubules. *PLoS Pathogens*, *5*(3), e1000332. https://doi.org/10.1371/journal.ppat.1000332

146. Gradoville, L., Gerlach, J., Grogan, E., Shedd, D., Nikiforow, S., Metroka, C., & Miller, G. (2000). Kaposi's sarcoma-associated herpesvirus open reading frame 50/Rta protein activates the entire viral lytic cycle in the HH-B2 primary effusion lymphoma cell line. *Journal of Virology*, *74*(13), 6207–6212. https://doi.org/10.1128/JVI.74.13.6207-6212.2000

147. Harrison, S. M., & Whitehouse, A. (2008). Kaposi's sarcoma-associated herpesvirus (KSHV) Rta and cellular HMGB1 proteins synergistically transactivate the KSHV ORF50 promoter. *FEBS Letters*, *582*(20), 3080–3084. https://doi.org/10.1016/j.febslet.2008.07.055

148. Bottero, V., Sharma-Walia, N., Kerur, N., Paul, A. G., Sadagopan, S., Cannon, M., & Chandran, B. (2009). Kaposi Sarcoma-associated herpes virus (KSHV) G protein-coupled receptor (vGPCR) activates the ORF50 lytic switch promoter: A potential positive feedback loop for sustained ORF50 gene expression. *Virology*, *392*(1), 34–51. https://doi.org/10.1016/j.virol.2009.07.002

149. Lu, F., Zhou, J., Wiedmer, A., Madden, K., Yuan, Y., & Lieberman, P. M. (2003). Chromatin remodeling of the Kaposi's sarcoma-associated herpesvirus ORF50 promoter correlates with reactivation from latency. *Journal of Virology*, *77*(21), 11425–11435. https://doi.org/10.1128/JVI.77.21.11425-11435.2003

150. Ye, J., Shedd, D., & Miller, G. (2005). An Sp1 response element in the Kaposi's sarcoma-associated herpesvirus open reading frame 50 promoter mediates lytic cycle induction by butyrate. *Journal of Virology*, *79*(3), 1397–1408. https://doi.org/10.1128/JVI.79.3.1397-1408.2005

151. Cheng, F., Weidner-Glunde, M., Varjosalo, M., Rainio, E.-M., Lehtonen, A., Schulz, T. F., Koskinen, P. J., Taipale, J., & Ojala, P. M. (2009). KSHV reactivation from latency requires Pim-1 and Pim-3 kinases to inactivate the latency-associated nuclear antigen LANA. *PLoS Pathogens*, *5*(3), e1000324. https://doi.org/10.1371/journal.ppat.1000324

152. Cai, Q., Lan, K., Verma, S. C., Si, H., Lin, D., & Robertson, E. S. (2006). Kaposi's Sarcoma-associated herpesvirus latent protein LANA interacts with HIF-1α to upregulate RTA expression during hypoxia: Latency control under low oxygen conditions. *Journal of Virology*, *80*(16), 7965–7975. https://doi.org/10.1128/JVI.00689-06

153. Wilson, S. J., Tsao, E. H., Webb, B. L. J., Ye, H., Dalton-Griffin, L., Tsantoulas, C., Gale, C. V., Du, M.-Q., Whitehouse, A., & Kellam, P. (2007). X Box binding protein XBP-1s transactivates the Kaposi's sarcoma-associated herpesvirus (KSHV) ORF50 promoter, linking plasma cell differentiation to KSHV reactivation from latency. *Journal of Virology*, *81*(24), 13578–13586. https://doi.org/10.1128/JVI.01663-07

154. Xie, J., Ajibade, A. O., Ye, F., Kuhne, K., & Gao, S.-J. (2008). Reactivation of Kaposi's sarcoma-associated herpesvirus from latency requires MEK/ERK, JNK and p38 multiple mitogen-activated protein kinase pathways. *Virology*, *371*(1), 139–154. https://doi.org/10.1016/j.virol.2007.09.040

155. Yoshida, H., Matsui, T., Yamamoto, A., Okada, T., & Mori, K. (2001). XBP1 mRNA is induced by ATF6 and spliced by IRE1 in response to ER stress to produce a highly active transcription factor. *Cell*, *107*(7), 881–891. https://doi.org/10.1016/S0092-8674(01)00611-0

156. Yu, F., Harada, J. N., Brown, H. J., Deng, H., Song, M. J., Wu, T.-T., Kato-Stankiewicz, J., Nelson, C. G., Vieira, J., Tamanoi, F., Chanda, S. K., & Sun, R. (2007). Systematic identification of cellular signals reactivating Kaposi sarcoma–associated herpesvirus. *PLoS Pathogens*, *3*(3), e44. https://doi.org/10.1371/journal.ppat.0030044

157. Qin, D., Feng, N., Fan, W., Ma, X., Yan, Q., Lv, Z., Zeng, Y., Zhu, J., & Lu, C. (2011). Activation of PI3K/AKT and ERK MAPK signal pathways is required for the induction of lytic cycle replication of Kaposi's Sarcoma-associated herpesvirus by herpes simplex virus type 1. *BMC Microbiology*, *11*(1), 240. https://doi.org/10.1186/1471-2180-11-240

158. Chen, J., Dai, L., Goldstein, A., Zhang, H., Tang, W., Forrest, J. C., Post, S. R., Chen, X., & Qin, Z. (2019). Identification of new antiviral agents against Kaposi's sarcoma-associated herpesvirus (KSHV) by high-throughput drug screening reveals the role of histamine-related signaling in promoting viral lytic reactivation. *PLOS Pathogens*, *15*(12), e1008156. https://doi.org/10.1371/journal.ppat.1008156

159. Merat, R., Amara, A., Lebbe, C., de The, H., Morel, P., & Saib, A. (2002). HIV-1 infection of primary effusion lymphoma cell line triggers Kaposi's sarcoma-associated herpesvirus (KSHV) reactivation. *International Journal of Cancer*, *97*(6), 791–795. https://doi.org/10.1002/ijc.10086

160. Gregory, S. M., West, J. A., Dillon, P. J., Hilscher, C., Dittmer, D. P., & Damania, B. (2009). Toll-like receptor signaling controls reactivation of KSHV from latency. *Proceedings of the National Academy of Sciences*, *106*(28), 11725–11730. https://doi.org/10.1073/pnas.0905316106

161. Stolz, M. L., & McCormick, C. (2020). The bZIP Proteins of Oncogenic Viruses. *Viruses*, *12*(7), 757. https://doi.org/10.3390/v12070757

162. Walter, P., & Ron, D. (2011). The unfolded protein response: From stress pathway to homeostatic regulation. *Science*, *334*(6059), 1081–1086. https://doi.org/10.1126/science.1209038

163. Xu, C., Bailly-Maitre, B., & Reed, J. C. (2005). Endoplasmic reticulum stress: Cell life and death decisions. *Journal of Clinical Investigation*, *115*(10), 2656–2664. https://doi.org/10.1172/JCI26373

164. Bertolotti, A., Zhang, Y., Hendershot, L. M., Harding, H. P., & Ron, D. (2000). Dynamic interaction of BiP and ER stress transducers in the unfolded-protein response. *Nature Cell Biology*, *2*(6), 326–332. https://doi.org/10.1038/35014014

165. Preissler, S., Rato, C., Perera, L. A., Saudek, V., & Ron, D. (2017). FICD acts bifunctionally to AMPylate and de-AMPylate the endoplasmic reticulum chaperone BiP. *Nature Structural & Molecular Biology*, *24*(1), 23–29. https://doi.org/10.1038/nsmb.3337

166. Kopp, M. C., Nowak, P. R., Larburu, N., Adams, C. J., & Ali, M. M. (2018). In vitro FRET analysis of IRE1 and BiP association and dissociation upon endoplasmic reticulum stress. *ELife*, *7*, e30257. https://doi.org/10.7554/eLife.30257

167. Sundaram, A., Appathurai, S., Plumb, R., & Mariappan, M. (2018). Dynamic changes in complexes of IRE1α, PERK, and ATF6α during endoplasmic reticulum stress. *Molecular Biology of the Cell*, *29*(11), 1376–1388. https://doi.org/10.1091/mbc.E17-10-0594

168. Haze, K., Yoshida, H., Yanagi, H., Yura, T., & Mori, K. (1999). Mammalian transcription factor ATF6 is synthesized as a transmembrane protein and activated by proteolysis in response to endoplasmic reticulum stress. *Molecular Biology of the Cell*, *10*(11), 3787–3799. https://doi.org/10.1091/mbc.10.11.3787

169. Chen, X., Shen, J., & Prywes, R. (2002). The luminal domain of ATF6 senses endoplasmic reticulum (ER) stress and causes translocation of ATF6 from the ER to the Golgi. *Journal of Biological Chemistry*, *277*(15), 13045–13052. https://doi.org/10.1074/jbc.M110636200

170. Oka, O. B., Lith, M., Rudolf, J., Tungkum, W., Pringle, M. A., & Bulleid, N. J. (2019). ERp18 regulates activation of ATF6α during unfolded protein response. *The EMBO Journal*, *38*(15), e100990. https://doi.org/10.15252/embj.2018100990

171. Koba, H., Jin, S., Imada, N., Ishikawa, T., Ninagawa, S., Okada, T., Sakuma, T., Yamamoto, T., & Mori, K. (2020). Reinvestigation of disulfide-bonded oligomeric forms of the unfolded protein response transducer ATF6. *Cell Structure and Function*, *45*(1), 9–21. https://doi.org/10.1247/csf.19030

172. Shen, J., Chen, X., Hendershot, L., & Prywes, R. (2002). ER stress regulation of ATF6 localization by dissociation of BiP/GRP78 binding and unmasking of Golgi localization signals. *Developmental Cell*, *3*(1), 99–111. https://doi.org/10.1016/S1534-5807(02)00203-4

173. Schindler, A. J., & Schekman, R. (2009). In vitro reconstitution of ER-stress induced ATF6 transport in COPII vesicles. *Proceedings of the National Academy of Sciences*, *106*(42), 17775–17780. https://doi.org/10.1073/pnas.0910342106

174. Shoulders, M. D., Ryno, L. M., Genereux, J. C., Moresco, J. J., Tu, P. G., Wu, C., Yates, J. R., Su, A. I., Kelly, J. W., & Wiseman, R. L. (2013). Stress-independent activation of XBP1s and/or ATF6 reveals three functionally diverse ER proteostasis environments. *Cell Reports*, *3*(4), 1279–1292. https://doi.org/10.1016/j.celrep.2013.03.024

175. Tam, A. B., Roberts, L. S., Chandra, V., Rivera, I. G., Nomura, D. K., Forbes, D. J., & Niwa, M. (2018). The UPR activator ATF6 responds to proteotoxic and lipotoxic stress by distinct mechanisms. *Developmental Cell*, *46*(3), 327–343. https://doi.org/10.1016/j.devcel.2018.04.023

176. Horimoto, S., Ninagawa, S., Okada, T., Koba, H., Sugimoto, T., Kamiya, Y., Kato, K., Takeda, S., & Mori, K. (2013). The unfolded protein response transducer ATF6 represents a novel transmembrane-type endoplasmic reticulum-associated degradation substrate requiring both mannose trimming and SEL1L protein. *Journal of Biological Chemistry*, *288*(44), 31517–31527. https://doi.org/10.1074/jbc.M113.476010

177. Thuerauf, D. J., Morrison, L. E., Hoover, H., & Glembotski, C. C. (2002). Coordination of ATF6-mediated transcription and ATF6 degradation by a domain that is shared with the viral transcription factor, VP16. *Journal of Biological Chemistry*, *277*(23), 20734–20739. https://doi.org/10.1074/jbc.M201749200

178. Cox, J. S., & Walter, P. (1996). A novel mechanism for regulating activity of a transcription factor that controls the unfolded protein response. *Cell*, *87*, 391–404.

179. Tirasophon, W., Welihinda, A. A., & Kaufman, R. J. (1998). A stress response pathway from the endoplasmic reticulum to the nucleus requires a novel bifunctional protein kinase/endoribonuclease (Ire1p) in mammalian cells. *Genes & Development*, *12*, 1812–1824. https://doi.org/10.1101/gad.12.12.1812

180. Niwa, M., Sidrauski, C., Kaufman, R. J., & Walter, P. (1999). A role for presenilin-1 in nuclear accumulation of Ire1 fragments and induction of the mammalian unfolded protein response. *Cell*, *99*(7), 691–702. https://doi.org/10.1016/S0092-8674(00)81667-0

181. Tirasophon, W., Lee, K., Callaghan, B., Welihinda, A., & Kaufman, R. J. (2000). The endoribonuclease activity of mammalian IRE1 autoregulates its mRNA and is required for the unfolded protein response. *Genes & Development*, *14*(21), 2725–2736. https://doi.org/10.1101/gad.839400

182. Zhou, J., Liu, C. Y., Back, S. H., Clark, R. L., Peisach, D., Xu, Z., & Kaufman, R. J. (2006). The crystal structure of human IRE1 luminal domain reveals a conserved dimerization interface required for activation of the unfolded protein response. *Proceedings of the National Academy of Sciences*, *103*(39), 14343–14348. https://doi.org/10.1073/pnas.0606480103

183. Prischi, F., Nowak, P. R., Carrara, M., & Ali, M. M. U. (2014). Phosphoregulation of Ire1 RNase splicing activity. *Nature Communications*, *5*(1), 3554. https://doi.org/10.1038/ncomms4554

184. Joshi, A., Newbatt, Y., McAndrew, P. C., Stubbs, M., Burke, R., Richards, M. W., Bhatia, C., Caldwell, J. J., McHardy, T., Collins, I., & Bayliss, R. (2015). Molecular mechanisms of human IRE1 activation through dimerization and ligand binding. *Oncotarget*, *6*(15), 13019–13035. https://doi.org/10.18632/oncotarget.3864

185. Credle, J. J., Finer-Moore, J. S., Papa, F. R., Stroud, R. M., & Walter, P. (2005). On the mechanism of sensing unfolded protein in the endoplasmic reticulum. *Proceedings of the National Academy of Sciences*, *102*(52), 18773–18784. https://doi.org/10.1073/pnas.0509487102

186. Yoshida, H., Okada, T., Haze, K., Yanagi, H., Yura, T., Negishi, M., & Mori, K. (2000). ATF6 activated by proteolysis binds in the presence of NF-Y (CBF) directly to the cis-acting element responsible for the mammalian unfolded protein response. *Molecular and Cellular Biology*, *20*(18), 6755–6767. https://doi.org/10.1128/MCB.20.18.6755-6767.2000

187. Yamamoto, K. (2004). Differential contributions of ATF6 and XBP1 to the activation of endoplasmic reticulum stress-responsive cis-acting elements ERSE, UPRE and ERSE-II. *Journal of Biochemistry*, *136*(3), 343–350. https://doi.org/10.1093/jb/mvh122

188. Yoshida, H., Haze, K., Yanagi, H., Yura, T., & Mori, K. (1998). Identification of the cis-acting endoplasmic reticulum stress response element responsible for transcriptional induction of mammalian glucose-regulated proteins. *Journal of Biological Chemistry*, *273*(50), 33741–33749. https://doi.org/10.1074/jbc.273.50.33741

189. Lee, A.-H., Iwakoshi, N. N., & Glimcher, L. H. (2003). XBP-1 regulates a subset of endoplasmic reticulum resident chaperone genes in the unfolded protein response. *Molecular and Cellular Biology*, *23*(21), 7448–7459. https://doi.org/10.1128/MCB.23.21.7448-7459.2003

190. Luo, S., Baumeister, P., Yang, S., Abcouwer, S. F., & Lee, A. S. (2003). Induction of Grp78/BiP by translational block. *Journal of Biological Chemistry*, *278*(39), 37375–37385. https://doi.org/10.1074/jbc.M303619200

191. Ma, Y., & Hendershot, L. M. (2004). Herp is dually regulated by both the endoplasmic reticulum stress-specific branch of the unfolded protein response and a branch that is shared with other cellular stress pathways. *Journal of Biological Chemistry*, *279*(14), 13792–13799. https://doi.org/10.1074/jbc.M313724200

192. Takayanagi, S., Fukuda, R., Takeuchi, Y., Tsukada, S., & Yoshida, K. (2013). Gene regulatory network of unfolded protein response genes in endoplasmic reticulum stress. *Cell Stress and Chaperones*, *18*(1), 11–23. https://doi.org/10.1007/s12192-012-0351-5

193. Amin-Wetzel, N., Neidhardt, L., Yan, Y., Mayer, M. P., & Ron, D. (2019). Unstructured regions in IRE1α specify BiP-mediated destabilisation of the luminal domain dimer and repression of the UPR. *ELife*, *8*, e50793. https://doi.org/10.7554/eLife.50793

194. Amin-Wetzel, N., Saunders, R. A., Kamphuis, M. J., Rato, C., Preissler, S., Harding, H. P., & Ron, D. (2017). A J-protein co-chaperone recruits BiP to monomerize IRE1 and repress the unfolded protein response. *Cell*, *171*(7), 1625–1637. https://doi.org/10.1016/j.cell.2017.10.040

195. Ali, M. M. U., Bagratuni, T., Davenport, E. L., Nowak, P. R., Silva-Santisteban, M. C., Hardcastle, A., McAndrews, C., Rowlands, M. G., Morgan, G. J., Aherne, W., Collins, I., Davies, F. E., & Pearl, L. H. (2011). Structure of the Ire1 autophosphorylation complex and implications for the unfolded protein response: Structure of the Ire1 autophosphorylation complex and implications for the UPR. *The EMBO Journal*, *30*(5), 894–905. https://doi.org/10.1038/emboj.2011.18

196. Wilkinson, M. E., Charenton, C., & Nagai, K. (2020). RNA splicing by the spliceosome. *Annual Review of Biochemistry*, *89*(1), 359–388. https://doi.org/10.1146/annurev-biochem-091719-064225

197. Sidrauski, C., & Walter, P. (1997). The transmembrane kinase Ire1p is a Site-specific endonuclease that initiates mRNA splicing in the unfolded protein response. *Cell*, *90*(6), 1031–1039. https://doi.org/10.1016/S0092-8674(00)80369-4

198. Korennykh, A. V., Korostelev, A. A., Egea, P. F., Finer-Moore, J., Stroud, R. M., Zhang, C., Shokat, K. M., & Walter, P. (2011). Structural and functional basis for RNA cleavage by Ire1. *BMC Biology*, *9*(1), 47. https://doi.org/10.1186/1741-7007-9-47

199. Hollien, J., Lin, J. H., Li, H., Stevens, N., Walter, P., & Weissman, J. S. (2009). Regulated Ire1-dependent decay of messenger RNAs in mammalian cells. *Journal of Cell Biology*, *186*(3), 323–331. https://doi.org/10.1083/jcb.200903014

200. Tam, A. B., Koong, A. C., & Niwa, M. (2014). Ire1 has distinct catalytic mechanisms for XBP1/HAC1 splicing and RIDD. *Cell Reports*, *9*(3), 850–858. https://doi.org/10.1016/j.celrep.2014.09.016

201. Liu, L., Cai, J., Wang, H., Liang, X., Zhou, Q., Ding, C., Zhu, Y., Fu, T., Guo, Q., Xu, Z., Xiao, L., Liu, J., Yin, Y., Fang, L., Xue, B., Wang, Y., Meng, Z.-X., He, A., Li, J.-L., … Gan, Z. (2019). Coupling of COPII vesicle trafficking to nutrient availability by the IRE1α-XBP1s axis. *Proceedings of the National Academy of Sciences*, *116*(24), 11776–11785. https://doi.org/10.1073/pnas.1814480116

202. Yoshida, H., Oku, M., Suzuki, M., & Mori, K. (2006). PXBP1(U) encoded in XBP1 pre-mRNA negatively regulates unfolded protein response activator pXBP1(S) in mammalian ER stress response. *Journal of Cell Biology*, *172*(4), 565–575. https://doi.org/10.1083/jcb.200508145

203. Yoshida, H., Uemura, A., & Mori, K. (2009). PXBP1(U), a negative regulator of the unfolded protein response activator pXBP1(S), targets ATF6 but not ATF4 in proteasome-mediated degradation. *Cell Structure and Function*, *34*(1), 1–10. https://doi.org/10.1247/csf.06028

204. Ma, K., Vattem, K. M., & Wek, R. C. (2002). Dimerization and release of molecular chaperone inhibition facilitate activation of eukaryotic initiation factor-2 kinase in response to endoplasmic reticulum stress. *Journal of Biological Chemistry*, *277*(21), 18728–18735. https://doi.org/10.1074/jbc.M200903200

205. Cui, W., Li, J., Ron, D., & Sha, B. (2011). The structure of the PERK kinase domain suggests the mechanism for its activation. *Acta Crystallographica Section D Biological Crystallography*, *67*(5), 423–428. https://doi.org/10.1107/S0907444911006445

206. Hamanaka, R. B., Bennett, B. S., Cullinan, S. B., & Diehl, J. A. (2005). PERK and GCN2 contribute to eIF2α phosphorylation and cell cycle arrest after activation of the unfolded protein response pathway. *Molecular Biology of the Cell*, *16*, 5493–5501. http://www.molbiolcell.org/cgi/doi/10.1091/mbc.E05– 03– 0268

207. Wang, P., Li, J., Tao, J., & Sha, B. (2018). The luminal domain of the ER stress sensor protein PERK binds misfolded proteins and thereby triggers PERK oligomerization. *Journal of Biological Chemistry*, *293*(11), 4110–4121. https://doi.org/10.1074/jbc.RA117.001294

208. Hinnebusch, A. G., & Lorsch, J. R. (2012). The mechanism of eukaryotic translation initiation: New insights and challenges. *Cold Spring Harbor Perspectives in Biology*, *4*(10), a011544. https://doi.org/10.1101/cshperspect.a011544

209. Gordiyenko, Y., Llácer, J. L., & Ramakrishnan, V. (2019). Structural basis for the inhibition of translation through eIF2α phosphorylation. *Nature Communications*, *10*(1), 2640. https://doi.org/10.1038/s41467-019-10606-1

210. Donnelly, N., Gorman, A. M., Gupta, S., & Samali, A. (2013). The eIF2α kinases: Their structures and functions. *Cellular and Molecular Life Sciences*, *70*(19), 3493–3511. https://doi.org/10.1007/s00018-012-1252-6

211. Harding, H. P., Zhang, Y., Zeng, H., Novoa, I., Lu, P. D., Calfon, M., Sadri, N., Yun, C., Popko, B., Paules, R., Stojdl, D. F., Bell, J. C., Hettmann, T., Leiden, J. M., & Ron, D. (2003). An integrated stress response regulates amino acid metabolism and resistance to oxidative stress. *Molecular Cell*, *11*(3), 619–633. https://doi.org/10.1016/S1097-2765(03)00105-9

212. Vattem, K. M., & Wek, R. C. (2004). Reinitiation involving upstream ORFs regulates ATF4 mRNA translation in mammalian cells. *Proceedings of the National Academy of Sciences*, *101*(31), 11269–11274. https://doi.org/10.1073/pnas.0400541101

213. Chen, H., Pan, Y.-X., Dudenhausen, E. E., & Kilberg, M. S. (2004). Amino acid deprivation induces the transcription rate of the human asparagine synthetase gene through a timed program of expression and promoter binding of nutrient-responsive basic region/leucine zipper transcription factors as well as localized histone acetylation. *Journal of Biological Chemistry*, *279*(49), 50829–50839. https://doi.org/10.1074/jbc.M409173200

214. Palii, S. S., Thiaville, M. M., Pan, Y.-X., Zhong, C., & Kilberg, M. S. (2006). Characterization of the amino acid response element within the human sodium-coupled neutral amino acid transporter 2 (SNAT2) System A transporter gene. *Biochemical Journal*, *395*(3), 517–527. https://doi.org/10.1042/BJ20051867

215. B'chir, W., Maurin, A.-C., Carraro, V., Averous, J., Jousse, C., Muranishi, Y., Parry, L., Stepien, G., Fafournoux, P., & Bruhat, A. (2013). The eIF2α/ATF4 pathway is essential for stress-induced autophagy gene expression. *Nucleic Acids Research*, *41*(16), 7683–7699. https://doi.org/10.1093/nar/gkt563

216. Luhr, M., Torgersen, M. L., Szalai, P., Hashim, A., Brech, A., Staerk, J., & Engedal, N. (2019). The kinase PERK and the transcription factor ATF4 play distinct and essential roles in autophagy resulting from tunicamycin-induced ER stress. *Journal of Biological Chemistry*, *294*(20), 8197–8217. https://doi.org/10.1074/jbc.RA118.002829

217. Ye, J., Kumanova, M., Hart, L. S., Sloane, K., Zhang, H., De Panis, D. N., Bobrovnikova-Marjon, E., Diehl, J. A., Ron, D., & Koumenis, C. (2010). The GCN2-ATF4 pathway is critical for tumour cell survival and proliferation in response to nutrient deprivation. *The EMBO Journal*, *29*(12), 2082–2096. https://doi.org/10.1038/emboj.2010.81

218. Matsumoto, H., Miyazaki, S., Matsuyama, S., Takeda, M., Kawano, M., Nakagawa, H., Nishimura, K., & Matsuo, S. (2013). Selection of autophagy or apoptosis in cells exposed to ER-stress depends on ATF4 expression pattern with or without CHOP expression. *Biology Open*, *2*(10), 1084–1090. https://doi.org/10.1242/bio.20135033

219. Zinszner, H., Kuroda, M., Wang, X., Batchvarova, N., Lightfoot, R. T., Remotti, H., Stevens, J. L., & Ron, D. (1998). CHOP is implicated in programmed cell death in response to impaired function of the endoplasmic reticulum. *Genes & Development*, *12*(7), 982–995. https://doi.org/10.1101/gad.12.7.982

220. Hu, H., Tian, M., Ding, C., & Yu, S. (2019). The C/EBP homologous protein (CHOP) transcription factor functions in endoplasmic reticulum stress-induced apoptosis and microbial infection. *Frontiers in Immunology*, *9*, 3083. https://doi.org/10.3389/fimmu.2018.03083

221. Brush, M. H., Weiser, D. C., & Shenolikar, S. (2003). Growth arrest and DNA damage-inducible protein GADD34 targets protein phosphatase 1α to the endoplasmic reticulum and promotes dephosphorylation of the α subunit of eukaryotic translation initiation factor 2. *Molecular and Cellular Biology*, *23*(4), 1292–1303. https://doi.org/10.1128/MCB.23.4.1292-1303.2003

222. Marciniak, S. J., Yun, C. Y., Oyadomari, S., Novoa, I., Zhang, Y., Jungreis, R., Nagata, K., Harding, H. P., & Ron, D. (2004). CHOP induces death by promoting protein synthesis and oxidation in the stressed endoplasmic reticulum. *Genes & Development*, *18*(24), 3066–3077. https://doi.org/10.1101/gad.1250704

223. Shaulian, E., & Karin, M. (2002). AP-1 as a regulator of cell life and death. *Nature Cell Biology*, *4*(5), E131–E136. https://doi.org/10.1038/ncb0502-e131

224. Nerlov, C. (2007). The C/EBP family of transcription factors: A paradigm for interaction between gene expression and proliferation control. *Trends in Cell Biology*, *17*(7), 318–324. https://doi.org/10.1016/j.tcb.2007.07.004

225. Luo, Q., Viste, K., Urday-Zaa, J. C., Senthil Kumar, G., Tsai, W.-W., Talai, A., Mayo, K. E., Montminy, M., & Radhakrishnan, I. (2012). Mechanism of CREB recognition and coactivation by the CREB-regulated transcriptional coactivator CRTC2. *Proceedings of the National Academy of Sciences*, *109*(51), 20865–20870. https://doi.org/10.1073/pnas.1219028109

226. Vinson, C., Myakishev, M., Acharya, A., Mir, A. A., Moll, J. R., & Bonovich, M. (2002). Classification of human b-ZIP proteins based on dimerization properties. *Molecular and Cellular Biology*, *22*(18), 6321–6335. https://doi.org/10.1128/MCB.22.18.6321-6335.2002

227. Vinson, C. R., Hai, T., & Boyd, S. M. (1993). Dimerization specificity of the leucine zipper-containing bZIP motif on DNA binding: Prediction and rational design. *Genes & Development*, *7*(6), 1047–1058. https://doi.org/10.1101/gad.7.6.1047

228. Vinson, C., Sigler, P., & McKnight, S. (1989). Scissors-grip model for DNA recognition by a family of leucine zipper proteins. *Science*, *246*(4932), 911–916. https://doi.org/10.1126/science.2683088

229. Jindrich, K., & Degnan, B. M. (2016). The diversification of the basic leucine zipper family in eukaryotes correlates with the evolution of multicellularity. *BMC Evolutionary Biology*, *16*(1), 28. https://doi.org/10.1186/s12862-016-0598-z

230. Rodríguez-Martínez, J. A., Reinke, A. W., Bhimsaria, D., Keating, A. E., & Ansari, A. Z. (2017). Combinatorial bZIP dimers display complex DNA-binding specificity landscapes. *ELife*, *6*, e19272. https://doi.org/10.7554/eLife.19272

231. Osada, S., Yamamoto, H., Nishihara, T., & Imagawa, M. (1996). DNA binding specificity of the CCAAT/enhancer-binding protein transcription factor family. *Journal of Biological Chemistry*, *271*(7), 3891–3896. https://doi.org/10.1074/jbc.271.7.3891

232. Parkin, S. E., Baer, M., Copeland, T. D., Schwartz, R. C., & Johnson, P. F. (2002). Regulation of CCAAT/enhancer-binding protein (C/EBP) activator proteins by heterodimerization with C/EBPγ (Ig/EBP). *Journal of Biological Chemistry*, *277*(26), 23563–23572. https://doi.org/10.1074/jbc.M202184200

233. Newman, J. R. S., & Keating, A. E. (2003). Comprehensive identification of human bZIP interactions with coiled-coil arrays. *Science*, *300*(5628), 2097–2101. https://doi.org/10.1126/science.1084648

234. Huggins, C. J., Mayekar, M. K., Martin, N., Saylor, K. L., Gonit, M., Jailwala, P., Kasoji, M., Haines, D. C., Quiñones, O. A., & Johnson, P. F. (2016). C/EBPγ Is a critical regulator of cellular stress response networks through heterodimerization with ATF4. *Molecular and Cellular Biology*, *36*(5), 693–713. https://doi.org/10.1128/MCB.00911-15

235. Cai, D. H., Wang, D., Keefer, J., Yeamans, C., Hensley, K., & Friedman, A. D. (2008). C/EBPα:AP-1 leucine zipper heterodimers bind novel DNA elements, activate the PU.1 promoter and direct monocyte lineage commitment more potently than C/EBPα homodimers or AP-1. *Oncogene*, *27*(19), 2772–2779. https://doi.org/10.1038/sj.onc.1210940

236. Kokame, K., Kato, H., & Miyata, T. (2001). Identification of ERSE-II, a new cis-acting element responsible for the ATF6-dependent mammalian unfolded protein response. *Journal of Biological Chemistry*, *276*(12), 9199–9205. https://doi.org/10.1074/jbc.M010486200

237. Wang, Y., Shen, J., Arenzana, N., Tirasophon, W., Kaufman, R. J., & Prywes, R. (2000). Activation of ATF6 and an ATF6 DNA binding site by the endoplasmic reticulum stress response. *Journal of Biological Chemistry*, *275*(35), 27013–27020. https://doi.org/10.1016/S0021-9258(19)61473-0

238. Yamamoto, K., Suzuki, N., Wada, T., Okada, T., Yoshida, H., Kaufman, R. J., & Mori, K. (2008). Human HRD1 promoter carries a functional unfolded protein response element to which XBP1 but not ATF6 directly binds. *Journal of Biochemistry*, *144*(4), 477–486. https://doi.org/10.1093/jb/mvn091

239. Yamamoto, K., Sato, T., Matsui, T., Sato, M., Okada, T., Yoshida, H., Harada, A., & Mori, K. (2007). Transcriptional induction of mammalian ER quality control proteins is mediated by single or combined action of ATF6α and XBP1. *Developmental Cell*, *13*(3), 365–376. https://doi.org/10.1016/j.devcel.2007.07.018

240. Yoshida, H., Matsui, T., Hosokawa, N., Kaufman, R. J., Nagata, K., & Mori, K. (2003). A time-dependent phase shift in the mammalian unfolded protein response. *Developmental Cell*, *4*(2), 265–271. https://doi.org/10.1016/S1534-5807(03)00022-4

241. Pramanik, J., Chen, X., Kar, G., Henriksson, J., Gomes, T., Park, J.-E., Natarajan, K., Meyer, K. B., Miao, Z., McKenzie, A. N. J., Mahata, B., & Teichmann, S. A. (2018). Genome-wide analyses reveal the IRE1a-XBP1 pathway promotes T helper cell differentiation by resolving secretory stress and accelerating proliferation. *Genome Medicine*, *10*(1), 76. https://doi.org/10.1186/s13073-018-0589-3

242. Kanemoto, S., Kondo, S., Ogata, M., Murakami, T., Urano, F., & Imaizumi, K. (2005). XBP1 activates the transcription of its target genes via an ACGT core sequence under ER stress. *Biochemical and Biophysical Research Communications*, *331*(4), 1146–1153. https://doi.org/10.1016/j.bbrc.2005.04.039

243. Dalton-Griffin, L., Wilson, S. J., & Kellam, P. (2009). X-Box binding protein 1 contributes to induction of the Kaposi's sarcoma-associated herpesvirus lytic cycle under hypoxic conditions. *Journal of Virology*, *83*(14), 7202–7209. https://doi.org/10.1128/JVI.00076-09

244. Harding, H. P., Novoa, I., Zhang, Y., Zeng, H., Wek, R., Schapira, M., & Ron, D. (2000). Regulated translation initiation controls stress-induced gene expression in mammalian cells. *Molecular Cell*, *6*(5), 1099–1108. https://doi.org/10.1016/S1097-2765(00)00108-8

245. Bruhat, A., Averous, J., Carraro, V., Zhong, C., Reimold, A. M., Kilberg, M. S., & Fafournoux, P. (2002). Differences in the molecular mechanisms involved in the transcriptional activation of the CHOP and asparagine synthetase genes in response to amino acid deprivation or activation of the unfolded protein response. *Journal of Biological Chemistry*, *277*(50), 48107–48114. https://doi.org/10.1074/jbc.M206149200

246. Averous, J., Bruhat, A., Jousse, C., Carraro, V., Thiel, G., & Fafournoux, P. (2004). Induction of CHOP expression by amino acid limitation requires both ATF4 expression and ATF2 phosphorylation. *Journal of Biological Chemistry*, *279*(7), 5288–5297. https://doi.org/10.1074/jbc.M311862200

247. Lopez, A. B., Wang, C., Huang, C. C., Yaman, I., Li, Y., Chakravarty, K., Johnson, P. F., Chiang, C.-M., Snider, M. D., Wek, R. C., & Hatzoglou, M. (2007). A feedback transcriptional mechanism controls the level of the arginine/lysine transporter cat-1 during amino acid starvation. *Biochemical Journal*, *402*(1), 163–173. https://doi.org/10.1042/BJ20060941

248. Rappoport, N., & Linial, M. (2012). Viral proteins acquired from a host converge to simplified domain architectures. *PLoS Computational Biology*, *8*(2), e1002364. https://doi.org/10.1371/journal.pcbi.1002364

249. Chang, Y. N., Dong, D. L., Hayward, G. S., & Hayward, S. D. (1990). The Epstein-Barr virus Zta transactivator: A member of the bZIP family with unique DNA-binding specificity and a dimerization domain that lacks the characteristic heptad leucine zipper motif. *Journal of Virology*, *64*(7), 3358–3369. https://doi.org/10.1128/JVI.64.7.3358-3369.1990

250. Lin, S.-F., Robinson, D. R., Miller, G., & Kung, H.-J. (1999). Kaposi's sarcoma-associated herpesvirus encodes a bZIP protein with homology to BZLF1 of Epstein-Barr virus. *Journal of Virology*, *73*(3), 1909–1917. https://doi.org/10.1128/JVI.73.3.1909-1917.1999

251. Gaudray, G., Gachon, F., Basbous, J., Biard-Piechaczyk, M., Devaux, C., & Mesnard, J.-M. (2002). The complementary strand of the human T-cell leukemia virus type 1 RNA genome encodes a bZIP transcription factor that down-regulates viral transcription. *Journal of Virology*, *76*(24), 12813–12822. https://doi.org/10.1128/JVI.76.24.12813-12822.2002

252. Welker, M.-W., Welsch, C., Meyer, A., Antes, I., Albrecht, M., Forestier, N., Kronenberger, B., Lengauer, T., Piiper, A., Zeuzem, S., & Sarrazin, C. (2010). Dimerization of the hepatitis C virus nonstructural protein 4B depends on the integrity of an aminoterminal basic leucine zipper: HCV NS4B-Dimerization via Leucine Zipper. *Protein Science*, *19*(7), 1327–1336. https://doi.org/10.1002/pro.409

253. Jones, D., Lee, L., Liu, J.-L., Kung, H.-J., & Tillotson, J. K. (1992). Marek disease virus encodes a basic-leucine zipper gene resembling the fos/jun oncogenes that is highly expressed in lymphoblastoid tumors. *Proceedings of the National Academy of Sciences*, *89*(9), 4042–4046. https://doi.org/10.1073/pnas.89.9.4042

254. Qian, Z., Brunovskis, P., Lee, L., Vogt, P. K., & Kung, H. J. (1996). Novel DNA binding specificities of a putative herpesvirus bZIP oncoprotein. *Journal of Virology*, *70*(10), 7161–7170. https://doi.org/10.1128/JVI.70.10.7161-7170.1996

255. Levy, A. M., Izumiya, Y., Brunovskis, P., Xia, L., Parcells, M. S., Reddy, S. M., Lee, L., Chen, H.-W., & Kung, H.-J. (2003). Characterization of the chromosomal binding sites and dimerization partners of the viral oncoprotein Meq in Marek's disease virus-transformed T-cells. *Journal of Virology*, *77*(23), 12841–12851. https://doi.org/10.1128/JVI.77.23.12841-12851.2003

256. Reinke, A. W., Grigoryan, G., & Keating, A. E. (2010). Identification of bZIP interaction partners of viral proteins HBZ, MEQ, BZLF1, and K-bZIP using coiled-coil arrays. *Biochemistry*, *49*(9), 1985–1997. https://doi.org/10.1021/bi902065k

257. Thébault, S., Basbous, J., Hivin, P., Devaux, C., & Mesnard, J.-M. (2004). HBZ interacts with JunD and stimulates its transcriptional activity. *Federation of European Biochemical Societies Letters*, *562*(1–3), 165–170. https://doi.org/10.1016/S0014-5793(04)00225-X

258. Kuhlmann, A.-S., Villaudy, J., Gazzolo, L., Castellazzi, M., Mesnard, J.-M., & Duc Dodon, M. (2007). HTLV-1 HBZ cooperates with JunD to enhance transcription of the human telomerase reverse transcriptase gene (hTERT). *Retrovirology*, *4*(1), 92. https://doi.org/10.1186/1742-4690-4-92

259. Matsumoto, J., Ohshima, T., Isono, O., & Shimotohno, K. (2005). HTLV-1 HBZ suppresses AP-1 activity by impairing both the DNA-binding ability and the stability of c-Jun protein. *Oncogene*, *24*(6), 1001–1010. https://doi.org/10.1038/sj.onc.1208297

260. Lemasson, I., Lewis, M. R., Polakowski, N., Hivin, P., Cavanagh, M.-H., Thébault, S., Barbeau, B., Nyborg, J. K., & Mesnard, J.-M. (2007). Human T-cell leukemia virus type 1 (HTLV-1) bZIP protein interacts with the cellular transcription factor CREB to inhibit HTLV-1 transcription. *Journal of Virology*, *81*(4), 1543–1553. https://doi.org/10.1128/JVI.00480-06

261. Mukai, R., & Ohshima, T. (2011). Dual effects of HTLV-1 bZIP factor in suppression of interferon regulatory factor 1. *Biochemical and Biophysical Research Communications*, *409*(2), 328–332. https://doi.org/10.1016/j.bbrc.2011.05.014

262. Ma, Y., Zheng, S., Wang, Y., Zang, W., Li, M., Wang, N., Li, P., Jin, J., Dong, Z., & Zhao, G. (2013). The HTLV-1 HBZ protein inhibits cyclin D1 expression through interacting with the cellular transcription factor CREB. *Molecular Biology Reports*, *40*(10), 5967–5975. https://doi.org/10.1007/s11033-013-2706-0

263. Wu, F. Y., Wang, S. E., Chen, H., Wang, L., Hayward, S. D., & Hayward, G. S. (2004). CCAAT/enhancer binding protein α binds to the Epstein-Barr virus (EBV) ZTA protein through oligomeric interactions and contributes to cooperative transcriptional activation of the ZTA promoter through direct binding to the ZII and ZIIIB motifs during Induction of the EBV lytic cycle. *Journal of Virology*, *78*(9), 4847–4865. https://doi.org/10.1128/JVI.78.9.4847–4865.2004

264. Wu, F. Y., Wang, S. E., Tang, Q.-Q., Fujimuro, M., Chiou, C.-J., Zheng, Q., Chen, H., Hayward, S. D., Lane, M. D., & Hayward, G. S. (2003). Cell cycle arrest by Kaposi's sarcoma-associated herpesvirus replication-associated protein is mediated at both the transcriptional and posttranslational levels by binding to CCAAT/enhancer-binding protein α and p21CIP-1. *Journal of Virology*, *77*(16), 8893–8914. https://doi.org/10.1128/JVI.77.16.8893–8914.2003

265. Kaul, R., Purushothaman, P., Uppal, T., & Verma, S. C. (2019). KSHV lytic proteins K-RTA and K8 bind to cellular and viral chromatin to modulate gene expression. *PLOS ONE*, *14*(4), e0215394. https://doi.org/10.1371/journal.pone.0215394

266. Lieberman, P. M., Hardwick, J. M., Sample, J., Hayward, G. S., & Hayward, S. D. (1990). The zta transactivator involved in induction of lytic cycle gene expression in Epstein-Barr virus-infected lymphocytes binds to both AP-1 and ZRE sites in target promoter and enhancer regions. *Journal of Virology*, *64*(3), 1143–1155. https://doi.org/10.1128/JVI.64.3.1143-1155.1990

267. Ohshima, T., Mukai, R., Nakahara, N., Matsumoto, J., Isono, O., Kobayashi, Y., Takahashi, S., & Shimotohno, K. (2010). HTLV-1 basic leucine-zipper factor, HBZ, interacts with MafB and suppresses transcription through a Maf recognition element. *Journal of Cellular Biochemistry*, *111*(1), 187–194. https://doi.org/10.1002/jcb.22687

268. Chang, P.-C., Izumiya, Y., Wu, C.-Y., Fitzgerald, L. D., Campbell, M., Ellison, T. J., Lam, K. S., Luciw, P. A., & Kung, H.-J. (2010). Kaposi's Sarcoma-associated herpesvirus (KSHV) encodes a SUMO E3 ligase that is SIM-dependent and SUMO-2/3-specific. *Journal of Biological Chemistry*, *285*(8), 5266–5273. https://doi.org/10.1074/jbc.M109.088088

269. Qian, Z., Brunovskis, P., Rauscher, F., Lee, L., & Kung, H. J. (1995). Transactivation activity of Meq, a Marek's disease herpesvirus bZIP protein persistently expressed in latently infected transformed T cells. *Journal of Virology*, *69*(7), 4037–4044. https://doi.org/10.1128/JVI.69.7.4037-4044.1995

270. Clerc, I., Polakowski, N., André-Arpin, C., Cook, P., Barbeau, B., Mesnard, J.-M., & Lemasson, I. (2008). An interaction between the human T cell leukemia virus type 1 basic leucine Zipper factor (HBZ) and the KIX domain of p300/CBP contributes to the down-regulation of Tax-dependent viral transcription by HBZ. *Journal of Biological Chemistry*, *283*(35), 23903–23913. https://doi.org/10.1074/jbc.M803116200

271. Hügle, T., Fehrmann, F., Bieck, E., Kohara, M., Kräusslich, H.-G., Rice, C. M., Blum, H. E., & Moradpour, D. (2001). The hepatitis C virus nonstructural protein 4B is an integral endoplasmic reticulum membrane protein. *Virology*, *284*(1), 70–81. https://doi.org/10.1006/viro.2001.0873

272. Egger, D., Wölk, B., Gosert, R., Bianchi, L., Blum, H. E., Moradpour, D., & Bienz, K. (2002). Expression of hepatitis C virus proteins induces distinct membrane alterations including a candidate viral replication complex. *Journal of Virology*, *76*(12), 5974–5984. https://doi.org/10.1128/JVI.76.12.5974-5984.2002

273. Frabutt, D. A., Wang, B., Riaz, S., Schwartz, R. C., & Zheng, Y.-H. (2018). Innate sensing of influenza A virus hemagglutinin glycoproteins by the host endoplasmic reticulum (ER) stress pathway triggers a potent antiviral response via ER-associated protein degradation. *Journal of Virology*, *92*(1), 14.

274. Li, S., Ye, L., Yu, X., Xu, B., Li, K., Zhu, X., Liu, H., Wu, X., & Kong, L. (2009). Hepatitis C virus NS4B induces unfolded protein response and endoplasmic reticulum overload response-dependent NF-κB activation. *Virology*, *391*(2), 257–264. https://doi.org/10.1016/j.virol.2009.06.039

275. Zheng, Y., Gao, B., Ye, L., Kong, L., Jing, W., Yang, X., Wu, Z., & Ye, L. (2005). Hepatitis C virus non-structural protein NS4B can modulate an unfolded protein response. *Journal of Microbiology*, *43*(6), 529–536.

276. Peña, J., & Harris, E. (2011). Dengue virus modulates the unfolded protein response in a time-dependent manner. *Journal of Biological Chemistry*, *286*(16), 14226–14236. https://doi.org/10.1074/jbc.M111.222703

277. Turpin, J., Frumence, E., Harrabi, W., Haddad, J. G., El Kalamouni, C., Desprès, P., Krejbich-Trotot, P., & Viranaïcken, W. (2020). Zika virus subversion of chaperone GRP78/BiP expression in A549 cells during UPR activation. *Biochimie*, *175*, 99–105. https://doi.org/10.1016/j.biochi.2020.05.011

278. Mulvey, M., Arias, C., & Mohr, I. (2007). Maintenance of endoplasmic reticulum (ER) homeostasis in herpes simplex virus type 1-infected cells through the association of a viral glycoprotein with PERK, a cellular ER stress sensor. *Journal of Virology*, *81*(7), 3377–3390. https://doi.org/10.1128/JVI.02191-06

279. Zhang, P., Su, C., Jiang, Z., & Zheng, C. (2017). Herpes simplex virus 1 UL41 protein suppresses the IRE1/XBP1 signal pathway of the unfolded protein response via its RNase activity. *Journal of Virology*, *91*(4), e02056-16. https://doi.org/10.1128/JVI.02056-16

280. Sun, C. C., & Thorley-Lawson, D. A. (2007). Plasma cell-specific transcription factor XBP-1s binds to and transactivates the Epstein-Barr virus BZLF1 promoter. *Journal of Virology*, *81*(24), 13566–13577. https://doi.org/10.1128/JVI.01055-07

281. Taylor, G. M., Raghuwanshi, S. K., Rowe, D. T., Wadowsky, R. M., & Rosendorff, A. (2011). Endoplasmic reticulum stress causes EBV lytic replication. *Blood*, *118*(20), 5528–5539. https://doi.org/10.1182/blood-2011-04-347112

282. Ke, P.-Y., & Chen, S. S.-L. (2011). Activation of the unfolded protein response and autophagy after hepatitis C virus infection suppresses innate antiviral immunity in vitro. *Journal of Clinical Investigation*, *121*(1), 37–56. https://doi.org/10.1172/JCI41474

283. Chen, L.-W., Wang, S.-S., Hung, C.-H., Hung, Y.-H., Lin, C.-L., & Chang, P.-J. (2021). The Epstein-Barr virus lytic protein BMLF1 induces upregulation of GRP78 expression through ATF6 activation. *International Journal of Molecular Sciences*, *22*(8), 4024. https://doi.org/10.3390/ijms22084024

284. Hinte, F., van Anken, E., Tirosh, B., & Brune, W. (2020). Repression of viral gene expression and replication by the unfolded protein response effector XBP1u. *ELife*, *9*, e51804. https://doi.org/10.7554/eLife.51804

285. Fan, Y., & He, J. J. (2016). HIV-1 Tat induces unfolded protein response and endoplasmic reticulum stress in astrocytes and causes neurotoxicity through glial fibrillary Acidic protein (GFAP) activation and aggregation. *Journal of Biological Chemistry*, *291*(43), 22819–22829. https://doi.org/10.1074/jbc.M116.731828

286. Johnston, B. P., Pringle, E. S., & McCormick, C. (2019). KSHV activates unfolded protein response sensors but suppresses downstream transcriptional responses to support lytic replication. *PLOS Pathogens*, *15*(12), e1008185. https://doi.org/10.1371/journal.ppat.1008185

287. Johnston, B. P. (2019). *Kaposi's sarcoma-associated herpesvirus modulates the unfolded protein response during lytic replication* [Doctoral thesis]. Dalhousie University.

288. Izumiya, Y., Ellison, T. J., Yeh, E. T. H., Jung, J. U., Luciw, P. A., & Kung, H.-J. (2005). Kaposi's sarcoma-associated herpesvirus K-bZIP represses gene transcription via SUMO modification. *Journal of Virology*, *79*(15), 9912–9925. https://doi.org/10.1128/JVI.79.15.9912-9925.2005

289. Lefort, S., Gravel, A., & Flamand, L. (2010). Repression of interferon-α stimulated genes expression by Kaposi's sarcoma-associated herpesvirus K-bZIP protein. *Virology*, *408*(1), 14–30. https://doi.org/10.1016/j.virol.2010.07.027

290. Lefort, S., & Flamand, L. (2009). Kaposi's sarcoma-associated herpesvirus K-bZIP protein is necessary for lytic viral gene expression, DNA replication, and virion production in primary effusion lymphoma cell lines. *Journal of Virology*, *83*(11), 5869–5880. https://doi.org/10.1128/JVI.01821-08

291. Wu, F. Y., Chen, H., Wang, S. E., Fujimuro, M., Farrell, C. J., Huang, J., Hayward, S. D., & Hayward, G. S. (2003). CCAAT/enhancer binding protein α interacts with ZTA and mediates ZTA-induced p21CIP-1 accumulation and G1 cell cycle arrest during the Epstein-Barr virus lytic cycle. *Journal of Virology*, *77*(2), 1481–1500. https://doi.org/10.1128/JVI.77.2.1481–1500.2003

292. Izumiya, Y., Lin, S.-F., Ellison, T. J., Levy, A. M., Mayeur, G. L., Izumiya, C., & Kung, H.-J. (2003). Cell cycle regulation by Kaposi's sarcoma-associated herpesvirus K-bZIP: Direct interaction with cyclin-CDK2 and induction of G1 growth arrest. *Journal of Virology*, *77*(17), 9652–9661. https://doi.org/10.1128/JVI.77.17.9652-9661.2003

293. Sinclair, A. J. (2003). BZIP proteins of human gammaherpesviruses. *Journal of General Virology*, *84*(8), 1941–1949. https://doi.org/10.1099/vir.0.19112-0

294. Wu, F. Y., Tang, Q.-Q., Chen, H., ApRhys, C., Farrell, C., Chen, J., Fujimuro, M., Lane, M. D., & Hayward, G. S. (2002). Lytic replication-associated protein (RAP) encoded by Kaposi sarcoma-associated herpesvirus causes p21CIP-1-mediated G1 cell cycle arrest through CCAAT/enhancer-binding protein-α. *Proceedings of the National Academy of Sciences*, *99*(16), 10683–10688. https://doi.org/10.1073/pnas.162352299

295. Teijaro, J. R. (2016). Type I interferons in viral control and immune regulation. *Current Opinion in Virology*, *16*, 31–40. https://doi.org/10.1016/j.coviro.2016.01.001

296. Lefort, S., Soucy-Faulkner, A., Grandvaux, N., & Flamand, L. (2007). Binding of Kaposi's sarcoma-associated herpesvirus K-bZIP to interferon-responsive factor 3 elements modulates antiviral gene expression. *Journal of Virology*, *81*(20), 10950–10960. https://doi.org/10.1128/JVI.00183-07

297. Regad, T., & Chelbi-Alix, M. K. (2001). Role and fate of PML nuclear bodies in response to interferon and viral infections. *Oncogene*, *20*(49), 7274–7286. https://doi.org/10.1038/sj.onc.1204854

298. Muñoz-Fontela, C., Macip, S., Martínez-Sobrido, L., Brown, L., Ashour, J., García-Sastre, A., Lee, S. W., & Aaronson, S. A. (2008). Transcriptional role of p53 in interferon-mediated antiviral immunity. *Journal of Experimental Medicine*, *205*(8), 1929–1938. https://doi.org/10.1084/jem.20080383

299. Pearson, M., Carbone, R., Sebastiani, C., Cioce, M., Fagioli, M., Saito, S., Higashimoto, Y., Appella, E., Minucci, S., Pandolfi, P. P., & Pelicci, P. G. (2000). PML regulates p53 acetylation and premature senescence induced by oncogenic Ras. *Nature*, *406*(6792), 207–210. https://doi.org/10.1038/35018127

300. Zhang, Q., Gutsch, D., & Kenney, S. (1994). Functional and physical interaction between p53 and BZLF1: Implications for Epstein-Barr virus latency. *Molecular and Cellular Biology*, *14*(3), 1929–1938. https://doi.org/10.1128/MCB.14.3.1929

301. Mauser, A., Saito, S., Appella, E., Anderson, C. W., Seaman, W. T., & Kenney, S. (2002). The Epstein-Barr virus immediate-early protein BZLF1 regulates p53 function through multiple mechanisms. *Journal of Virology*, *76*(24), 12503–12512. https://doi.org/10.1128/JVI.76.24.12503-12512.2002

302. Katano, H., Ogawa-Goto, K., Hasegawa, H., Kurata, T., & Sata, T. (2001). Human-herpesvirus-8-encoded K8 protein colocalizes with the promyelocytic leukemia protein (PML) bodies and recruits p53 to the PML bodies. *Virology*, *286*(2), 446–455. https://doi.org/10.1006/viro.2001.1005

303. Hossain, Md. G., Ohsaki, E., Honda, T., & Ueda, K. (2018). Importance of promyelocytic leukemia protein (PML) for Kaposi's sarcoma-associated herpesvirus lytic replication. *Frontiers in Microbiology*, *9*, 2324. https://doi.org/10.3389/fmicb.2018.02324

304. Zerby, D., Chen, C.-J., Poon, E., Lee, D., Shiekhattar, R., & Lieberman, P. M. (1999). The amino-terminal C/H1 domain of CREB binding protein mediates Zta transcriptional activation of latent Epstein-Barr virus. *Molecular and Cellular Biology*, *19*(3), 1617–1626. https://doi.org/10.1128/MCB.19.3.1617

305. Adamson, A. L., & Kenney, S. (1999). The Epstein-Barr virus BZLF1 protein interacts physically and functionally with the histone acetylase CREB-binding protein. *Journal of Virology*, *73*(8), 6551–6558. https://doi.org/10.1128/JVI.73.8.6551-6558.1999

306. Hwang, S., Gwack, Y., Byun, H., Lim, C., & Choe, J. (2001). The Kaposi's sarcoma-associated herpesvirus K8 protein interacts with CREB-binding protein (CBP) and represses CBP-mediated transcription. *Journal of Virology*, *75*(19), 9509–9516. https://doi.org/10.1128/JVI.75.19.9509-9516.2001

307. Tomita, M., Choe, J., Tsukazaki, T., & Mori, N. (2004). The Kaposi's sarcoma-associated herpesvirus K-bZIP protein represses transforming growth factor β signaling through interaction with CREB-binding protein. *Oncogene*, *23*(50), 8272–8281. https://doi.org/10.1038/sj.onc.1208059

308. Martínez, F. P., & Tang, Q. (2012). Leucine zipper domain is required for Kaposi sarcoma-associated herpesvirus (KSHV) K-bZIP protein to interact with histone deacetylase and is important for KSHV replication. *Journal of Biological Chemistry*, *287*(19), 15622–15634. https://doi.org/10.1074/jbc.M111.315861

309. Hwang, S., Lee, D., Gwack, Y., Min, H., & Choe, J. (2003). Kaposi's sarcoma-associated herpesvirus K8 protein interacts with hSNF5. *Journal of General Virology*, *84*(3), 665–676. https://doi.org/10.1099/vir.0.18699-0

310. Hunter, O. V., Sei, E., Richardson, R. B., & Conrad, N. K. (2013). Chromatin immunoprecipitation and microarray analysis suggest functional cooperation between Kaposi's sarcoma-associated herpesvirus ORF57 and K-bZIP. *Journal of Virology*, *87*(7), 4005–4016. https://doi.org/10.1128/JVI.03459-12

311. Izumiya, Y., Izumiya, C., Van Geelen, A., Wang, D.-H., Lam, K. S., Luciw, P. A., & Kung, H.-J. (2007). Kaposi's sarcoma-associated herpesvirus-encoded protein kinase and its interaction with K-bZIP. *Journal of Virology*, *81*(3), 1072–1082. https://doi.org/10.1128/JVI.01473-06

312. Lowrey, A. J., Cramblet, W., & Bentz, G. L. (2017). Viral manipulation of the cellular sumoylation machinery. *Cell Communication and Signaling*, *15*(1), 27. https://doi.org/10.1186/s12964-017-0183-0

313. Bossis, G., Malnou, C. E., Farras, R., Andermarcher, E., Hipskind, R., Rodriguez, M., Schmidt, D., Muller, S., Jariel-Encontre, I., & Piechaczyk, M. (2005). Down-regulation of c-Fos/c-Jun AP-1 dimer activity by sumoylation. *Molecular and Cellular Biology*, *25*(16), 6964–6979. https://doi.org/10.1128/MCB.25.16.6964-6979.2005

314. Eaton, E. M., & Sealy, L. (2003). Modification of CCAAT/enhancer-binding protein-β by the small ubiquitin-like modifier (SUMO) family members, SUMO-2 and SUMO-3. *Journal of Biological Chemistry*, *278*(35), 33416–33421. https://doi.org/10.1074/jbc.M305680200

315. Hou, X., Yang, Z., Zhang, K., Fang, D., & Sun, F. (2017). SUMOylation represses the transcriptional activity of the unfolded protein response transducer ATF6. *Biochemical and Biophysical Research Communications*, *494*(3–4), 446–451. https://doi.org/10.1016/j.bbrc.2017.10.103

316. Chen, H., & Qi, L. (2010). SUMO modification regulates the transcriptional activity of XBP1. *Biochemical Journal*, *429*(1), 95–102. https://doi.org/10.1042/BJ20100193

317. Rosonina, E., Akhter, A., Dou, Y., Babu, J., & Sri Theivakadadcham, V. S. (2017). Regulation of transcription factors by sumoylation. *Transcription*, *8*(4), 220–231. https://doi.org/10.1080/21541264.2017.1311829

318. Chang, P.-C., & Kung, H.-J. (2014). SUMO and KSHV replication. *Cancers*, *6*(4), 1905–1924. https://doi.org/10.3390/cancers6041905

319. Yang, W.-S., Hsu, H.-W., Campbell, M., Cheng, C.-Y., & Chang, P.-C. (2015). K-bZIP mediated SUMO-2/3 specific modification on the KSHV genome negatively regulates lytic gene expression and viral reactivation. *PLOS Pathogens*, *11*(7), e1005051. https://doi.org/10.1371/journal.ppat.1005051

320. Wang, M., Sang, J., Ren, Y., Liu, K., Liu, X., Zhang, J., Wang, H., Wang, J., Orian, A., Yang, J., & Yi, J. (2016). SENP3 regulates the global protein turnover and the Sp1 level via antagonizing SUMO2/3-targeted ubiquitination and degradation. *Protein & Cell*, *7*(1), 63–77. https://doi.org/10.1007/s13238-015-0216-7

321. Izumiya, Y., Kobayashi, K., Kim, K. Y., Pochampalli, M., Izumiya, C., Shevchenko, B., Wang, D.-H., Huerta, S. B., Martinez, A., Campbell, M., & Kung, H.-J. (2013). Kaposi's sarcoma-associated herpesvirus K-Rta exhibits SUMO-targeting ubiquitin ligase (STUbL) like activity and is essential for viral reactivation. *PLoS Pathogens*, *9*(8), e1003506. https://doi.org/10.1371/journal.ppat.1003506

322. Yang, W.-S., Campbell, M., Kung, H.-J., & Chang, P.-C. (2018). In vitro SUMOylation assay to study SUMO E3 ligase activity. *Journal of Visualized Experiments*, *131*, 56629. https://doi.org/10.3791/56629

323. Myoung, J., & Ganem, D. (2011). Generation of a doxycycline-inducible KSHV producer cell line of endothelial origin: Maintenance of tight latency with efficient reactivation upon induction. *Journal of Virological Methods*, *174*(1–2), 12–21. https://doi.org/10.1016/j.jviromet.2011.03.012

324. Nakamura, H., Lu, M., Gwack, Y., Souvlis, J., Zeichner, S. L., & Jung, J. U. (2003). Global changes in Kaposi's sarcoma-associated virus gene expression patterns following expression of a tetracycline-inducible Rta transactivator. *Journal of Virology*, *77*(7), 4205–4220. https://doi.org/10.1128/JVI.77.7.4205-4220.2003

325. Aranda, P. S., LaJoie, D. M., & Jorcyk, C. L. (2012). Bleach gel: A simple agarose gel for analyzing RNA quality. *ELECTROPHORESIS*, *33*(2), 366–369. https://doi.org/10.1002/elps.201100335

326. Senichkin, V. V., Prokhorova, E. A., Zhivotovsky, B., & Kopeina, G. S. (2021). Simple and efficient protocol for subcellular fractionation of normal and apoptotic cells. *Cells*, *10*(4), 852. https://doi.org/10.3390/cells10040852

327. Diner, E. J., Burdette, D. L., Wilson, S. C., Monroe, K. M., Kellenberger, C. A., Hyodo, M., Hayakawa, Y., Hammond, M. C., & Vance, R. E. (2013). The innate immune DNA sensor cGAS produces a noncanonical cyclic dinucleotide that activates human STING. *Cell Reports*, *3*(5), 1355–1361. https://doi.org/10.1016/j.celrep.2013.05.009

328. Fitzgerald, K. A., McWhirter, S. M., Faia, K. L., Rowe, D. C., Latz, E., Golenbock, D. T., Coyle, A. J., Liao, S.-M., & Maniatis, T. (2003). IKKε and TBK1 are essential components of the IRF3 signaling pathway. *Nature Immunology*, *4*(5), 491–496. https://doi.org/10.1038/ni921

329. Tanaka, Y., & Chen, Z. J. (2012). STING specifies IRF3 phosphorylation by TBK1 in the cytosolic DNA signaling pathway. *Science Signaling*, *5*(214). https://doi.org/10.1126/scisignal.2002521

330. Field, A. K., Tytell, A. A., Piperno, E., Lampson, G. P., Nemes, M. M., & Hilleman, M. R. (1972). Poly I:C, an inducer of interferon and interference against virus infection. *Medicine*, *51*(3), 169–174.

331. Field, R., Campion, S., Warren, C., Murray, C., & Cunningham, C. (2010). Systemic challenge with the TLR3 agonist poly I:C induces amplified IFNα/β and IL-1β responses in the diseased brain and exacerbates chronic neurodegeneration. *Brain, Behavior, and Immunity*, *24*(6), 996–1007. https://doi.org/10.1016/j.bbi.2010.04.004

332. Lytton, J., Westlin, M., & Hanley, M. R. (1991). Thapsigargin inhibits the sarcoplasmic or endoplasmic reticulum Ca-ATPase family of calcium pumps. *Journal of Biological Chemistry*, *266*(26), 17067–17071. https://doi.org/10.1016/S0021-9258(19)47340-7

333. Austgen, K., Oakes, S. A., & Ganem, D. (2012). Multiple defects, including premature apoptosis, prevent Kaposi's sarcoma-associated herpesvirus replication in murine cells. *Journal of Virology*, *86*(3), 1877–1882. https://doi.org/10.1128/JVI.06600-11

334. Patil, C., & Walter, P. (2001). Intracellular signaling from the endoplasmic reticulum to the nucleus: The unfolded protein response in yeast and mammals. *Current Opinion in Cell Biology*, *13*(3), 349–355. https://doi.org/10.1016/S0955-0674(00)00219-2

335. Wen, H.-J., Minhas, V., & Wood, C. (2009). Identification and characterization of a new Kaposi's sarcoma-associated herpesvirus replication and transcription activator (RTA)-responsive element involved in RTA-mediated transactivation. *Journal of General Virology*, *90*(4), 944–953. https://doi.org/10.1099/vir.2008.006817-0

336. Boyne, J. R., Jackson, B. R., Taylor, A., Macnab, S. A., & Whitehouse, A. (2010). Kaposi's sarcoma-associated herpesvirus ORF57 protein interacts with PYM to enhance translation of viral intronless mRNAs. *The EMBO Journal*, *29*(11), 1851–1864. https://doi.org/10.1038/emboj.2010.77

337. Kirshner, J. R., Lukac, D. M., Chang, J., & Ganem, D. (2000). Kaposi's sarcoma-associated herpesvirus open reading frame 57 encodes a posttranscriptional regulator with multiple distinct activities. *Journal of Virology*, *74*(8), 3586–3597. https://doi.org/10.1128/JVI.74.8.3586-3597.2000

338. Palmeri, D., Spadavecchia, S., Carroll, K. D., & Lukac, D. M. (2007). Promoter- and cell-specific transcriptional transactivation by the Kaposi's sarcoma-associated herpesvirus ORF57/Mta protein. *Journal of Virology*, *81*(24), 13299–13314. https://doi.org/10.1128/JVI.00732-07

339. Waser, M., Mesaeli, N., Spencer, C., & Michalak, M. (1997). Regulation of calreticulin gene expression by calcium. *Journal of Cell Biology*, *138*(3), 547–557. https://doi.org/10.1083/jcb.138.3.547

340. Nguyen, T. Q., Donald Capra, J., & Sontheimer, R. D. (1996). Calreticulin is transcriptionally upregulated by heat shock, calcium and heavy metals. *Molecular Immunology*, *33*(4–5), 379–386. https://doi.org/10.1016/0161-5890(95)00149-2

341. Launay, S., Giannı, M., Zassadowski, F., Chomienne, C., & Enouf, J. (1999). Lineage-specific modulation of calcium pump expression during myeloid differentiation. *Phagocytes*, *93*(12), 4395–4405.

342. Papp, B., Brouland, J.-P., Gélébart, P., Kovàcs, T., & Chomienne, C. (2004). Endoplasmic reticulum calcium transport ATPase expression during differentiation of colon cancer and leukaemia cells. *Biochemical and Biophysical Research Communications*, *322*(4), 1223–1236. https://doi.org/10.1016/j.bbrc.2004.08.030

343. Portes-Sentis, S., Manet, E., Gourru, G., Sergeant, A., & Gruffat, H. (2001). Identification of a short amino acid sequence essential for efficient nuclear targeting of the Kaposi's sarcoma-associated herpesvirus/human herpesvirus-8 K8 protein. *Journal of General Virology*, *82*(3), 507–512. https://doi.org/10.1099/0022-1317-82-3-507

344. Li, J., Zhao, J., Xu, S., Zhang, S., Zhang, J., Xiao, J., Gao, R., Tian, M., Zeng, Y., Lee, K., Tarakanova, V., Lan, K., Feng, H., & Feng, P. (2019). Antiviral activity of a purine synthesis enzyme reveals a key role of deamidation in regulating protein nuclear import. *Science Advances*, *5*(10), eaaw7373. https://doi.org/10.1126/sciadv.aaw7373

345. Majerciak, V., Yamanegi, K., Nie, S. H., & Zheng, Z.-M. (2006). Structural and functional analyses of Kaposi sarcoma-associated herpesvirus ORF57 nuclear localization signals in living cells. *Journal of Biological Chemistry*, *281*(38), 28365–28378. https://doi.org/10.1074/jbc.M603095200

346. Vieira, J., & O'Hearn, P. M. (2004). Use of the red fluorescent protein as a marker of Kaposi's sarcoma-associated herpesvirus lytic gene expression. *Virology*, *325*(2), 225–240. https://doi.org/10.1016/j.virol.2004.03.049

347. Majerciak, V. (2009). Kaposi's sarcoma-associated herpesvirus ORF57 in viral RNA processing. *Frontiers in Bioscience*, *Volume*(14), 1516. https://doi.org/10.2741/3322

348. Gruffat, H., Batisse, J., Pich, D., Neuhierl, B., Manet, E., Hammerschmidt, W., & Sergeant, A. (2002). Epstein-Barr virus mRNA export factor EB2 is essential for production of infectious virus. *Journal of Virology*, *76*(19), 9635–9644. https://doi.org/10.1128/JVI.76.19.9635-9644.2002

349. Hiriart, E., Bardouillet, L., Manet, E., Gruffat, H., Penin, F., Montserret, R., Farjot, G., & Sergeant, A. (2003). A region of the Epstein-Barr virus (EBV) mRNA export factor EB2 containing an arginine-rich motif mediates direct binding to RNA. *Journal of Biological Chemistry*, *278*(39), 37790–37798. https://doi.org/10.1074/jbc.M305925200

350. Ricci, E. P., Mure, F., Gruffat, H., Decimo, D., Medina-Palazon, C., Ohlmann, T., & Manet, E. (2009). Translation of intronless RNAs is strongly stimulated by the Epstein–Barr virus mRNA export factor EB2. *Nucleic Acids Research*, *37*(15), 4932–4943. https://doi.org/10.1093/nar/gkp497

351. Juillard, F., Hiriart, E., Sergeant, N., Vingtdeux-Didier, V., Drobecq, H., Sergeant, A., Manet, E., & Gruffat, H. (2009). Epstein-Barr virus protein EB2 contains an N-terminal transferable nuclear export signal that promotes nucleocytoplasmic export by directly binding TAP/NXF1. *Journal of Virology*, *83*(24), 12759–12768. https://doi.org/10.1128/JVI.01276-09

352. Yuan, F., Gao, Z.-Q., Majerciak, V., Bai, L., Hu, M.-L., Lin, X.-X., Zheng, Z.-M., Dong, Y.-H., & Lan, K. (2018). The crystal structure of KSHV ORF57 reveals dimeric active sites important for protein stability and function. *PLOS Pathogens*, *14*(8), e1007232. https://doi.org/10.1371/journal.ppat.1007232

353. Freitas, N., & Cunha, C. (2009). Mechanisms and signals for the nuclear import of proteins. *Current Genomics*, *10*(8), 550–557.

354. Pemberton, L. F., & Paschal, B. M. (2005). Mechanisms of receptor-mediated nuclear import and nuclear export: Nucleocytoplasmic transport. *Traffic*, *6*(3), 187–198. https://doi.org/10.1111/j.1600-0854.2005.00270.x

355. Lin, R., Heylbroeck, C., Pitha, P. M., & Hiscott, J. (1998). Virus-dependent phosphorylation of the IRF-3 transcription factor regulates nuclear translocation, transactivation potential, and proteasome-mediated degradation. *Molecular and Cellular Biology*, *18*(5), 2986–2996. https://doi.org/10.1128/MCB.18.5.2986

356. Khokhlatchev, A. V., Canagarajah, B., Wilsbacher, J., Robinson, M., Atkinson, M., Goldsmith, E., & Cobb, M. H. (1998). Phosphorylation of the MAP kinase ERK2 promotes its homodimerization and nuclear translocation. *Cell*, *93*(4), 605–615. https://doi.org/10.1016/S0092-8674(00)81189-7

357. Lidke, D. S., Huang, F., Post, J. N., Rieger, B., Wilsbacher, J., Thomas, J. L., Pouysségur, J., Jovin, T. M., & Lenormand, P. (2010). ERK nuclear translocation is dimerization-independent but controlled by the rate of phosphorylation. *Journal of Biological Chemistry*, *285*(5), 3092–3102. https://doi.org/10.1074/jbc.M109.064972

358. Surguladze, N., Patton, S., Cozzi, A., Fried, M. G., & Connor, J. R. (2005). Characterization of nuclear ferritin and mechanism of translocation. *Biochemical Journal*, *388*(3), 731–740. https://doi.org/10.1042/BJ20041853

359. Geetha, T., Kenchappa, R. S., Wooten, M. W., & Carter, B. D. (2005). TRAF6-mediated ubiquitination regulates nuclear translocation of NRIF, the p75 receptor interactor. *The EMBO Journal*, *24*(22), 3859–3868. https://doi.org/10.1038/sj.emboj.7600845

360. Terui, Y., Saad, N., Jia, S., McKeon, F., & Yuan, J. (2004). Dual role of sumoylation in the nuclear localization and transcriptional activation of NFAT1. *Journal of Biological Chemistry*, *279*(27), 28257–28265. https://doi.org/10.1074/jbc.M403153200

361. Haze, K., Okada, T., Yoshida, H., Yanagi, H., Yura, T., Negishi, M., & Mori, K. (2001). Identification of the G13 (cAMP-response-element-binding protein-related protein) gene product related to activating transcription factor 6 as a transcriptional activator of the mammalian unfolded protein response. *Journal of Biochemistry*, *355*, 19–28.

362. Thuerauf, D. J., Morrison, L., & Glembotski, C. C. (2004). Opposing Roles for ATF6α and ATF6β in Endoplasmic Reticulum Stress Response Gene Induction. *Journal of Biological Chemistry*, *279*(20), 21078–21084. https://doi.org/10.1074/jbc.M400713200

363. Yang, H., Niemeijer, M., van de Water, B., & Beltman, J. B. (2020). ATF6 is a critical determinant of CHOP dynamics during the unfolded protein response. *IScience*, *23*(2), 100860. https://doi.org/10.1016/j.isci.2020.100860

364. Gade, P., Ramachandran, G., Maachani, U. B., Rizzo, M. A., Okada, T., Prywes, R., Cross, A. S., Mori, K., & Kalvakolanu, D. V. (2012). An IFN-γ–stimulated ATF6–C/EBP-β–signaling pathway critical for the expression of death associated protein kinase 1 and induction of autophagy. *Proceedings of the National Academy of Sciences*, *109*(26), 10316–10321. https://doi.org/10.1073/pnas.1119273109

365. Gade, P., Roy, S. K., Li, H., Nallar, S. C., & Kalvakolanu, D. V. (2008). Critical role for transcription factor C/EBP-β in regulating the expression of death-associated protein kinase 1. *Molecular and Cellular Biology*, *28*(8), 2528–2548. https://doi.org/10.1128/MCB.00784-07

366. Choi, Y., Bowman, J. W., & Jung, J. U. (2018). Autophagy during viral infection— A double-edged sword. *Nature Reviews Microbiology*, *16*(6), 341–354. https://doi.org/10.1038/s41579-018-0003-6

367. Granato, M., Santarelli, R., Filardi, M., Gonnella, R., Farina, A., Torrisi, M. R., Faggioni, A., & Cirone, M. (2015). The activation of KSHV lytic cycle blocks autophagy in PEL cells. *Autophagy*, *11*(11), 1978–1986. https://doi.org/10.1080/15548627.2015.1091911

368. Liang, Q., Chang, B., Brulois, K. F., Castro, K., Min, C.-K., Rodgers, M. A., Shi, M., Ge, J., Feng, P., Oh, B.-H., & Jung, J. U. (2013). Kaposi's sarcoma-associated herpesvirus K7 modulates rubicon-mediated inhibition of autophagosome maturation. *Journal of Virology*, *87*(22), 12499–12503. https://doi.org/10.1128/JVI.01898-13

369. Pattingre, S., Tassa, A., Qu, X., Garuti, R., Liang, X. H., Mizushima, N., Packer, M., Schneider, M. D., & Levine, B. (2005). Bcl-2 antiapoptotic proteins inhibit beclin 1-dependent autophagy. *Cell*, *122*(6), 927–939. https://doi.org/10.1016/j.cell.2005.07.002

370. Lee, J.-S., Li, Q., Lee, J.-Y., Lee, S.-H., Jeong, J. H., Lee, H.-R., Chang, H., Zhou, F.-C., Gao, S.-J., Liang, C., & Jung, J. U. (2009). FLIP-mediated autophagy regulation in cell death control. *Nature Cell Biology*, *11*(11), 1355–1362. https://doi.org/10.1038/ncb1980

371. Arias, C., Weisbrud, B., Stern-Ginossar, N., Mercier, A., Madrid A. S., Bellare, P., Holdorf, M., Weissman, J. S., & Ganem, D. (2014). KSHV 2.0: a comprehensive annotation of the Kaposi's sarcoma-associated herpesvirus genome using next-generation sequencing reveals novel genomic and functional features. *PLoS Pathogens, 10*(1), e1003847. https://doi.org/10.1371/journal.ppat.1003847

372. Yan, L., Majerciak, V., Zheng, Z.-H., & Lan, K. (2019). Towards better understanding of KSHV life cycle: from transcription and posttranscriptional regulations to pathogenesis. *Virologica Sinica, 34*(2), 135–161. https://doi.org/10.1007/s12250-019-00114-3